

# **The role of SENP1 in B cell development and differentiation**

Dissertation  
Zur Erlangung des Grades  
Doktor der Naturwissenschaft

Am Fachbereich Biologie  
der Johannes Gutenberg-Universität Mainz

vorgelegt von  
**Christian Reichhold**  
geb. am 07. August 1981  
in Frankfurt am Main, Deutschland

Mainz, 2013



## Table of Contents

<b>1. INTRODUCTION .....</b>	<b>1</b>
1.1 SUMO .....	2
1.2 MECHANISM OF SUMOYLATION.....	4
1.3 SUMO PROTEASES (SENPs) .....	6
1.3.1 SENP1 .....	7
1.3.2 SENP2 .....	8
1.4 CELLULAR FUNCTIONS OF SUMO AND SENP .....	8
1.4.1 SENP1 in mouse development.....	9
1.4.2 Lethal defects in erythropoiesis in SENP1 KO mice.....	9
1.4.3 Early lymphoid development.....	9
1.4.4 SENP1 in plasma cell development.....	10
1.4.5 Regulation of senescence .....	11
1.4.6 PML and nuclear body formation.....	11
1.4.7 SENP1 in Transcription .....	13
1.4.8 SENP1 in DNA repair .....	14
1.4.9 SUMO and NEMO in response to genotoxic stress, V(D)J and class switch recombination.....	15
1.4.10 SENP1 in cancer.....	17
1.5 RATIONALE & AIMS.....	18
<b>2. MATERIALS AND METHODS.....</b>	<b>19</b>
2.1 CHEMICAL AND BIOLOGICAL MATERIAL .....	19
2.2 MOLECULAR BIOLOGY.....	20
2.2.1 Competent cells and isolation of plasmid DNA.....	20
2.2.2 Plasmid cloning.....	20
2.2.3 Isolation of genomic DNA from mouse organs.....	22
2.2.4 Isolation of genomic DNA from ES cells.....	22
2.2.5 Polymerase Chain Reaction (PCR) .....	22
2.2.6 Agarose gel electrophoresis and DNA gell extraction.....	23
2.2.7 DNA & RNA quantification.....	24
2.2.8 Southern blot analysis.....	24
2.2.9 Quantitative real time PCR .....	25
2.3 CELL BIOLOGY .....	27
2.3.1 Embryonic stem cell cultur.....	27
2.3.2 Preperation of cells from lymphoid organs.....	28
2.3.3 Magnetic cell sorting and FACS sorting.....	28

2.3.4	<i>Cell counting</i> .....	29
2.3.5	<i>Flow Cytometry</i> .....	29
2.3.6	<i>Culture and activation of ex vivo B cells</i> .....	30
2.3.7	<i>Proliferation assays</i> .....	31
2.3.8	<i>Cell cycle analysis</i> .....	31
2.4	IMMUNOHISTOCHEMISTRY.....	31
2.5	MOUSE EXPERIMENTS.....	32
2.5.1	<i>Mice</i> .....	32
2.5.2	<i>Immunization with Sheep Red Blood Cells (SRBC)</i> .....	32
2.5.3	<i>Generation of mixed bone marrow chimeras</i> .....	32
2.5.4	<i>In vivo BrdU labeling</i> .....	32
2.6	SOFTWARE & STATISTICS.....	33
<b>3.</b>	<b>RESULTS</b> .....	<b>34</b>
3.1	SEN1 <sup>FF</sup> .....	34
3.1.1	<i>Reduced B cell numbers in naive SEN1<sup>ff</sup> and SEN1<sup>ff</sup> CD19-Cre mice</i> .....	34
3.1.2	<i>Transcriptional network in naive SEN1<sup>ff</sup> CD19 B cells</i> .....	42
3.1.3	<i>Impaired survival after in vitro stimulation due to activation induced cell death (AICD)</i> .....	45
3.1.4	<i>In vitro class switch recombination and plasma cell differentiation</i> .....	49
3.1.5	<i>Reduction of B cell subsets in naive JHT<sup>-/-</sup>/SEN1<sup>ff</sup> RFP CD19-Cre mixed bone marrow chimeras</i> .....	53
3.1.6	<i>SEN1<sup>ff</sup> CD19-Cre mice experience a higher B cell turnover</i> .....	63
3.1.7	<i>Block of de novo B cell generation through all7R treatment results in B cell reduction</i> .....	64
3.1.8	<i>Sheep red blood cell immunization of JHT/SEN1<sup>ff</sup> CD19-Cre bone marrow chimeras</i> .....	65
3.2	GENERATION OF SEN2 <sup>FLOX</sup> MICE.....	74
<b>4.</b>	<b>DISCUSSION</b> .....	<b>78</b>
4.1	SEN1 IN B CELL SURVIVAL.....	78
4.2	SEN1 IN CSR & PC DEVELOPMENT.....	85
4.3	SEN2.....	88
<b>5.</b>	<b>SUMMARY</b> .....	<b>89</b>
<b>6.</b>	<b>ZUSAMMENFASSUNG</b> .....	<b>91</b>
<b>7.</b>	<b>REFERENCE LIST</b> .....	<b>93</b>

---

<b>8. ACKNOWLEDGEMENTS .....</b>	<b>107</b>
<b>9. VERSICHERUNG.....</b>	<b>108</b>
<b>10. LEBENSLAUF.....</b>	<b>109</b>
<b>11. PUBLIKATIONEN.....</b>	<b>110</b>

---

## List of Abbreviations

°C	degrees Celsius
3'	3 prime end of DNA sequence
5'	5 prime end of DNA sequence
7AAD	7-Aminoactinomycin D
aa	amino acid
AICD	activation induced cell death
AID	activation-induced (cytidine) deaminase
$\alpha$ IL7R	anti IL7 receptor blocking antibody
APC	allophycocyanin
APC Cy7	allophycocyanin Cy7
approx.	approximately
AR	androgen receptor
ATM	ataxia telangiectasia mutated serine threonine kinase
$\beta$ -ME	beta-mercapto ethanol
BAC	bacterial artificial chromosome
Bcl2	B-cell lymphoma 2 protein
Bcl6	B-cell lymphoma 6 protein
BCR	B cell receptor
BER	base excision repair
Bio	biotin
BLIMP1	PR domain zinc finger protein 1
BM	bone marrow
bp	base pair
BrdU	bromodeoxyuridine
BSA	bovine serum albumin
CCND2	cyclin D2
CCND3	cyclin D3
cDNA	complementary DNA
cps	counts per second
Cre	Cre recombinase
CSR	class switch recombination
ddH <sub>2</sub> O	double distilled water
DMEM	Dulbecco's modified Eagle's medium
DMSO	dimethyl sulfoxide

---

DNA	desoxyribonucleic acid
dNTP	desoxyribonucleotide triphosphate
DP	double positive
DSB	double strand break
DTT	dithiothritole
DUB	deubiquitin protease
e.g.	exempli gratia
E2A	NeuroD basic helix loop helix transcription factor
EBF1	transcription factor COE1
EDTA	ethylen-diaminetetraacetic acid
ELISA	enzyme-linked immuno-sorbent assay
ES cell	embryonic stem cell
et al.	<i>et alii</i>
EtOH	ethanol
F	Farad
FACS	fluorescence activated cell sorting
FCS	fetal calf serum
Fig.	Figure
FITC	fluorescein isothiocyanate
flp	flp recombinase
fol	follicular B cell
FoxP3	forkhead box protein 3
frt	flippase recognition target
g	gram
G418	Geneticin
GC	germinal centre
Gly	glycine
Gy	gray
h	hour
Hepes	4-(2-hydroxyethyl)-1-piperazineethanesulfonic acid
HR	homologous recombination
i.e.	<i>id est</i>
i.p.	intra peritoneal
i.v.	intro venous
Ig	Immunoglobulin
IgA	Immunoglobulin A

---

IgE	Immunoglobulin E
IgD	Immunoglobulin D
IgG1	Immunoglobulin G1
IgG2a	Immunoglobulin G2a
IgG2b	Immunoglobulin G2b
IgG3	Immunoglobulin G3
IgM	Immunoglobulin M
IKEA	nuclear factor of kappa light polypeptide gene enhancer in B-cells inhibitor, alpha
IL4	interleukin 4
IL7R	interleukin 7 receptor
IRF4	interferon regulatory factor 4
IRF5	interferon regulatory factor 5
iso control	isotype control
JHT	Jh targeted mutation mice
kb	kilo base pair
KO	knock out
l	litre
LAH	left arm of homology
LIF	leukaemia inhibiting factor
LN	lymph node
loxP	locus of X-over P1
LPS	lipopolysachharide
Lys	lysine
M	molar
MACS	magnetic-activated cell sorting
mF	milli Farad
mg	milli gram
MHC	major histocompatibility complex
min	minute
ml	millilitre
mM	milli molar
mRNA	messenger RNA
MZ	marginal zone
MZP	marginal zone precursor
NB	nuclear body



---

NDSM	negatively charged amino acid dependant SUMOylation motif
neg	negative
NEMO	NF-kappa-B essential modulator, aka IKK-γ
neo	neomycin resistance
NER	nucleotide excision repair
NES	nuclear export signal
NF-KB	nuclear factor kappa-light-chain-enhancer of activated B cells
ng	nano gram
NHEJ	non-homologous end joining
NLS	nuclear localisation signal
nm	nano molar
NPC	nuclear pore complex
OD	optical density
PC	plasma cell
PCNA	proliferating cell nuclear antigen
PCR	polymerase chain reaction
PDSM	phosphorylation dependant SUMOylation motif
Pe	phycoerythrin
PeCy7	phycoerythrin Cy7
PerCP	peridinin-chlorophyll-protein complex
PIAS	protein inhibitor of activated STAT
PML	promyelocytic leukaemia protein
pos	positive
PP	Peyer's patches
PTM	posttranslational modification
RAG	recombination activating gene
RAH	right arm of homology
RFP	red fluorescent protein
RIPA	radioimmunoprecipitation assay buffer
RNA	ribonucleic acid
RT	room temperature
RT-PCR	reverse transcription PCR
SA	streptavidin
SD	standard deviation
SDS	sodium dodecyl sulfate
sec	second

---

SEM	standard error of mean
SENP	SUMO protease
SHM	somatic hypermutation
SIM	SUMO interaction motif
SRBC	sheep red blood cells
SSC	saline sodium citrate buffer
SUMO	small ubiquitin like modifier
T1	transitional 1 B cells
T2	transitional 2 B cells
T3	transitional 3 B cells
TAE	tris base, acetic acid and EDTA buffer
Taq	thermus aquaticus DNA polymerase
TK	thymidin kinase
TLR4	Toll-like receptor
Tris	tris(hydroxymethyl)aminomethane
U	unit
Ub	ubiquitin
Ubl	ubiquitin like modifier
ug	micro gram
ul	micro litre
Ulp	Ubl-specific protease
V	volt
v/v	volume per volume
V450	fluorochrome
V500	fluorochrome
w/o	without
w/v	weight per volume
WT	wild type

## List of Figures

<i>Figure 1-1 Overview on most prominent ubiquitin (Ub) and ubiquitin like (Ubl) posttranslational modifications</i> .....	2
<i>Figure 1-2: Mechanism of SUMOylation</i> .....	5
<i>Figure 1-3: Primary structure of Ubls and SENPs</i> .....	7
<i>Figure 1-4: SUMO targets grouped by function or localisation</i> .....	8
<i>Figure 1-5: Assembly of the Promyelocytic leukemia protein (PML) nuclear bodies (NB)</i> .....	12
<i>Figure 1-6: Interplay of IKK<math>\gamma</math> (NEMO) and ATM in response to DNA damage</i> .....	17
<i>Figure 3-1: B cell development in the bone marrow</i> .....	35
<i>Figure 3-2: B/T cell ration in the spleen</i> .....	37
<i>Figure 3-3: B cell subsets in the spleen</i> .....	38
<i>Figure 3-4: GC B cells in the Peyer's patches of naive mice</i> .....	39
<i>Figure 3-5: Verification of SENP1 knockout by PCR typing and qRT-PCR</i> .....	40
<i>Figure 3-6: Schematic of SENP1<sup>f</sup> and KO mouse targeting strategy</i> .....	41
<i>Figure 3-7: quantitative real-time RT-PCR analysis of B cell, apoptosis and cell cycle relevant genes</i> ..	42
<i>Figure 3-8: in vitro stimulation of total splenocyte culture</i> .....	46
<i>Figure 3-9: Cell cycle analysis</i> .....	48
<i>Figure 3-10: in vitro proliferation assay</i> .....	49
<i>Figure 3-11: in vitro CSR and PC differentiation of total splenocyte culture</i> .....	51
<i>Figure 3-12: MHC II expression after in vitro stimulation</i> .....	52
<i>Figure 3-13: Schematic of mixed bone marrow chimera generation</i> .....	54
<i>Figure 3-14: Total cell number of splenocytes in JHT/SENP1<sup>f</sup> RFP CD19 bone marrow chimeras</i> .....	55
<i>Figure 3-15: B cell subsets in the spleen of JHT/SENP1<sup>f</sup> RFP CD19 bone marrow chimeras 8 weeks after reconstitution</i> .....	56
<i>Figure 3-16: B cell subsets in the spleen of JHT/SENP1<sup>f</sup> RFP CD19 bone marrow chimeras</i> .....	58
<i>Figure 3-17: Statistical analysis of B cell subsets in the spleen of JHT/SENP1<sup>f</sup> RFP CD19 bone marrow chimeras</i> .....	59
<i>Figure 3-18: B cell subsets in the lymph nodes of JHT/SENP1<sup>f</sup> RFP CD19 bone marrow chimeras</i> .....	60
<i>Figure 3-19: B cells in the Peyer's patches and peritoneal cavity of naive JHT/SENP1<sup>f</sup> RFP CD19 bone marrow chimeras</i> .....	61
<i>Figure 3-20: Analysis of RFP expression in splenic B cells of naive JHT/SENP1<sup>f</sup> RFP CD19 bone marrow chimeras 8 weeks after reconstitution</i> .....	62
<i>Figure 3-21: in vivo BrdU incorporation indicates increased B cell turnover</i> .....	64
<i>Figure 3-22: Block of de novo B cell generation through in vivo <math>\alpha</math>L7R treatment</i> .....	65
<i>Figure 3-23: Schematic of mixed bone marrow chimera generation</i> .....	66
<i>Figure 3-24: Total cell number of all bone marrow and spleen cells in JHT/SENP1<sup>f</sup> CD19-Cre mice after SRBC immunization</i> .....	67

---

<i>Figure 3-25: B cell subsets in the BM of JHT/SEN1<sup>fl</sup> CD19 bone marrow chimeras after SRBC immunization</i> .....	68
<i>Figure 3-26 Splenic B cell populations in SRBC immunized JHT/SEN1<sup>fl</sup> CD19-Cre BM chimeras</i> .....	69
<i>Figure 3-27: Splenic B cell populations in SRBC immunized JHT/SEN1<sup>fl</sup> CD19-Cre BM chimeras</i> .....	70
<i>Figure 3-28: Statistical analysis of splenic B cell populations in SRBC immunized JHT/SEN1<sup>fl</sup> CD19-Cre BM chimeras</i> .....	71
<i>Figure 3-29: Analysis of CSR and plasma cell differentiation in SRBC immunized JHT/SEN1<sup>fl</sup> CD19-Cre BM chimeras</i> .....	72
<i>Figure 3-30: IgM expression on plasma cells</i> .....	73
<i>Figure 3-31: Immunoglobulin ELISA from serum of SRBC immunized JHT/SEN1<sup>fl</sup> CD19-Cre mice</i> .....	74
<i>Figure 3-32: Schematic representation of targeting strategy</i> .....	75
<i>Figure 3-33: Schematic representation of targeting vector</i> .....	76
<i>Figure 3-34: Southern blot analysis of BglI digested ES cell DNA</i> .....	76
<i>Figure 3-35: Picture of chimeric mouse after blastocyst ES cell injection &amp; Results of chromosome counting in metaphase</i> .....	77

## List of Tables

<i>Table 2-1: List of chemical substances</i> .....	19
<i>Table 2-2: Sequences for primers used in cloning. Red letters mark in-fusion sequence</i> .....	21
<i>Table 2-3: Primer for sequencing of cloning products</i> .....	21
<i>Table 2-4: Primer sequences for genotyping</i> .....	23
<i>Table 2-5: Primer sequences for Southern blot probes</i> .....	25
<i>Table 2-6: List of qRT-PCR primers</i> .....	26
<i>Table 2-7: List of antibodies used for FACS stainings</i> .....	30

## 1. Introduction

Post-translational protein modifications (PTM) are a highly sophisticated means to fine tune cellular processes and redirect protein functions. PTMs can take on many different form such as phosphorylation, hydroxylation, glycosylation, methylation, etc. The most studied form of post-translational modifications with a protein as modifier is ubiquitination. Ubiquitin (Ub), a highly conserved 76 amino acid (aa) polypeptide, is able to covalently attach to other proteins and is therefore able to regulate the fate of the target protein in a dynamic and reversible manner. Target proteins are able to undergo mono- and polyubiquitination with each form of ubiquitination resulting in a different outcome of modification. Ub itself has Ub binding sites and can therefore build polyubiquitination chains by linking either through Lys48 or Lys63, whereas Lys48 (Flick et al., 2004) linked Ub moieties mainly results in proteasomal degradation (Hershko and Ciechanover, 1992) and Lys63 chains regulates DNA repair mechanisms, endocytosis and activates protein kinases (Figure 1-1) (Haglund and Dikic, 2005).

Besides Ub many ubiquitin-like modifications (Ubl) are known. These ubiquitin-like proteins follow a similar mechanism of post-translational modification, however with different protein structures and distinct physiological consequences. The most prominent Ubl is the small ubiquitin-like modifier, known as SUMO (also known as sentrin, Pic-1, GMP-1 UBL1, SMT3C). However, besides many others, also NEDDylation (Nedd8) (Kamitani et al., 1997), ISGylation (ISG15) (Haas et al., 1987; Loeb and Haas, 1992) and FATylation (FAT10) are well known Ubls (Liu et al., 1999).

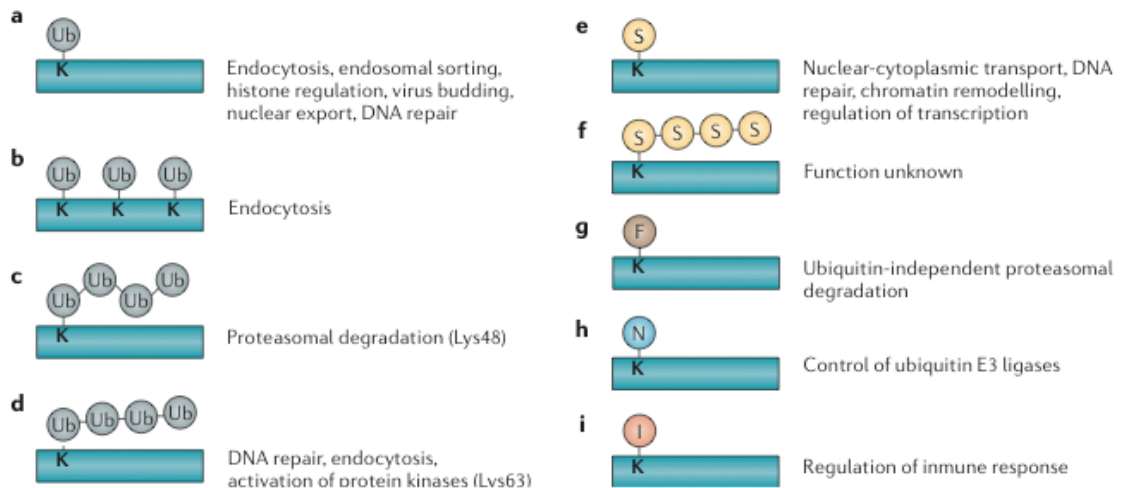


**Figure 1-1 Overview on most prominent ubiquitin (Ub) and ubiquitin like (Ubl) posttranslational modifications.** In a process known as monoubiquitination (A) a single Ub is covalently bound to a target lysine (K) resulting in a range of different functions of the target protein. Multi monoubiquitination on the same protein is often used in endocytosis (B), whereas polyubiquitination, where Ub chains are formed via Lys48, targets proteins for proteasomal degradation (C). Polyubiquitination through Lys63-linked chains (D) regulates DNA repair mechanisms, endocytosis and activates protein kinases. SUMOylation regulates many cellular mechanisms, such as nuclear transport, DNA damage repair and chromatin remodelling, besides many others (E). SUMO chain formation has been observed, however it's function is unknown (F). Fatylation regulates rapid proteasomal degradation in a ubiquitin like manner (G). NEDDylation (H) has been shown to modify Ub E3 ligases and ISGylation regulates immune responses induced through interferons. (Adapted from Hoeller et al., 2006)

## 1.1 SUMO

First discovered as an ubiquitin-like protein in 1996 by several groups (Boddy et al. 1996, Mannen et al. 1996, Matunis et al. 1996, Shen et al. 1996a, Kamitani et al. 1997b, Lapenta et al. 1997), SUMO has since then immensely gained on scientific weight. SUMO is ubiquitously expressed in eukaryotic cells and is essential for survival. In *Saccharomyces cerevisiae* SUMO defects result in G2/M cell cycle arrest (Seufert et al., 1995) and in mice SUMO deficiency leads to embryonic lethality (Nacerddine et al., 2005). SUMOylation is a highly dynamic process and reversible by deconjugation through Ubl-specific proteases, referred to as SUMO proteases (SENPs).

SUMO has only 18 % primary sequence homology to ubiquitin, but the characteristic ubiquitin-fold tertiary structure is virtually identical (Bayer et al., 1998; Jin et al., 2001; Sheng and Liao, 2002). SUMO is initially expressed as an

immature form with an C-terminal tail (Muller et al., 2001). For SUMO to be able to bind to target proteins this tail is cleaved off by SENPs to expose the mature diglycine motif (Gly-Gly) at the C-terminus that is found in most UbIs (Jentsch and Pyrowolakis, 2000). Once matured, SUMO forms an isopeptide bond between the  $\epsilon$ -amino group of the lysine within the SUMO consensus motif of the target protein and the C-terminal glycine of SUMO. The SUMOylation consensus motif is defined by  $\psi$ KXE/D, where  $\psi$  resembles a hydrophobic residue, K the lysine residue, X any amino acid and E/D an acidic residue (Bayer et al., 1998; Jentsch and Pyrowolakis, 2000; Jin et al., 2001; Rodriguez et al., 2001; Sheng and Liao, 2002). Restricted or preferential binding to a consensus motif is unique for SUMOylation as it is not found in ubiquitin target conjugation. However many other binding motives or SUMO targets without any binding motifs have so far been discovered (Hoege et al., 2002; Pichler et al., 2005).

Yeast and invertebrates express only one form of SUMO (Smt3)(Meluh and Koshland, 1995), plants express up to eight SUMO isoforms, whereas vertebrates express three isoforms: SUMO-1, SUMO-2 and SUMO-3 (Melchior, 2000). SUMO-2 and SUMO-3 share approximately 95% sequence homology between each other, but SUMO-1 compared to SUMO-2 and SUMO-3 only about 50%. SUMO-2 and SUMO-3 differ only in three aminoterminal residues and are here referred to as SUMO2/3. The C-terminal tails of SUMO are four aa long in SUMO-1, 11 aa in SUMO-2 and two aa in SUMO-3. In contrast to SUMO-1 SUMO-2/3 has an internal SUMO consensus motif found at the N-terminal region at Lys11 and thus, just as ubiquitin, is able to form poly-SUMO chains (Hay, 2007; Mukhopadhyay and Dasso, 2007; Tatham et al., 2001). It is believed that monomeric SUMO-1 and polymeric SUMO-2/3 chains have very distinct cellular functions. SUMO-1 modification often counteracts ubiquitin mediated proteasomal degradation, as seen for I $\kappa$ B $\alpha$ , Smad4, Rad52 and Mdm2 (Desterro et al., 1998; Lee et al., 2006; Lin et al., 2003; Sacher et al., 2006; Zhao, 2007), whereas SUMO-2/3 polySUMOylation in BMAL1 may serve as a signal for ubiquitin mediated proteasomal degradation (Lee et al., 2008). It is also shown that SUMO-2/3 mostly exist in a free pool in the cytoplasm and is therefore readily available for fast conjugation upon cellular stress. SUMO-1,



however, is mostly found conjugated to target proteins. This again underlines the notion that SUMO-1 and SUMO2/3 have very different biological functions.

A fourth isoform, SUMO-4, has been reported for humans. SUMO-4 has an 86 % aa similarity to SUMO-2 and is mainly expressed in the kidney, lymph nodes and spleen (Guo et al., 2004). However, it is so far unclear if SUMO-4 is able to covalently bind to target proteins (Owerbach et al., 2005).

## 1.2 Mechanism of SUMOylation

The reversible process of SUMOylation depends on the formation of an isopeptide bond between the C-terminal Gly-Gly motif of SUMO and the  $\epsilon$ -amino group of the lysine within the conserved or unique SUMO consensus motif of the target protein and a subsequent non-destructive deSUMOylation. This process is a highly regulated cascade involving three classes of enzymes: activation enzymes (E1); conjugation enzymes (E2); ligation enzymes (E3). As similar as this process is to ubiquitination, the enzymes of the SUMOylation cascade are unique and have no similarities to the enzymes of the ubiquitination cascade. The only exception being their similarity in function.

The first step of the SUMOylation mechanism is the proSUMO maturation (Muller et al., 2001), by cleaving the C-terminal tail and freeing the di-glycin motif necessary for further conjugation. Endopeptidic maturation is achieved by the deSUMOylating proteases SENP. Once SUMO is matured it can be activated through the E1 activation enzyme complex AOS1-UBA2. The heterodimers AOS1-UBA2 form a SUMO-adenylate complex in an ATP dependant manner. This complex consists of a thioester bond between the C-terminal carboxy group of SUMO and the catalytic Cys residue of UBA2 which resembles an intermediate to the subsequent complex, which is formed between SUMO and the E2 enzyme UBC9 (Figure 1-2).

In the following step SUMO is transferred from the E1 enzyme complex to the E2 conjugation enzyme UBC9 where a thioester linkage between the catalytic Cys residue of UBC9 and the C-terminal carboxy group of SUMO is formed (Muller et

al., 2001). UBC9 then transfers SUMO to its final target protein. The two proteins are linked by an isopeptide bond between C-terminal Gly residue of SUMO and the Lys of the substrate. This step is in most cases aided by E3 ligases which catalyse the transfer from UBC9 to the target. This catalytic help is not always necessary, however it is believed to increase substrate specificity of UBC9 (Yang and Sharrocks, 2013).

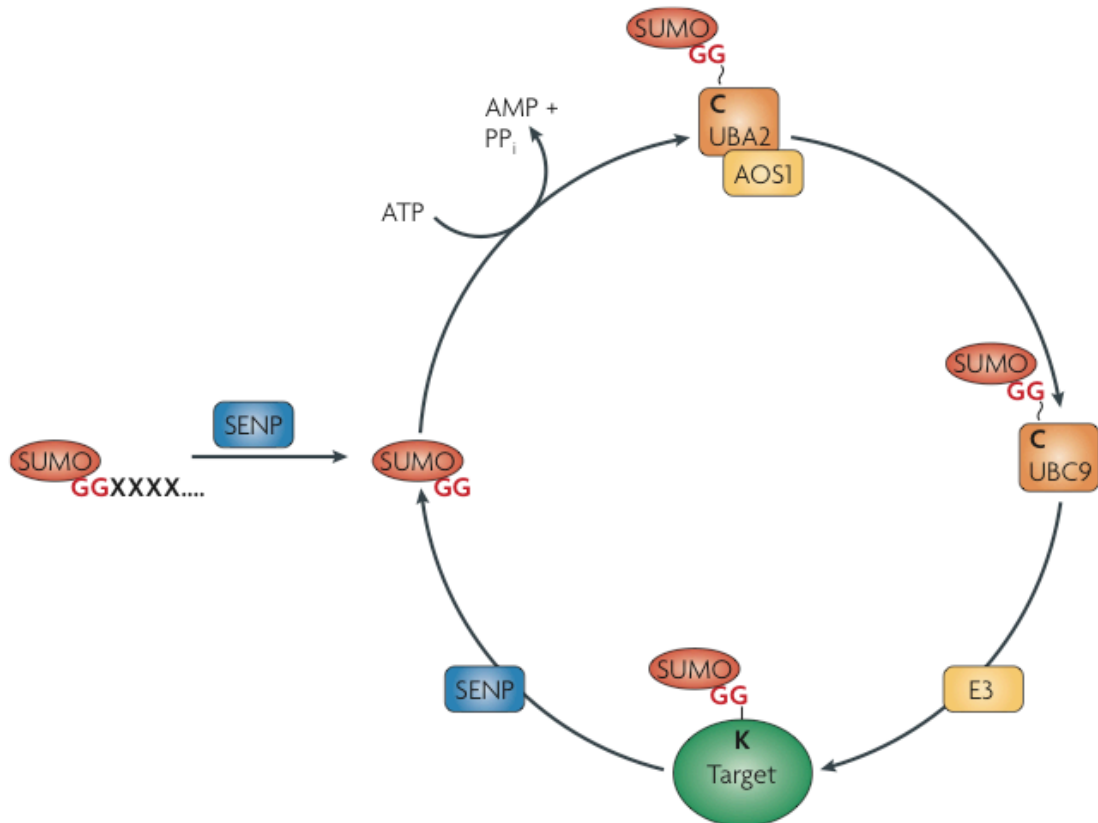


**Figure 1-2: Mechanism of SUMOylation.** Immature SUMO is processed by SENPs through C-terminal tail cleavage to expose di-glycine motif. Mature SUMO is then activated by E1 heterodimer AOS1-UBA2 in an ATP dependent manner and subsequently transferred to the catalytic Cys residue of the E2 enzyme UBC9. At last an isopeptide bond between the C-terminal Gly residue of SUMO and a Lys residue of the target protein is formed. E3 ligases usually catalyse this step. SENPs then deconjugate SUMO again from their target proteins in a non-destructive process. (Geiss-Friedlander and Melchior, 2007)

Interestingly within the SUMOylation cycle only one E2 enzyme, UBC9, has so far been discovered. The uniqueness of UBC9 is in that way remarkable that it alone has to govern substrate specificity. In contrast, in ubiquitination more than 20 E2 enzymes have been identified. To overcome the problem of being restricted to only one conjugation enzyme it is believed that consensus motifs in the SUMO acceptor

sites of target proteins increase target specificity (Geiss-Friedlander and Melchior, 2007). And these consensus motifs, in turn, have not been shown in ubiquitin target proteins.

The E3 SUMO ligases, in some cases thought to be redundant, consist of four groups. The biggest of the four groups is the SP-RING motif group (Hochstrasser, 2001; Jackson, 2001). The SP-RING motif is related to the RING motif of ubiquitin E3 ligases and binds SUMO in a non-covalent manner through SUMO interaction and SUMO binding motifs (SIM/SBM) (Minty et al., 2000). The PIAS family ligases, MMS21 and Zip3 are part of the SP-RING group (Hochstrasser, 2001; Jackson, 2001). Other E3 ligase groups are the RanBP2, CBX4 (in humans Polycomb group PC2) and HDAC4 (Gao et al., 2008; Kagey et al., 2003; Pichler et al., 2002; Yang et al., 2011). Interestingly, HDAC4 itself is SUMOylated with the help of the RanBP ligase (Kirsh et al., 2002).

As this thesis solely deals with the regulatory effects of SUMO-1, if not otherwise stated, for simplicity reasons SUMO-1 will be referred to as SUMO.

### **1.3 SUMO proteases (SENPs)**

As previously mentioned SUMO is ubiquitously expressed in every eukaryotic cell, hence it regulates a vast amount of different cellular processes. These different processes and pathways include transcriptional regulation, embryonic development, cell cycle control, DNA damage response, apoptosis, PML nuclear body formation and many more, which will be discussed below.

Yeast Ulp1 and Ulp2 (Ubl-specific proteases) were the first two deSUMOylation proteases that were identified and characterized (Li and Hochstrasser, 1999, 2000). Both proteases can deconjugate Smt3 (yeast orthologue of SUMO) target proteins and cleave the C-terminal tail for Smt3 maturation. However, their structural similarity is confined to the approximate 200 aa sequence of the catalytic Ulp domain (Li and Hochstrasser, 2000).

In humans and mice eight genes were found with similar sequence to the Ulp genes, coding for possible SUMO proteases (Yeh et al., 2000), SENP1-8. It was not

long after discovery where SENP3 and SENP4 were found out to be the same gene, and SENP8 was not specific for SUMO, rather it was deconjugating a different ubiquitin-like protein, NEDD8 (Mendoza et al., 2003; Wu et al., 2003). The six remaining SENP members can be divided into three groups. SENP1 and SENP2 with a very similar, but broad, substrate specificity. SENP3 and SENP5 with a preference to SUMO-2/3, and SENP6 and SENP7, which are in contrast to SENP1-5 more closely related to Ulp2 than Ulp1 and contain a so far unelucidated insertion in the catalytic domain (Figure 1-3) (Hay, 2007; Kim et al., 2002; Mukhopadhyay and Dasso, 2007).

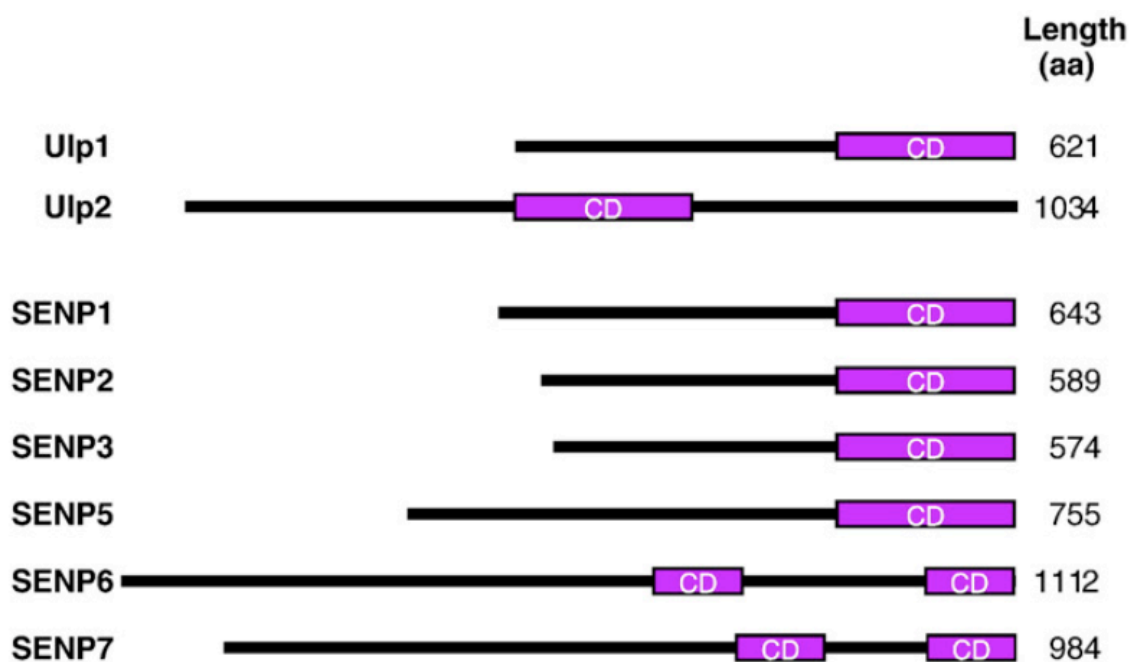


**Figure 1-3: Primary structure of Ulp1 and SENPs.** The conserved catalytic domains are marked in purple (Kim and Baek, 2009)

### 1.3.1 SENP1

SENP1 is a cysteine protease with a highly conserved catalytic domain at the C-terminus. The core of the catalytic domain consists of a catalytic triad with a His-Asp-Cys sequence. Proteases are grouped in different clans according to their structure and function. All SENPs belong to the CE cysteine proteases clan, whereas the deubiquitin proteases (DUBs), for example, are part of the clan of CA papain-like proteases. Despite similar function of SENPs and DUBs there is no sequence similarity. SENP1 contains a N-terminal localisation signal (NLS) and nuclear export signal (NES) and is mainly found in the nucleus.

### 1.3.2 SENP2

SENP2 is closely related to SENP1 and shares many targets and functions (Drag and Salvesen, 2008). SENP2 is primarily found in the nuclear envelope close to the nuclear pore complex (NPC) (Hang and Dasso, 2002). It accumulates in distinct subnuclear bodies and has both NLS and NES in the non-conserved N-terminus (Hang and Dasso, 2002). SENP2 constantly shuttles between cytoplasm and the nucleus, whereas in cytoplasm it is polyubiquitinated and degraded by the 26S proteasom pathway.

## 1.4 Cellular functions of SUMO and SENP

Since the discovery of SUMO and its first target (RanGAP), the list of SUMO modified proteins and therefore the involvement and regulation of a vast array of different cellular processes is ever increasing (Figure 1-4).

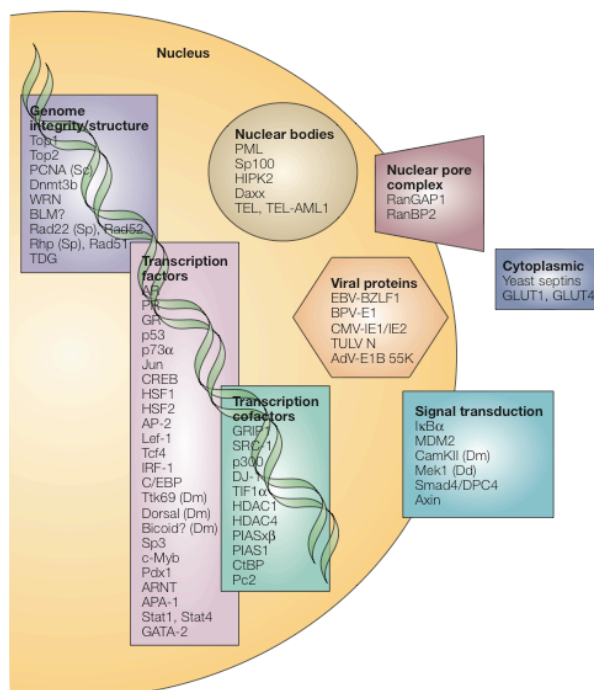


**Figure 1-4: SUMO targets grouped by function or localisation.** All proteins are of mammalian origin unless otherwise stated; (Sc) budding yeast, (Sp) fission yeast, (Dm) *Drosophila*, (Dd) Dictyostelium. Adapted from (Seeler and Dejean, 2003)

### 1.4.1 *SENP1 in mouse development*

*Yamaguchi et al. (2005)* generated a mouse model with a randomly integrated retroviral insertion into SENP1, which led to a reduced SUMO-1 deconjugation and a decrease in mature SUMO-1. Impaired deSUMOylation capability led to increase in SUMOylated targets, including RanGAP, showing that RanGAP is mainly SUMOylated by SUMO-1. In contrast, SUMO-2 and SUMO-3 levels were unchanged. Furthermore they could show that homozygous SENP1 gene disruption caused severe defects in placental development from e12.5 on and embryonic lethality between day e12.5 and e14.5.

### 1.4.2 *Lethal defects in erythropoiesis in SENP1 KO mice*

Yu and colleagues from the Wang Min Lab have constructed a conditional SENP1 knockout (KO), which was crossed to a  $\beta$ -Actin Cre resulting in a full SENP1 KO (Yu et al., 2010). In parallel Cheng, from the Edward Yeh Lab, also generated a full SENP1 knockout (Cheng et al., 2007). In both models embryonic lethality could be observed due to hypoxia. As show by Yamaguchi (Yamaguchi et al., 2005) previously, in a different mutagenesis approach by random retroviral insertion mutation into *Senp1*, the complete SENP1 absence caused embryonic lethality between embryonic day 13.5 and postnatal day one. Only three of the 384 littermates survived until two weeks of age, each developing a strong anaemia. In general embryos died at day E13.5 caused by erythropoiesis defects in fetal liver, less erythroblasts, less erythropoietic islands in fetal liver, decreased haemoglobin (Hbb-a1, Hbb-b1) and increased embryonic haemoglobin levels (Hbb-x & Hbb-y).

These fatal defects in erythropoiesis are based on the impaired GATA1 regulation through SUMO. GATA1, a transcription factor regulating erythropoiesis, is repressed by SUMOylation. The subsequent expression of GATA1 targets was also decreased in the SENP1 KO. Yu et al. (2010) could also show that SENP1 but not SENP2 regulates GATA1 and alters the GATA1 DNA binding ability.

### 1.4.3 *SENP1 in early lymphoid development*

Until today only few papers were published on the regulation of lymphocyte development through SUMOylation. The publication by Van Nguyen et al. (2012)

from the Edward Yeh Lab shows that impaired deSUMOylation in *in vitro* generated SENP1 KO cells and embryonic SENP1<sup>-/-</sup> cells leads to excess SUMOylated STAT5 in early B and T cells, resulting in subsequent maturation defects, namely in severe intrinsic impairment of B and T cell development. They demonstrated that the constant SUMOylation in SENP1 KO cells inhibits the tyrosine phosphorylation and therefore inhibits the activation-inactivation cycle of STAT5 in lymphocytes. This again highlights the close interplay between different post-translational modifications and the competition for common modification sites. In addition to the SUMOylation/phosphorylation interplay, SUMOylation and acetylation compete for the same lysine residue K696. The STAT5 acetylation is hypothesised to be necessary for STAT5 dimerisation and SUMOylated STAT5 is unable to acetylate.

#### 1.4.4 SENP1 in plasma cell development

Shimshon et al. (2011) and Ying et al. (2012) both showed the importance of SUMOylation on plasma cell differentiation. Shimshon et al. (2011) first showed how SUMOylation regulates the transcriptional repression of BLIMP-1, and how SUMOylation of BLIMP-1 leads to its proteasomal degradation. BLIMP-1 is one of the master regulators of plasma cell differentiation. BLIMP-1 tightly regulates the balance between the germinal centre (GC) B cells and plasma cells (PCs), where BLIMP-1 represses the pro-germinal centre transcription factors, such as Pax5 and Bcl6 (Shapiro-Shelef and Calame, 2005). BLIMP-1, however, is in turn suppressed by important GC transcriptional factors and is additionally regulated by SUMOylation. SUMOylation of BLIMP-1 leads to its proteasomal degradation and therefore to a decreased repression of BLIMP-1 targets. This was shown in an *in vitro* SENP1 knockout, which results in deSUMOylation defects. Shimshon *et al.* (2011) could also display that an increase in SENP1 led to a stabilisation of BLIMP-1.

Ying et al. (2012), using BLIMP-1 SUMOylation consensus site mutations, could also demonstrate the importance of SUMOylation in plasma cell differentiation. They could show that Lys816 is the SUMO target lysine on BLIMP-1 and by site mutagenesis of Lys into Arg they observed a lack of BLIMP1 SUMOylation and

further a decrease in IgM secretion, a decrease in the repression of *Pax5*, *Ciita*, *Bcl2a1* and *Xbp1* and a decrease in plasma cell development.

#### 1.4.5 Regulation of senescence

P53, being the most well known tumour suppressor gene and cell cycle regulator has been known to be regulated through SUMOylation (Rodriguez et al., 1999) as well as ubiquitination (Bode and Dong, 2004). The physiological dead end of a cell, senescence, is highly regulated by p53, other tumour suppressors and cell cycle regulators. In 2008 Yates *et al.* illustrated that PIASy, a SUMO ligase, increases during replicative senescence. It was also shown that overexpression of PIASy or overexpression of SUMO2/3 could induce premature senescence through increase of SUMOylated p53 and retinoblastoma protein (p105<sup>Rb</sup>, as well a tumour suppressor gene) (Li et al., 2006). The responsible deSUMOylation proteases for p53 regulation were shown, in RNAi studies, to be SENP1, SENP2 and SENP7. Again, the increased SUMOylation by defective deSUMOylation induced replicative senescence and underlines the importance of SUMO in cell cycle regulation, apoptosis and senescence.

#### 1.4.6 PML and nuclear body formation

Promyelocytic leukaemia protein (PML) nuclear bodies (NBs) are spheres of 0.1–1.0 µm in diameter and are found mainly in the nucleus of most cell types (Seeler and Dejean, 1999; Zhong et al., 1999). PML NBs are matrix-associated protein complexes that recruit large varieties of more than 100 different proteins, with the SUMOylated PML building the shell of the NBs (Johnson, 2004). The assembled nuclear factors are in the core of the complex and can be themselves SUMOylated, their only common feature seems to be their ability to be SUMOylated (Bernardi and Pandolfi, 2007).



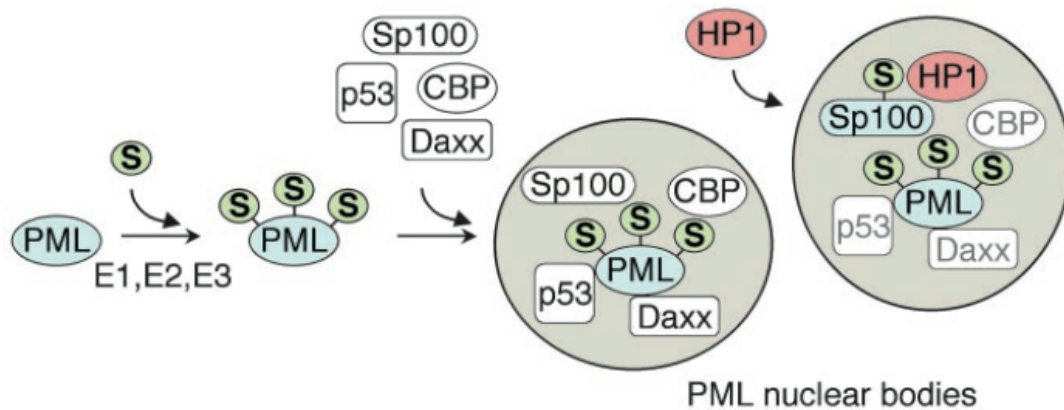


**Figure 1-5: Assembly of the Promyelocytic leukaemia protein (PML) nuclear bodies (NB).** PML is SUMOylated on three different lysines. This recruits a variety of different proteins to form the nuclear body (NB). The assembled proteins can also be SUMOylated to attract other binding partners such as HP1 (Johnson, 2004).

PML NBs regulate a multitude of nuclear functions, such as DNA replication, transcription, or epigenetic silencing (Stuurman et al., 1990). NBs themselves are regulated by cellular stress derived from viral infection (Everett et al., 2006), DNA-damage (Gurrieri et al., 2004; Koken et al., 1995; Terris et al., 1995), and oxidative stress (Villagra et al., 2006). The expression of PML and NB associated proteins is controlled by interferon  $\alpha$ ,  $\beta$  or  $\gamma$ , but also by p53 (de Stanchina et al., 2004), which regulate the number and the size of the NBs.

The function of PML NBs itself is not very clear at this stage, one hypothesis states that NBs provide an accumulation or storage unit of nuclear factors, readily available or that NBs provide a space for specific modifications or assembly of transcription factors. PML SUMOylation plays a critical role in the recruitment of partners proteins and is essential for normal morphology of NBs as seen in *Ubc9*<sup>-/-</sup> cells, which display strong defects in the formation of NBs (Nacerddine et al., 2005). SUMOylated proteins in the NB complex can then again recruit new protein partners. It is believe that SUMO acts as a form of glue or net to hold the NB complex together. This is based on the fact that mutations in single SUMO consensus motif or binding sites may not always lead to defects in form or function of the NB (Johnson, 2004), suggesting that SUMOylation in general is necessary, but small defects can be compensated and are redundant. SUMO seems not to be

fundamental for PML aggregation, however it is important for the recruitment of protein partners.

Despite the strong influence and regulatory effects of PML NBs on the cell, NBs are dispensable for most basic biological functions as *Pml*<sup>-/-</sup> mice survive without major physiological problems (Johnson, 2004).

It is interesting to note the amount of p53 modifying enzymes that are present in the PML NBs which are all SUMOylated (e.g. CBP, HDM2, HIPK2, and HAUSP). Hence, it is not surprising that a major function of PML NBs is the regulation of senescence by a pathway involving p53 enhancement through acetylation, SUMOylation, and phosphorylation (Bischof et al., 2002; Bischof et al., 2005; Mallette et al., 2004).

#### 1.4.7 *SENP1 in Transcription*

66% of all SUMO targets are transcription factors (Dohmen, 2004; Zhao, 2007), where SUMOylation mainly results in their repression and deSUMOylation by SENPs leads to the relieve of transcriptional repression. Modification of transcription factors can be divided into two groups: transcription factors that are bound in or modified by PML NBs, as described above, or transcription factors that are bound at a specific promoter and are suppressed by SUMOylation. It has been shown that transcription factors, such as Elk-1, SP-3 or STAT-1 (Ross et al., 2002; Saitoh et al., 1998; Ungureanu et al., 2003), with mutated SUMOylation sites, and therefore unable to be SUMOylated, have an increased transcriptional activity on the respective promoter. It has further been shown that binding SUMO to the DNA binding motif of a transcription factor reduces the transcriptional activity on the promoter (Ross et al., 2002; Yang et al., 2003).

Transcriptional repression by SUMO can also be indirect. SUMOylated HDAC6 for example binds the repressor domain of p300, whereas RNAi knockdown of HDAC6 inhibits the transcriptional repression and p300 can be expressed (Girdwood et al., 2003). Also HDAC1 and HDAC4 are SUMOylated and thereby repress transcription (David et al., 2002; Kirsh et al., 2002; Petrie et al., 2003).

In contrast to the vast majority of transcriptional repression, SUMO can also increase transcriptional activity for example in HSF1 and HSF2, whose DNA binding is increased through SUMOylation after heat shock *in vitro* (Goodson et al., 2001; Hong et al., 2001).

#### 1.4.8 *SENP1 in DNA repair*

There are seven DNA repair mechanisms reacting to all kinds of different damage done to DNA. SUMOylation has been shown to regulate or to be involved in repair mechanisms such as non-homologous end joining (NHEJ), homologous recombination (HR), base-excision repair (BER) and nucleotide-excision repair (NER). The failure to recognize or respond to DNA damage may result in apoptosis or chromosomal rearrangement, which may lead to tumorigenesis (Jeggo and Lobrich, 2007).

The most well understood involvement of posttranslational modification in DNA repair is the ubiquitination and SUMOylation of mammalian and yeast proliferating cell nuclear antigen (PCNA). PCNA is mono- and poly-ubiquitinated at Lys164 and SUMOylated also on Lys164 and additionally on Lys127 (Hoegge et al., 2002). PCNA is a homotrimeric ring like structure that encircles and moves along the DNA forming a base for polymerases and other factors involved in replication and repair (Moldovan et al., 2007). The four different modification alternatives each lead to different functions of PCNA.

PCNA ubiquitination and SUMOylation both occur during S-phase of the cell cycle. PCNA, however, is monoubiquitinated in response to DNA damage during faulty replication and then mediates translesion synthesis (TLS) to repair damaged sites. This repair mechanism is very error prone and in case of incorrect repair PCNA is then polyubiquitinated, which switches the repair mechanism to an error free recombination related pathway. Details and specific factors of this pathway still have to be elucidated (Bienko et al., 2005; Friedberg et al., 2005; Kannouche et al., 2004).

SUMOylation of PCNA only occurs at Lys164 and Lys127 and takes place in yeast and in birds. SUMOylation of Lys164 leads to Srs2 recruitment to PCNA which

subsequently regulates recombination through Rad51 (Papouli et al., 2005; Pfander et al., 2005). In contrast, Lys127 SUMOylation prevents binding of factors that interact with PCNA, such as Eco1 which establishes sister chromatid cohesion in S-phase (Moldovan et al., 2006).

BRCA1, being a E3 ubiquitin ligase and a very prominent oncogene in breast cancer development (Lorick et al., 1999), has been shown to be negatively regulated by SUMO-1, by direct *Brca1* promoter repression (Park et al., 2008). It was also shown that regulated through PIAS1 and PIAS4 SUMO-1 co-localizes with BRCA1 and  $\gamma$ H2AX, a chromatin marker for DNA damage, in response to endogenous genotoxic stress and that this co-localisation is required for DNA DSB repair (Mabb et al., 2006; Morris et al., 2006).

An important molecule in non-homologous end joining (NHEJ) repair mechanism of DSBs is XRCC4. This is in the presented thesis of interest as NHEJ is the major repair mechanism in V(D)J recombination of the rearranged B cell and T cell receptor (Lieber et al., 2004; Rooney et al., 2004). XRCC4 builds complexes with itself and with DNA ligase IV (Critchlow et al., 1997; Modesti et al., 2003). It has been reported by Yurchenko et al. (2006) that a decrease of the SUMOylation capacity of XRCC4 also decreases V(D)J recombination and a sensitivity to DNA DSBs in CHO.XR-1 cells. Other factors that are SUMOylated in NHEJ are Ku70 (Golebiowski et al., 2009; Yurchenko et al., 2008), which is protected from proteasomal degradation through SUMO and LIF1, which has an important regulatory function in NHEJ (Vigasova et al., 2013).

Further SUMOylated proteins in DNA damage repair are topoisomerases (Azuma et al., 2003; Jacquiau et al., 2005), base excision glycosylase TDG (Hardeland et al., 2002; Steinacher and Schar, 2005), Rad 51 (Shen et al., 1996b), Rad52 (Shen et al., 1996b), Ku80 (Gocke et al., 2005) and BLM helicase (Eladad et al., 2005).

#### *1.4.9 SUMO and NEMO in response to genotoxic stress, V(D)J and class switch recombination*

V(D)J recombination in B and T cell receptors are essential for lymphocyte development. During RAG1 induced V(D)J recombination DSBs are induced and

repaired by NHEJ, as mentioned above. In class switch recombination (CSR), where the isotype of a mature immunoglobulin is switched in response to B cell stimulation, the same process takes place, however regulated and induced by AID. Both processes take place in the G1 phase of the cell cycle.

As DSBs possess a possible threat to a cell the DNA damage response mechanism is activated to repair the damage. This response is orchestrated through the ataxia telangiectasia mutated (ATM) serine threonine kinase and further by the p53 induced transcriptional program (which induces apoptosis or senescence in response to extensive DNA damage). ATM in turn needs to be activated in the nucleus by NEMO (an IKK complex regulatory subunit of the NF- $\kappa$ B pathway, also known as IKK $\gamma$ ), whereas NEMO needs to be SUMOylated for nuclear transport (Huang et al., 2003). This was shown as SUMOylated NEMO accumulates in the nucleus upon genotoxic stress signals and that the inactivation of NEMO SUMOylation sites results in inhibition of NF- $\kappa$ B activation. However the dependence of SUMO for the NF- $\kappa$ B activation is only in respect to genotoxic stress and not generally essential for other NF- $\kappa$ B pathways, such as induction through TNF $\alpha$  or LPS (Huang et al., 2003; Wuerzberger-Davis et al., 2007).

It was further shown that NF- $\kappa$ B activates SENP1 and SENP2 expression upon genotoxic stress and that mainly SENP2 is responsible for NEMO deSUMOylation (Lee et al., 2011). The transcriptional activity is modulated through ATM-dependant histone methylation of the SENP promoter regions and subsequent NF- $\kappa$ B recruitment (Lee et al., 2011). Lee et al. (2011) propose a negative feedback loop of genotoxic stress induced NF- $\kappa$ B dependant SENP1 and SENP2 induction, which in turn inhibits NF- $\kappa$ B induced cell survival responses. However, this mechanism has only been shown in response to exogenous DNA damaging agents, it is still unclear how this mechanism reacts in the situation of endogenous RAG and AID induced DNA damage in V(D)J and class switch recombination. The significance of SENP2 is also not clear as SENP2 is mainly located in the nucleus at the nuclear core complex, however NEMO needs to be SUMOylated to translocate into the nucleus (Hoeller et al., 2006), implicating its SUMOylation to take place in the cytoplasm.

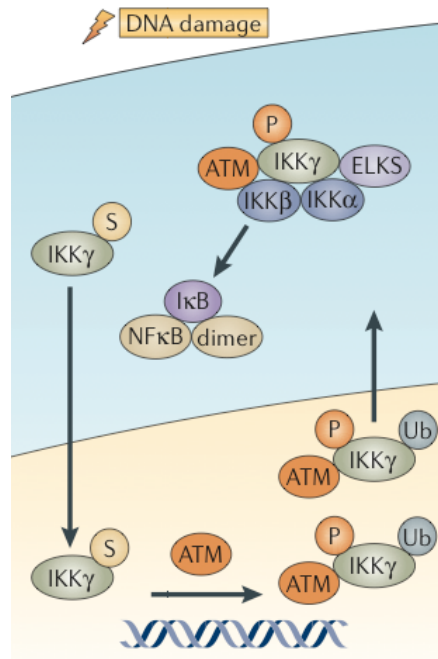


**Figure 1-6: Interplay of IKK $\gamma$  (NEMO) and ATM in response to DNA damage.** In response to DNA damage events NEMO is SUMOylated in the cytoplasm and translocated into the nucleus. At the same time ATM is phosphorylated and then co-localizes with NEMO. This leads to NEMO phosphorylation, ubiquitination and deSUMOylation. The p-Ub-NEMO-ATM complex then shuttles to the cytoplasm where it interacts with the IKK complex to activate NF- $\kappa$ B signalling. (Adapted from Hoeller et al. (2006))

#### 1.4.10 SENP1 in cancer

The most prominent example for the involvement of SUMO, especially SENP1, in cancer development is the regulation of androgen receptor (AR) and four of the AR co-receptors, SRC-1, SRC-2, p300 and HDAC1 by SUMO-1 (Matic et al., 2008). SUMOylation of AR is furthermore regulated by androgen itself, as expression of SENP1 is regulated through an androgen response element in the promoter region of the SENP1 gene. As androgen receptor signalling is one of the most important factors of prostate cancer development, SUMOylation of AR and its co-receptors may play a large role in tumourigenesis. And indeed a study by Hurley, Lee and Prag (Hurley et al., 2006) found a SENP1 overexpression in 50 % of high-grade prostatic intraepithelial neoplasias (PIN) and in prostate cancer in over 100 observed cases. They could similarly observe in mouse models that SENP1 transgenic mice developed an increased proliferation of prostate epithelial cells.

Besides prostate cancer, SENP1 was found to be 2-fold overexpressed in thyroid oncocytic tumours (Jacques et al., 2005).

## 1.5 Rationale & Aims

Our laboratory investigates various aspects of the adaptive immune response with interests in the humoral B cell response and B cell development, in connection with effects of ubiquitination on NF- $\kappa$ B signalling. It was recently discovered how SUMOylation, a close relative to ubiquitination, regulates early B cell development through its modification of STAT5 (Van Nguyen et al., 2012) and plasma cell differentiation through modification of BLIMP-1 (Shimshon et al., 2011; Ying et al., 2012). However, no B cell specific *in vivo* analyses have so far been published, hence it was decided to obtain the SENP1 conditional knockout from the Wang Min Lab in Yale and cross it to the CD19-Cre strain to generate a B cell specific conditional knockout mouse model.

The aims of this thesis were the phenotypic analysis of the conditional SENP1 knockout in B cells. As it was reported by Shimshon et al. (Shimshon et al., 2011) in *in vitro* analyses SUMOylation regulates BLIMP-1 degradation, therefore it is hypothesised that defective deSUMOylation in the SENP1<sup>ff</sup> CD19-Cre mice will lead to a decrease in nuclear BLIMP1 and therefore, in an inability of activated B cells to undergo plasma cell differentiation. However, as SUMO regulates many different transcription factors involved in B cell development, apoptosis, senescence, in class switch recombination, and in proliferation, the expected range of phenotypes and cellular disorders is very high.

Furthermore, as SENP1 and SENP2 share many of their targets for deSUMOylation it was aimed to generate a conditional SENP2 knockout mice for comparative studies between SENP1 and SENP2.

## 2. Materials and Methods

### 2.1 Chemical and Biological Material

Chemicals were purchased from Sigma (Steinheim), Fluka Chemie (Switzerland), Merck (Darmstadt) or AppliChem (Darmstadt) unless stated otherwise. Solutions were prepared with double distilled water (ddH<sub>2</sub>O). Bacterial media were autoclaved prior to use. Sterility of solutions and chemicals used in cell culture was maintained by working under a sterile hood (Heraeus, Germany).

**Table 2-1: List of chemical substances**

Substance	Supplier
Agar	Life Technologies, Darmstadt
Agarose, electrophoresis grade	AppliChem, Darmstadt
Ampicillin	Sigma-Aldrich, Steinheim
Bovine serum albumine (BSA)	Sigma-Aldrich, Steinheim
Chloroform	Merck, Darmstadt
Dimethylsulfoxide (DMSO)	Merck, Darmstadt
Dithiothreitol (DTT)	Boehringer GmbH, Mannheim
dNTPs	Pharmacia Biotech, USA
Ethanol, abs.	AppliChem, Darmstadt
Ethidium bromide	Sigma-Aldrich, Steinheim
Ethylenediamine tetraacetate (EDTA)	Sigma-Aldrich, Steinheim
Fetal calf serum (FCS)	Boehringer GmbH, Mannheim
Ficoll 400	Amersham Pharmacia, Freiburg
Glacial acetic acid	Sigma-Aldrich, Steinheim
Hydrochloric acid (37%)	Merck, Darmstadt
Isopropanol	AppliChem, Darmstadt
Magnesium chloride	Sigma-Aldrich, Steinheim
$\beta$ -Mercaptoethanol ( $\beta$ -ME)	Sigma-Aldrich, Steinheim
Mineral oil	Sigma-Aldrich, Steinheim
Phenol	Sigma-Aldrich, Steinheim
Potassium chloride	Merck, Darmstadt
Potassium hydrogenphosphate	Merck, Darmstadt



Proteinase K	Roche, Switzerland
Sodium azide	Sigma-Aldrich, Steinheim
Sodium carbonate	Sigma-Aldrich, Steinheim
Sodium chloride	AppliChem, Darmstadt
Sodium citrate	Sigma-Aldrich, Steinheim
Sodium dodecyl sulfate	AppliChem, Darmstadt
Sodium hydrogen carbonate	Sigma-Aldrich, Steinheim
Sodium hydrogenphosphate	Sigma-Aldrich, Steinheim
Sodium hydroxide	Sigma-Aldrich, Steinheim
Tris base	Sigma-Aldrich, Steinheim
Tween 20	Sigma-Aldrich, Steinheim

## 2.2 Molecular Biology

### 2.2.1 Competent cells and isolation of plasmid DNA

Competent *Escherichia coli* (*E. coli*) DH5 $\alpha$  cells were prepared according to the protocol of Inoue *et al.* (Inoue *et al.*, 1990) and used in heat shock transformation of plasmid DNA. DNA ligation was performed with the Takara DNA ligation Kit (Takara, Japan) according to the manufacturer's instructions. Plasmid DNA was isolated from transformed *E. coli* DH5 $\alpha$  bacteria with an alkaline lysis method (QIAGEN, Hilden, Germany). The procedure was performed according to the protocol of Zhou *et al.* (Zhou *et al.*, 1990). Plasmid DNA of higher purity was obtained with QIAGEN columns (QIAGEN, Hilden, Germany) following the supplier's instructions.

### 2.2.2 Plasmid cloning

For molecular cloning of plasmids restriction enzymes and CIP phosphatase from New England Biolabs and T4 DNA Ligase from Invitrogen were used according to manufacturers instructions. Additionally In-Fusion<sup>®</sup> HD Cloning Kit (Clontech Laboratories Inc, Mountain View, CA) and Phusion Flash High-Fidelity PCR Master Mix (Thermo Scientific) was used. Primers with specific In-Fusion<sup>®</sup> sequences are listed in Table 2-2. Restriction enzymes used for plasmid linearization and subsequent insertion of exon 3, left arm of homology and right arm of homology were Sall, NotI and XhoI respectively. Cloning techniques were applied according to Sambrook

(Sambrook and Gething, 1989). Sequencing was performed by Genterprise (Mainz) with self made primers (Table 2-3)

**Table 2-2: Sequences for primers used in cloning. Red letters mark In-Fusion<sup>®</sup> sequence**

Name	Sequence (5'-3')
<b>Exon 3</b>	
CR SENP2 Ex3 for	CGG CCC TAG AGT CGA CGC TCA CTG ATG CCG GTG GTG CC
CR SENP2 Ex3 rev	ACG AAG TTA TGT CGA CGC CAG AAC GGC GCA GAG GCA GGT GTA TCT CTG TGA G
<b>Left arm of homology</b>	
CR SENP2 LA for	ATG GCC ATA GCG GCC GCG GAT GTG TCC TGG CCA GCC
CR SENP2 LA rev	TAT GGA TCC GCG GCC GCG ATA TCA CTC ACA TTC ACT CAC TAG TTT GCC C
<b>Right arm of homology</b>	
CR SENP2 RA for	CGG CCG CCA CCT CGA GCT TCT GAG TGC TGA GAT TAA AGG TG
CR SENP2 RA rev	AAC CAC ACT GCT CGA GGG CCA ATGT ACA GAG AAT AAG TGA C

**Table 2-3: Primer for sequencing of cloning products**

Name	Sequence (5'-3')
<b>Exon 3</b>	
CR SENP2 Ex3 Seq1	GCT TCT GAG GCG GAA AGA ACC
CR SENP2 Ex3 Seq2	GTT GTA CTG TGA CTT GTC TGT GG
CR SENP2 Ex3 Seq3	CCA TGG TGT CTT CTG CTT GTA ATG G
<b>Left arm of homology</b>	
CR SENP2 LAH Seq1.rev	GAC ACT GGC CCT AAA GAC AGA C
CR SENP2 LAH Seq1.1	GGG TAT AGG GGT CGG GAG AC
CR SENP2 LAH Seq1	GAC CAT GAT TAC GCC AAG CGC
CR SENP2 LAH Seq2	GAC CAT GAT TAC GCC AAG CGC
CR SENP2 LAH Seq3	CAG ACA ATG AGA AGT TTC CTC TTT CCT G
CR SENP2 LAH Seq4	CCT GGC TAA CAG CCT GTG GC
CR SENP2 LAH Seq5	GCC ATC ACA CCC CAG TAA AGA GC
CR SENP2 LAH Seq6	GCT GTG CAG GGA GTG AGG AAG

<b>Right arm of homology</b>	
CR SENP2 RAH Seq1	CTC ACA GAG ATA CAC CTG CCT CTG C
CR SENP2 RAH Seq1.rev	GAC ACT GGC CCT AAA GAC AGA C
CR SENP2 RAH Seq1.1	GCA TAT TTG AGA GCC AGC CAG ATG
CR SENP2 RAH Seq1.2	GCC TTA GGG GCG TCG AC
CR SENP2 RAH Seq1.3	GCT CAC TTT GTA GAC CAG GCT G
CR SENP2 RAH Seq2	GCA CAA GAG CTG GGT AGA TAT CTA C
CR SENP2 RAH Seq2.1	GCC TTA AAC AGC ACA AGA GCT G
CR SENP2 RAH Seq2.2	GGG TTT CTA CTC TGC CTT TGA C
CR SENP2 RAH Seq2.3rev	CCT GTA AAA ACC TGA TAC TGA TGC C
CR SENP2 RAH Seq3	GAC TGG CCT CGA ACT CAG AAA TCC
CR SENP2 RAH Seq4	GGA AGG ATG TTT AAC CCA GAG CTC
CR SENP2 RAH Seq5	GAG GAA AGC TCA GCA GAG GC
CR SENP2 RAH Seq6	CAG TCT CTT CAG TCA AGT TGG CAC
CR SENP2 RAH Seq7	GCT TTA GTT CTA CAT GTA AGT AAG CTT TC
CR SENP2 RAH Seq8	GAT CAT GTT CAT CTC CAA CTT CTC CT

### 2.2.3 Isolation of genomic DNA from mouse organs

Cells or tail biopsies were lysed over night (o/n) at 56°C in lysis buffer (10 mM Tris- HCl, pH 8; 10 mM EDTA; 150 mM NaCl; 0.2% (w/v) SDS) and 400 mg/ml proteinase K. Undigested tissue was pelleted by centrifugation and the supernatant was mixed with an equal volume of isopropanol for genomic DNA precipitation. Finally, DNA was retrieved by centrifugation, washed twice in 70% (v/v) EtOH, dried at RT, and resuspended in dH<sub>2</sub>O

### 2.2.4 Isolation of genomic DNA from ES cells

ES cells were grown on 96 well tissue culture plates. DNA was extracted according to the protocol of (Pasparakis & Kollias, 1995, Torres & Kühn, 1997).

### 2.2.5 Polymerase Chain Reaction (PCR)

PCR (Mullis and Faloona, 1987; Saiki et al., 1988) was used to screen mice and ES cells for the presence of targeted alleles or transgenes and to amplify fragments for sequencing (primers shown in Table 2-3 and Table 2-4). Reactions were

performed in Triothermocyclers (Biometra, Göttingen, Germany). Genotyping of mice and ES cells was generally performed in a total volume of 20  $\mu$ l in the following reaction mix: 50 pmol of each primer, 1.5 U of *Thermus aquaticus* (Taq) DNA polymerase (Sigma), 250 mM dNTPs, 10 mM Tris-HCl pH 8.3, 50 mM KCl, 2.5 mM MgCl<sub>2</sub>, 100 ng template DNA. Amplification started with denaturation for 10 min at 94 °C followed by 30-35 cycles of denaturation, annealing and elongation at 94 °C for 30 sec, 52-60 °C for 30 sec, 72 °C for 30 sec respectively. Finalising extension step at 72 °C for 10 min.

**Table 2-4: Primer sequences for genotyping**

Name	Sequence (5'-3')	T <sub>m</sub> (°C)
Senp1loxF	AGG AAG GCA TAG AAG TTA CTC TA	61
Senp1loxR	GGT TGC TAC TAT AGT CAG ACT G	61
Senp1CreWtF	CCT GGG AGT GCT TGC AAG ATA	61
Senp1CreWtR	CAT TGT CCA TTT GCA CTT TGA CC	61
Senp1CreKoF	AGG AAG GCA TAG AAG TTA CTC TA	61
Senp1CreKoR	CAC TAT CTC AGT CTC ATC CTG T	61
CD19c	AAC CAG TCA ACA CCC TTC C	58
CD19d2	CCA GAC TAG ATA CAG ACC AGG A	58
CD19cre7	TCA GCT ACA CCA GAG ACG G	58
Allg-Cre For	GGA CAT GTT CAG GGA TCG CCA GGC G	58
Allg-Cre Rev	GCA TAA CCA GTG AAA CAG CAT TGC TG	58
Allg-Actin For	TGT TAC CAA CTG GGA CGA CA	58
Allg-Actin Rev	GAC ATG CAA GGA GTG CAA GA	58
Rosa 1	AAA GTC GCT CTG AGT TGT TAT	58
Rosa 2	GGA GCG GGA GAA ATG GAT ATG	58
Rosa 3	CAT CAA GGA AAC CCT GGA CTA CTG	58

### 2.2.6 Agarose gel electrophoresis and DNA gel extraction

Separation of DNA fragments by size was achieved by electrophoresis in agarose gels (0.8% - 2% (w/v); 1x TAE (Sambrook and Gething, 1989); 0.5 mg/ml ethidium bromide). DNA fragments were recovered from agarose gel slices with either the QIAEX II or the QIAquick Gel Extraction Kit (QIAGEN, Hilden, Germany) following the manufacturer's instructions.

### 2.2.7 DNA & RNA quantification

The concentration of nucleic acids was determined by measuring the absorption of the sample at 260 nm and 280 nm, respectively, in a spectrophotometer. An OD<sub>260</sub> of 1 corresponds to approximately 50 µg/ml for double stranded DNA or 40 µg/ml for RNA and single stranded DNA. Purity of nucleic acids was estimated by the ratio OD<sub>260</sub>/OD<sub>280</sub>, with 1.8 and 2.0 optimal for DNA and RNA, respectively.

### 2.2.8 Southern blot analysis

Digestion of 5-15 µg DNA was performed overnight with 50-100 U of the appropriate restriction enzyme (EcoRI, EcoRV and BglI for Exon 3, left arm of homology and right arm of homology, respectively). Subsequently, the DNA fragments were separated by agarose gel electrophoresis and transferred onto Hybond<sup>TM</sup>-N+ (Amersham, Illinois, USA) nylon membranes by an alkaline capillary transfer according to the method of (Chomczynski and Qasba, 1984). Membranes were baked at 80°C for 1 h to cross-link the DNA to the membrane, equilibrated in 2x SSC (Sambrook and Gething, 1989) and then prehybridised at 65 °C for 4 h in hybridisation solution (1 M NaCl, 1% (w/v) SDS, 10% (w/v) dextran sulfate, 50 mM Tris-HCl pH 7.5, 250 µg/ml sonicated salmon sperm DNA). The radioactively labelled probe (Table 2-5) was added to the hybridization solution and allowed to hybridize at 65 °C for 10 h in a rotating cylinder

**Table 2-5: Primer sequences for Southern blot probes**

Name	Sequence (5'-3')	T <sub>m</sub> (°C)
<b>Exon 3</b>		
CR SENP2 Sonde1 EcoRI for	GCG ACT ATC CAA AGA TCA GAG TG AC	57
CR SENP2 Sonde1 EcoRI rev	GGC CAA TGT ACA GAG AAT AAG TGA	56
<b>Left arm of homology</b>		
CR SENP2 Sonde1 EcoRV for	GGA CAG GAG AGA TGG ACA GAC GGC	63
CR SENP2 Sonde1 EcoRV rev1	GCT TCC CCT GGC TTG CTC AGC CTG	64
<b>Right arm of homology</b>		
CR SENP2 Sonde5 BglI for	ACACAAAGCCAGTCTCAATACAAATGTA GGAAGAT	60
CR SENP2 Sonde5 BglI rev	CAA GGA GGC TGG AGA GAT TGC TCA ATT TAA	60

Aliquots of 50 ng DNA of the above probes were radioactively labelled with 2.5 µCi [<sup>32</sup>P]dATP (Amersham, Braunschweig, Germany) using the Ladderman™ Labelling Kit (Takara, Japan), based on the principle of random primed oligolabelling (Feinberg and Vogelstein, 1984). Unincorporated radiolabeled nucleotides were removed with Illustra MicroSpin G-25 Columns (GE Healthcare) to reduce background during hybridisation. The probe was denatured at 90°C for 5 min., cooled on ice for 5 min., and then added to 10ml hybridization solution. After hybridisation over night, stringent washes were initially performed twice in 2x SSC / 0.1 % (w/v) SDS and then followed by washes in 1x SSC / 0.1 % (w/v) SDS and 0.5x SSC / 0.1 % (w/v) SDS, if necessary. All washes were performed at 65 °C by rotation for 10-30 min. After each wash, the membrane was monitored with a Geiger counter and wash steps were stopped when specific signals reached 50 to 200 cps. The membrane was sealed in a plastic bag and exposed to X-ray film (BioMAX MS; Eastman Kodak) at -80°C. Films were developed in an automatic developer.

### 2.2.9 Quantitative real time PCR

RNA from mouse B cells and mouse embryonic fibroblasts (MEFs) was prepared using the RNeasy mini kit (QIAGEN, Hilden, Germany) according to the

manufacturer's protocol. DNA was removed by DNaseI digestion (Promega, Mannheim, Germany). cDNA synthesis of 5 µg total RNA was performed as described in superscript II protocol (GIBCO, Karlsruhe, Germany). cDNA was subsequently used for RT- and Real-Time PCR. Quantitative Real-Time PCR was performed using primers from QIAGEN as described on their homepage <https://www1.qiagen.com/GeneGlobe/Default.aspx> or with self designed primers.

**Table 2-6: List of qRT-PCR primers. Self-designed and commercial**

Primer Mix	Sequence (5'-3')	Supplier
<b>Senp1/1</b>		
SENP1 NorthProb Ex13/14 For	CCA TCT AAA CTG GCT CAA TGA TGA GAT CAT C	Home made
SENP1 NorthProb Ex14/15 Rev	CCT TCT AAA GTC TAC AAC AGC TAG ACA CC	Home made
<b>Senp1/4</b>		
sSENP1 ExS1 For	GTC ATG GAT CTG CTC TCT AGC AG	Home made
sSENP1 ExFL10/11 Rev	GAG AGT CAT AAA CGC TAG TTA ATT CTT TGA TC	Home made
<b>Senp1/5</b>		
sSENP1 ExS1 For	GTC ATG GAT CTG CTC TCT AGC AG	Home made
sSENP1 ExS5/6 Rev	CCA TTT CCT CTG TAA TTT CAG GAA ATT CG	Home made
Senp1	-	Quiagen
Senp2	-	Quiagen
SUMO1	-	Quiagen
<i>Stat3</i>	-	Quiagen
<i>Stat5</i>	-	Quiagen
<i>Tftp</i> (E2A)	-	Quiagen
<i>Pax5</i>	-	Quiagen
<i>PU.1</i>	-	Quiagen
<i>Bcl6</i>	-	Quiagen
<i>Irf4</i>	-	Quiagen
<i>Xbp1</i>	-	Quiagen
<i>Mitf</i>	-	Quiagen
<i>Stat3</i>	-	Quiagen
<i>Prdm1</i> (Blimp1)	-	Quiagen

## 2.3 Cell Biology

### 2.3.1 Embryonic stem cell culture

All gene targeting experiments were performed in V6.5 and JM8 ES cells. Culturing and transfection of ES cells was performed according to published protocols (Pasparakis & Kollias 1995, Torres & Kühn 1997). To maintain the pluripotency of the ES cells, they were cultured in ES cell medium in the presence of leukaemia inhibiting factor (LIF) on a layer of embryonic feeder (EF) cells. The ES cell medium (DMEM, 15% (v/v) FCS, 1 mM sodium pyruvate, 2 mM L-glutamine, 1 x non essential amino acids, 1:1000 diluted LIF supernatant, 0.1 mM 2- $\beta$ -mercaptoethanol) contained FCS that had been tested to promote ES cell growth and to prevent *in vitro* differentiation (Gibco, Karlsruhe, Germany). ES and EF cells were grown in tissue culture dishes (Falcon, Bedford, USA) and kept at 37°C under humid atmosphere with 10% CO<sub>2</sub>. EF cells in DMEM supplemented with 10% (v/v) FCS, 1 mM sodium pyruvate, 2 mM L-glutamine, were never passaged more than three times and then mitotically inactivated by mitomycin C treatment (10  $\mu$ g/ml for 2 h), before seeding with ES cells. ES cell colony growth was stopped before they became confluent. Colonies were washed twice with PBS and then treated shortly with trypsin (0.05 % (w/v), 0.02 % (v/v) EDTA in PBS; Gibco, Karlsruhe, Germany) at 37°C, until the cells detached from the dish. The cell suspension was then used for passaging, transfection or freezing. ES cells were frozen in 90% (v/v) FCS, 10% (v/v) DMSO at -80°C and later transferred into liquid nitrogen for long-term storage. For transfection,  $1 \times 10^7$  ES cells were mixed with 30 to 40  $\mu$ g DNA in 800  $\mu$ l transfection buffer (RPMI w/o phenol red, Gibco, Karlsruhe, Germany) and electroporated at 23°C (500 mF, 240 V). After 5 minutes of incubation, ES cells were transferred onto an embryonic feeder layer and 48 h later placed under G418 (300  $\mu$ g/ml, 71% active) selection. Selection against HSV-*tk* containing random integrants started at day five after transfection by supplementing the medium with 2 mM ganciclovir (Cymeven, Syntex). On approximately day 9 after transfection, double resistant colonies were picked and split into EF-containing 96-well tissue culture dishes for expansion.



Specific deletion of the *loxP* flanked exon 3 of the *Senp2* gene and FRT flanked *neo* selection marker cassette from targeted ES cells was achieved by transiently transfecting 30 µg of the Cre-expressing plasmid pGKCre. Three days after transfection, colonies were isolated as single clones, trypsinised and separated into a master and a duplicate 96-well plate. Cells in the duplicate plate were incubated with 900 µg/ml G418, which induced cell death in G418-sensitive clones. Sensitive clones were then recovered and expanded from the master plate.

### 2.3.2 Preparation of cells from lymphoid organs

Spleen, lymph nodes and Peyer's patches were removed from mice and passed through a sterile sieve to obtain single cell suspensions. Bones were flushed with PBS containing 10% (v/v) FCS to extract bone marrow. Erythrocytes were lysed from the spleen and the bone marrow in 140 mM NH<sub>4</sub>Cl, 17 mM Tris-HCl pH 7.65 for 2 min at room temperature. To obtain lymphocytes from the peritoneal cavity the latter was flushed with a syringe with 8 ml PBS containing 10% (v/v) FCS.

### 2.3.3 Magnetic cell sorting and FACS sorting

Specific cell populations were either sorted or depleted from a heterogeneous cell suspension by magnetic cell sorting (MACS; Miltenyi Biotec, Bergisch Gladbach, Germany). Cell populations were labelled with antibody-coupled microbeads (10 µl beads, 90 µl PBS-BSA-N<sub>3</sub> per 1x10<sup>7</sup> cells) and separated on LS MACS columns in a magnetic field (Miltenyi et al., 1990). For cell sorting by FACS, B cells were first purified by MACS and then stained with antibodies against various cell surface markers. B cells of individual B cell subsets were then sorted using FACSAria™ (Becton Dickinson, Franklin Lakes, USA). The purity of isolated populations was subsequently tested by FACS analysis: MACS-isolated B cells were normally >95% pure and sorted B cell subpopulations were >98% pure. FACS sorting was performed with the help of Sebastian Attig and Alexander Hohberger (Flow Cytometry Core Facility of the 3rd Medical Clinic of the University Medical Center, Mainz, Germany).

### 2.3.4 Cell counting

Viable cells were assessed using the trypan blue dye exclusion test and counted using a Neubauer chamber (Assistent, Sondheim, Germany). To this end, an aliquot of the cell suspension was diluted with physiological trypan blue solution (Gibco, Long Island, NY, USA). Dead cells are stained blue whereas live cells cannot take up the dye due to their intact membrane. After counting 16 single quadrants, the counted cell number (N) was multiplied by the dilution factor (V) and the 'chamber factor' ( $1 \times 10^4$ ) resulting in the number of live cells per ml ( $N \times V \times 1 \times 10^4 = \text{cell number/ml}$ ).

### 2.3.5 Flow Cytometry

Single cell suspensions were prepared from all tested organs as in 2.3.2.  $1 \times 10^6$  cells per sample were surface stained in 25  $\mu\text{l}$  PBS, 0.1% (w/v) BSA, 0.01% (w/v)  $\text{NaN}_3$  with combinations of fluoresceine isothiocyanate (FITC), phycoerythrine (PE), Peridinin-Chlorophyll (PerCP), tandem fluorochrome PE and cyanine dye Cy7 (Pe-Cy7), Allophycocyanin (APC), tandem fluorochrome APC and cyanine dye Cy7 (APC-Cy7), BD Horizon™ V450 and BD Horizon™ V500 or bio-conjugated mAbs for 20 min on ice. Stainings with biotinylated mAbs were followed by a secondary staining step with Streptavidin-APC-Cy7 (Pharmingen). Bio-conjugated CD138 mAbs were stained for 45 min. Intracellular stainings with IRF4 APC conjugated mAbs were first surface stained and then further treated with materials of the Foxp3 Staining Set from Natutec (Frankfurt, Germany). Surface stained cells were permeabilized with Cytotfix/Cytoperm for 20 min. at 4°C. Subsequently cells were washed twice with wash buffer and stained for IRF4-APC in wash buffer for 30 min. at 4°C. After intracellular staining, the samples were washed and resuspended in PBS-BSA- $\text{NaN}_3$ . Stained cells were analysed on a FACSCanto (Becton Dickinson, Mountain View, USA) and data were evaluated using FlowJo 887 software (Tree Star Inc., Stanford University USA). Dead cells were labelled with Popro1 and excluded from the analysis. Monoclonal antibodies are listed in Table 2-7.

**Table 2-7: List of antibodies used for FACS stainings**

Specificity	Clone	Supplier
CD93 (AA4.1)	AA4.1	BD Bioscience
B220	RA3-6B2	BD Bioscience
BrdU	BU20A	eBioscience
CD4	GK1.5, L3T4	BD Bioscience
CD8	5H10, YTS 169,4	eBioscience
CD19	1D3	BD Bioscience
CD21/35	7E9	biolegend
CD23	M-L233	BD Bioscience
CD86	GL1	BD Bioscience
CD90.2	53-2.1	eBioscience
CD138	MI15	BD Bioscience
CXCR5	RF8B2	BD Bioscience
Fas	Jo2	BD Bioscience
PNA	-	Sigma
IgA	M18-254	BD Bioscience
IgD	11-26c	eBioscience
IgG1	MOPC-31C	BD Bioscience
IgM	II/41	eBioscience
IRF4	3E4	eBioscience
MHCII	NIMR-4	eBioscience
PD-1	J43	eBioscience
SA	-	BD Bioscience

### 2.3.6 Culture and activation of ex vivo B cells

Spleens and lymph nodes were aseptically removed from mice and then pressed through a sterile sieve. Erythrocytes were lysed for 2 min. with ACK lysis buffer (140 mM NH<sub>4</sub>Cl, 17 mM Tris-HCl pH 7.65). Splenocytes were kept in DMEM supplemented with 10% (v/v) FCS, 1 mM sodium pyruvate, 2 mM L-glutamine, 1x non-essential amino acids, 0.1 mM 2-β mercaptoethanol and further supplemented with 50µg/ml LPS (Sigma) and 20ng/ml IL4 (R&D Systems) for not longer than four days.

### 2.3.7 Proliferation assays

For proliferation analysis B cells were purified using  $\alpha$ CD19 MACS beads and resuspended in 1 ml per  $1 \times 10^7$  cells with 5  $\mu$ M CellTrace™ Violet (Invitrogen) in PBS at RT for 6 min (Lyons and Parish, 1994). The labelling reaction was stopped by addition of 10 ml DMEM/10% (v/v) FCS medium. The cells were then washed once in medium. Labelled B cells were plated at  $0.5 \times 10^6$  cells per well in round bottom 96-well plates. The cells were incubated in DMEM medium plus 10% (v/v) FCS, untreated or treated with 50  $\mu$ g/ml LPS (Sigma) and 20 ng/ml IL4 (R&D Systems). Labelled cells were analysed at day four.

### 2.3.8 Cell cycle analysis

*Ex vivo* MACS sorted splenic B cells were stimulated with 50  $\mu$ g/ml LPS (Sigma) and 20 ng/ml IL4 (R&D Systems) to induce proliferation and CSR. Cell cycle analysis was performed on day one and two by FACS analysis according to BrdU (APC) FACS staining kit (eBioscience).

## 2.4 Immunohistochemistry

Immunoglobulin serum concentrations after SRBC immunization were determined with ELISA as described previously (Roes and Rajewsky, 1993). Microtiter plates (Greiner, Frickenhausen, Germany) were coated with the respective coating antibody (IgM, IgG1, IgG2a, IgG2b, IgG3) at 4°C o/n, and subsequently blocked at RT for 30 min. in 0.5% (w/v) BSA. Next, serially diluted sera samples were applied to the wells and incubated at 37°C for 1 h together with the standard. Secondary biotinylated antibody was then added for 1 h at 37°C. Detection of the biotinylated anti-sera was achieved with incubation of SA-conjugated alkaline phosphatase (AP, Boehringer) 30 min. incubation at RT and p-nitrophenylphosphate as substrate (Boehringer). Following each incubation step, unbound antibodies or SA-conjugated AP were removed by three washes with tap water. The OD<sub>405</sub> was measured with an ELISA-photometer (Nano Quant infinite M200 Pro, Tecan) and the relative antibody concentration was determined by calculating the association constant as described by Cumano (Cumano and Rajewsky, 1986), following a method developed by Herzenberg (Herzenberg and Black, 1980).

## 2.5 Mouse Experiments

Tail bleeding as well as the general handling of mice was performed according to Hogan (Hogan et al., 1987) and Silver (Silver 1995).

### 2.5.1 Mice

The following mouse strains were used in experiments of this thesis: C57BL/6, CD19-Cre (Rickert *et al.* 1997), JHT<sup>-/-</sup> (Gu et al., 1993) and ROSA-RFP were all obtained from breedings of our animal facility, ZVTE Mainz. The SENP1<sup>fl<sup>ox</sup>/+</sup> mice (Yu et al., 2010) were a kind gift from Prof. Wang Min, Yale, and were further bred to CD19-Cre mice to generate homozygous B cell specific knockouts.

### 2.5.2 Immunization with Sheep Red Blood Cells (SRBC)

Immune activation was induced by immunisation with sheep red blood cells (SRBC, Sheep Blood in Alsevers Solutions, Thermo Scientific). 1 ml SRBC are washed three times with 50 ml PBS and centrifuged at 2500rpm for 10 min. at 4°C.  $1 \times 10^8$  cells were injected i.p. per mouse. Analysis followed 14 days post immunization.

### 2.5.3 Generation of mixed bone marrow chimeras

Host mice were lethally irradiated on day 0 or day -1 with 9,5 Gy. Bone marrow of donor mice was extracted on day 0 from *femur, tibia, os coxae, scapula* and *humerus*. 80% of bone marrow of JHT mice was mixed with 20% of bone marrow of experimental mice (Senp1<sup>ff</sup>, Senp1<sup>ff</sup> CD19-Cre, CD19-Cre, Senp1<sup>ff</sup> CD19-Cre RFP).  $5 \times 10^6$  cells were injected i.v. into the previously irradiated host mice. Mice received 3,5 % Borgall in their drinking water. Analysis or further experiments followed eight weeks after transfer.

### 2.5.4 In vivo BrdU labelling

To analyse B cell turnover, mice were fed with 0,8mg/ml bromdesoxyuridin (BrdU, Sigma) and 1 % (w/v) succrose in the drinking water for 14 days. Water bottles were wrapped in aluminium foil to prevent degradation of BrdU and was changed

once a week. BrdU uptake in splenic B cells was analysed by FACS according to the BrdU Staining Kit for Flow Cytometry APC (eBioscience)

## 2.6 Software & Statistics

For molecular cloning, Gene Construction Kit (Textco BioSoftware Inc.) was used. For analyzing FACS data CellQuest (BD) and FlowJo<sup>®</sup> (Treestar) were used. For statistics, Prism<sup>®</sup> (GraphPad Software Inc.) and Microsoft Excel were used. Values are typically represented as mean  $\pm$ SD (standard deviation) or  $\pm$  SEM (standard error of mean). Statistical significance was assessed using 2-tailed Student's t-test. p-values < 0.05 were regarded significant, displayed by '\*' in the figures (\*\* = p-value < 0.01; \*\*\* = p-value < 0.001).

### 3. Results

#### 3.1 SENP1<sup>ff</sup>

##### 3.1.1 *Reduced B cell numbers in naive SENP1<sup>ff</sup> and SENP1<sup>ff</sup> CD19-Cre mice*

Van Nguyen et al. (2012) demonstrated the importance of SENP1 in early B cell development. He demonstrated this through the severe reduction of B cells in fetal livers of SENP1<sup>-/-</sup> embryos at day E14.5 and through the decreased ability of fetal liver hematopoietic stem cells (FL-HSCs) co-cultured with OP9 stromal cells to proliferate into the subsequent B cell subsets. These early B cell development defects are dependant on the regulation through SUMOylated STAT5. In our model, having crossed the SENP1 conditional knock out to the B cell specific CD19-Cre mouse, we were able to show similar developmental defects in B cells. CD19 is expressed from the pro B cell stage on (Hardy Fraction B/C (Hardy and Hayakawa, 2001)) generating the SENP1 specific deficiency from this developmental stage on.

In primary lymphoid organs such as the bone marrow (BM), lymphoid progenitors (pro- and pre- B cells) undergo a process of sequential recombination of the B cell receptor (BCR), induced by RAG1 initiated V(D)J genes rearrangement (Johnson et al., 2005). These cells, referred to as immature B cells (IgM<sup>hi</sup>IgD<sup>lo</sup>) exit from the BM and enter the spleen as transitional 1 (T1) B cells. In the spleen, T1 B cells undergo further maturation to transitional 2 (T2) B cells (IgM<sup>hi</sup>IgD<sup>hi</sup>), which are the direct precursors of mature B cells .

In the BM of SENP1<sup>ff</sup> CD19-Cre mice we observed a significant reduction in the total cell number of recirculating B cells (B220<sup>high</sup>IgM<sup>+</sup>), whereas B cell precursors and naïve B cells showed no significant difference in percentage as well as in total cell number (Figure 3-1). This indicates, that early B cell development in the BM is not affected by the knockout of SENP1 in B cells.

To test for any phenotypic effects of the targeted SENP1 allele, SENP1<sup>ff</sup> mice with the appropriate controls (C57BL/6 mice, here indicated as WT) were also analysed (Figure 3-1). In the BM of these mice a similar phenotype as in the SENP1<sup>ff</sup> CD19-Cre mice could be observed, namely a significant reduction of mature recirculating

B cells. However in the *Senp1<sup>ff</sup>* mice the percentual decrease of the mature B cell population was significant whereas in the *SENP1<sup>ff</sup> CD19-Cre* the total cell number of mature recirculating B cells was significantly decreased.

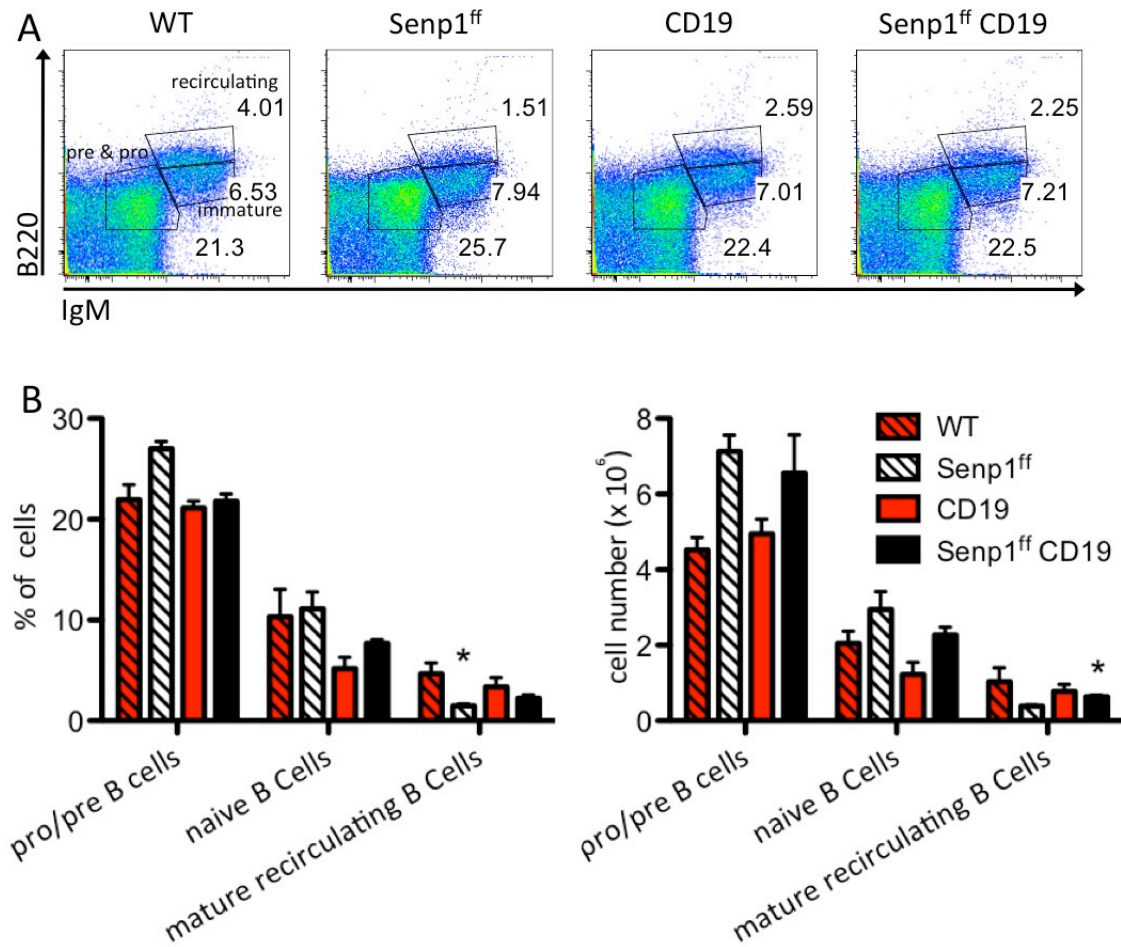


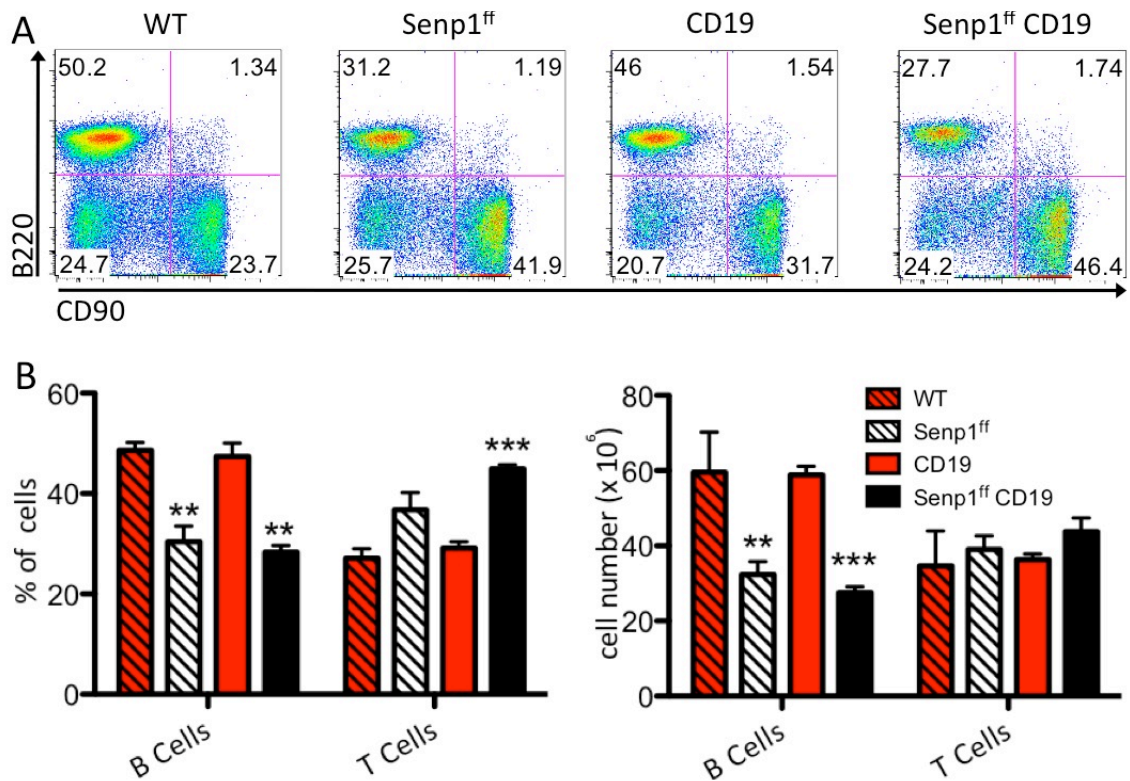
**Figure 3-1: B cell development in the bone marrow.** (A) FACS analysis of naive bone marrow (BM) cells of indicated genotypes. Cells were analysed for the expression of B220 and IgM surface markers and pregated on *popro1<sup>-</sup>* live cells. (B) Statistical evaluation of BM B cell populations. Left, percentage of cell population, right, number of cells per population. Statistical significance is calculated for WT vs. *SENP1<sup>ff</sup>* and CD19 vs. *SENP1<sup>ff</sup> CD19*. For each group n=3; \* p<0,05, \*\* p<0,01, \*\*\* p<0,001

The occurrence of a significant phenotype in the *SENP1<sup>ff</sup>* mice is unexpected as the floxed *SENP1* allele genetically resembles a WT allele. To investigate if the *SENP1<sup>f</sup>* allele has the same phenotype as the conditional *SENP1* knockout allele in other B cell subsets, further experiments included *SENP1<sup>ff</sup>* mice with the respective WT controls.



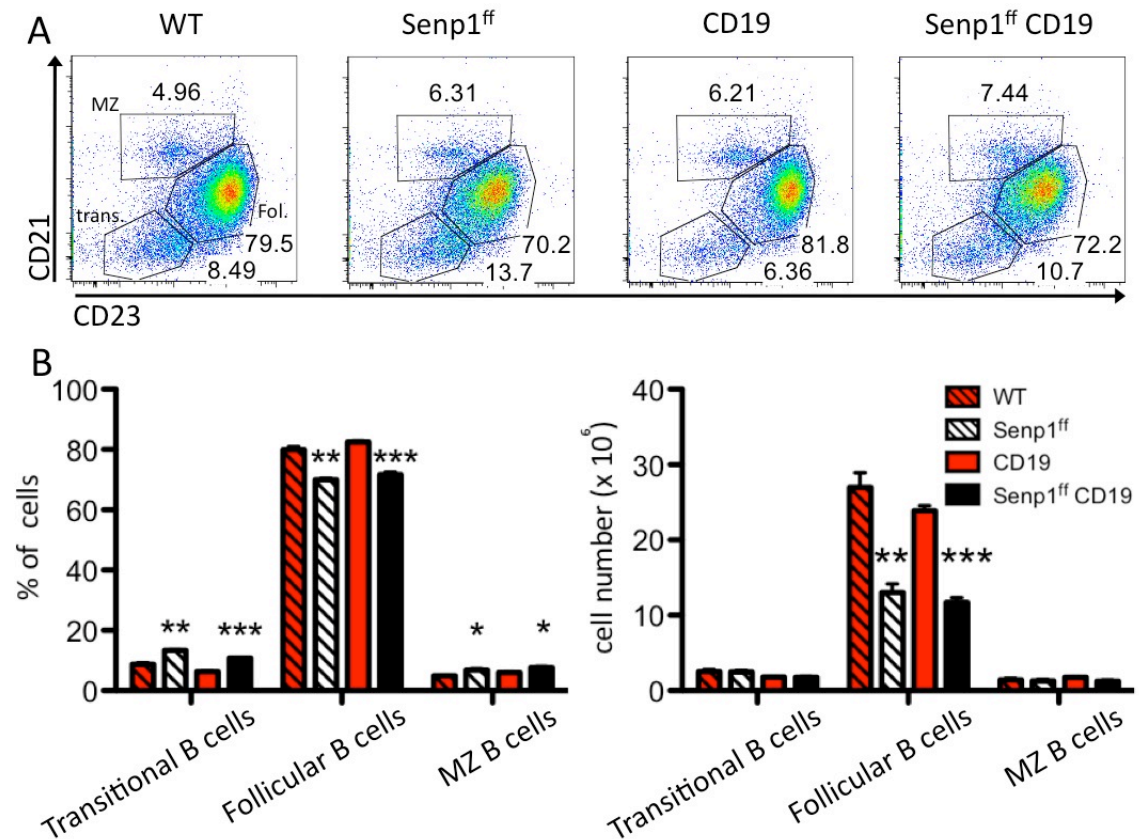
Once T1 B cells from the BM reach the secondary lymphoid organs (spleen and lymph nodes), they can differentiate and develop further in different mature B cell subsets. From the T1 stage they develop into T2 and T3 B cells from where they then either migrate into the follicles of the spleen to become follicular (Fol) B cells (CD21<sup>hi</sup> CD23<sup>hi</sup>) or to the marginal zone (MZ) to become MZ B cells (CD21<sup>hi</sup> CD23<sup>low</sup>). Fol B cells are then, upon antigen encounter, able to enter the germinal centre (GC) reaction where they undergo class switch recombination (CSR) and somatic hypermutation (SHM) to switch Ig isotype and increase their antigen specificity and affinity (Stavnezer et al., 2008). They subsequently develop into long lived plasma cells or memory B cells, which both then travel back to the BM. Fol as well as MZ B cells are also able to respond more quickly to antigen encounter by forming extra follicular foci and developing into short lived plasma cells, which only undergo CSR and not SH (Stavnezer et al., 2008).

Figure 3-2 shows, using B220 as a B cell marker and CD90 as a T cells marker, a highly significant reduction of B220<sup>+</sup> B cells in the spleens of SENP1<sup>ff</sup> CD19-Cre mice (30%) compared to controls (50%). This difference can be seen in percentage as well as total cell number (Figure 3-2B). Even though T cells were significantly increased in percentage in the SENP1<sup>ff</sup> CD19-Cre mice, this difference was not statistically significant looking at total cell numbers (Figure 3-2B).



**Figure 3-2: B/T cell ration in the spleen.** (A) FACS analysis of naive splenocytes of indicated genotypes. Cells were analysed for the expression of B220 and CD90 surface markers. (B) Statistical evaluation of splenic B cell and T cells. Left, percentage of cell population, right, number of cells per population. For each group n=3; \* p<0,05, \*\* p<0,01, \*\*\* p<0,001

When analysing splenic B cell populations by discriminating between immature (CD21<sup>-</sup>CD23<sup>-</sup>), Fol (CD21<sup>int</sup>CD23<sup>high</sup>) and MZ (CD21<sup>high</sup>CD23<sup>neg-low</sup>) B cells, we detected a significant increase in the percentage of transitional B cell, and MZ B cells in SENP1<sup>ff</sup> and SENP1<sup>ff</sup> CD19-Cre mice compared to the respective controls (Figure 3-3). However, this difference was not observed when looking at total cell numbers (Figure 3-3). Total cell numbers of transitional and MZ B cells were unchanged, however, cell numbers of Fol B cell were nearly halved in SENP1<sup>ff</sup> and SENP1<sup>ff</sup> CD19-Cre mice compared to controls (Figure 3-3B). This indicates that the effect of a SENP1 knockout in transitional and MZ B cells is only marginal, but substantially affects Fol B cells. The cause for this reduction may be a result of decreased proliferation or impaired survival.



**Figure 3-3: B cell subsets in the spleen.** (A) FACS analysis of naive splenocytes of indicated genotypes. Cells were analysed for the expression of CD21 and CD23 surface markers after pre-gating on B220<sup>+</sup>popro1<sup>-</sup> cells. (B) Statistical evaluation of splenic B cell subsets. Left, percentage of cell population, right, number of cells per population. For each group n=3; \* p<0,05, \*\* p<0,01, \*\*\* p<0,001

As Peyer's patches (PP) are a secondary lymphoid organ, where B cells encounter high amounts of antigen due to their direct vicinity to the small intestine, their ability to form germinal centres (GC) was analysed. B cells from the PP of naïve SENP1<sup>ff</sup> CD19-Cre mice and SENP1<sup>ff</sup> mice were stained for the surface markers Fas and PNA. Both genotypes showed a 1,5 fold increase in the percentage of GC B cell formation compared to their respective controls, indicating a stronger response to pathogenic antigens (Figure 3-4). In concert with a general reduction of B cell numbers in the PP in SENP1<sup>ff</sup> CD19-Cre mice, the total number of GC B cells was also decreased 1,3 fold compared to the CD19-Cre controls. However, due to a high variability of the percentages and cell numbers non of these differences are statistically significant.

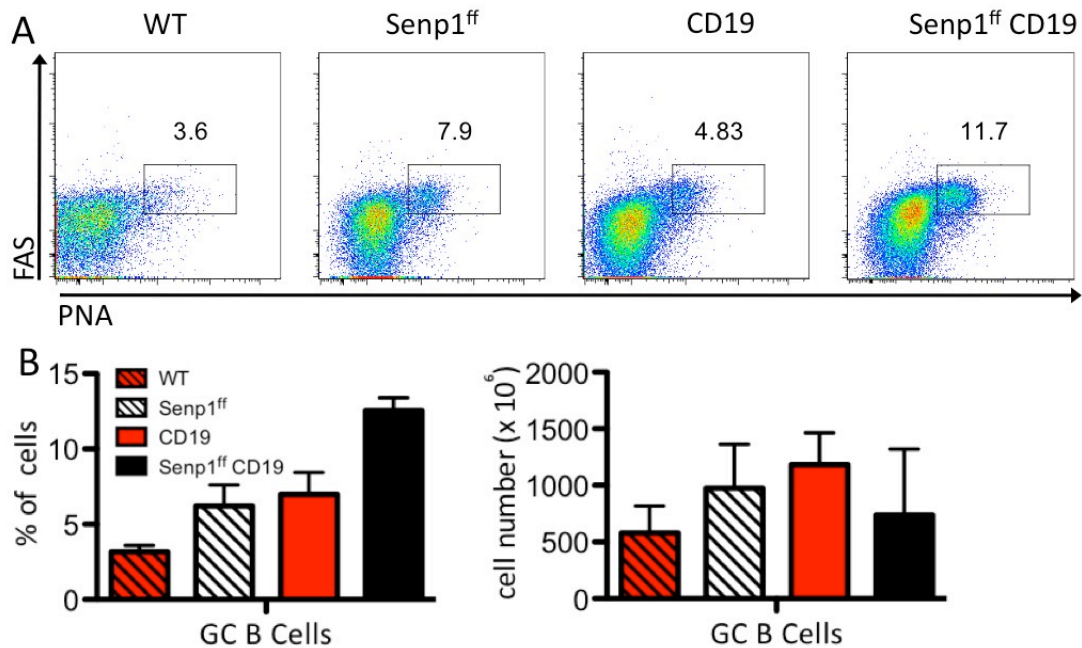


**Figure 3-4: GC B cells in the Peyer's patches of naive mice.** (A) FACS analysis of naive Peyer's patches (PP) of indicated genotypes. Cells were analysed for the expression of Fas and PNA surface markers after pre-gating on B220<sup>+</sup>popro1-cells. (B) Statistical evaluation. Left, percentage of cell population, right, number of cells per population. For each group n=3; \* p<0,05, \*\* p<0,01, \*\*\* p<0,001

As seen in Figure 3-2 the total reduction of splenic B cells in the SENP1<sup>ff</sup> was nearly as strong as in the SENP1<sup>ff</sup> CD19-Cre mice, although SENP1<sup>ff</sup> mice do not contain the B cell specific CD19-Cre induced knockout. PCR genotyping of SENP1<sup>ff</sup> CD19-Cre, SENP1<sup>ff</sup> and control B cells revealed that in the SENP1<sup>ff</sup> CD19-Cre B cells SENP1 is indeed knocked out as expected (Figure 3-5A). It could also be confirmed in B cells of the SENP1<sup>ff</sup> mice that the targeted exon 5 and 6 is still present (Figure 3-5A).

SENP1 mRNA expression in the same splenic B cells of SENP1<sup>ff</sup> CD19-Cre mice was analysed by quantitative real-time RT-PCR and showed a 70% reduction of SENP1 expression compared to CD19-Cre control mice (Figure 3-5B). The 30% of residual SENP1 expression can be explained in two ways: a small percentage may arise from CD19<sup>-</sup> cell contamination which occurs during the process of B cell purification, however the purity of the isolated B cells was between 94% and 98%. The main source of SENP1 mRNA is therefore hypothesised to originate from CD19 positive cells that escaped Cre mediated recombination and did not delete SENP1. In order to identify these potential Cre escapees the SENP1<sup>ff</sup> CD19-Cre mice were crossed to a red fluorescent protein (RFP) expressing reporter strain.

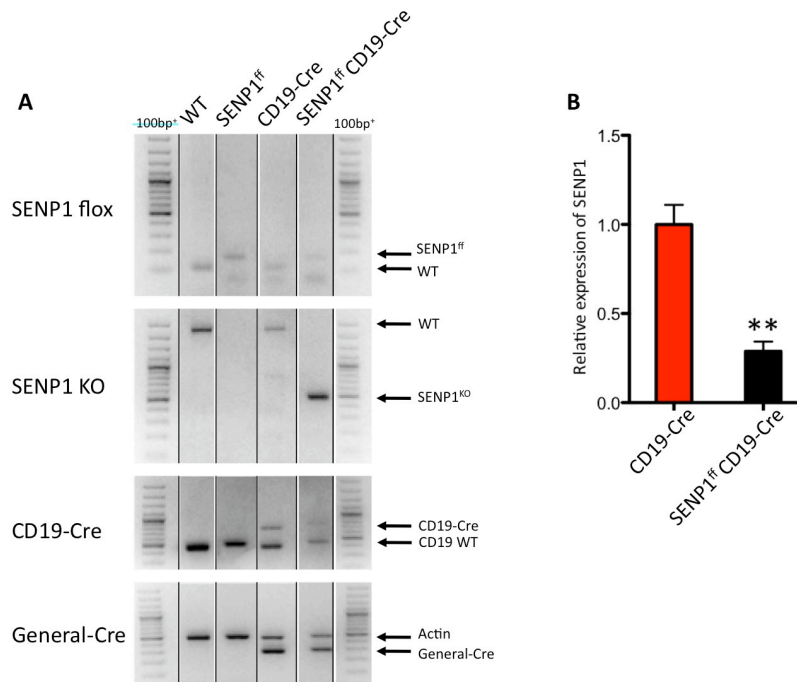


**Figure 3-5: Verification of SENP1 knockout by PCR typing and qRT-PCR.** (A) PCR genotyping of splenic B cells of the indicated genotypes with primers for the floxed and knockout SENP1 allele, specific CD19-Cre and a general Cre. Arrows indicate the expected band height. (B) mRNA expression of SENP1 in SENP1<sup>ff</sup> CD19-Cre B cells, compared to CD19-Cre controls, measured by quantitative RT-PCR. For each group n=3; \* p<0,05, \*\* p<0,01, \*\*\* p<0,001

To understand the phenomenon of the B cell phenotypes in the SENP1<sup>ff</sup> mice the available data on the generation of the SENP1<sup>fllox</sup> allele was carefully studied and validated. In the targeting strategy of the SENP1<sup>ff</sup> mice, generated by Luyang Yu (Yu et al., 2010) (Figure 3-6) it can be seen that the *neomycine resistance* (*neo*) cassette is not flanked by *frt* sites, as meanwhile common practice, but flanked by an additional *loxP* site. A *loxP* site is located 5' of exon 5 and 3' of the *neo* cassette as well as between exon 6 and the *neo* cassette. This makes the selective excision of the *neo* cassette very complicated and has not been done by Yu *et al.* Therefore the *neo* cassette still remains in the SENP1<sup>f</sup> allele.

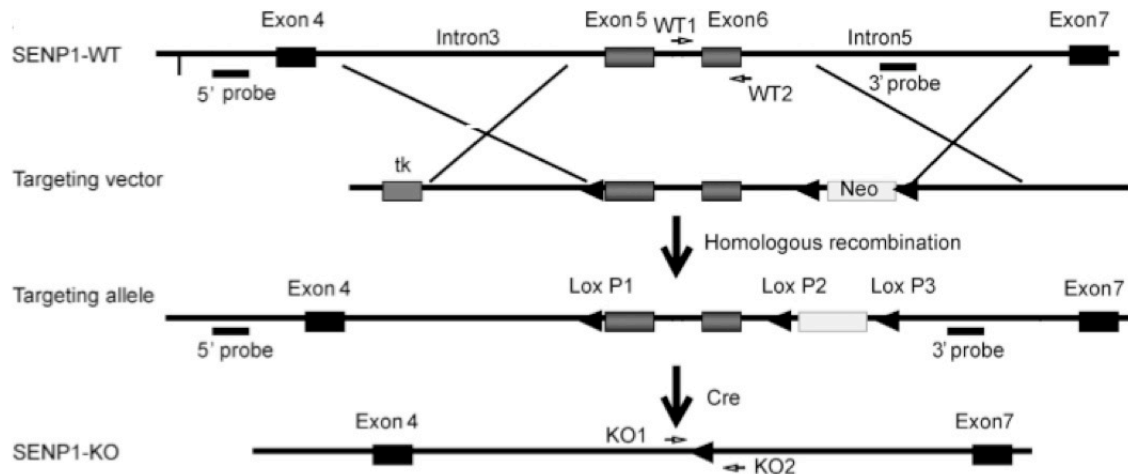


**Figure 3-6: Schematic of SENP1<sup>fl</sup> and KO mouse targeting strategy (Yu et al., 2010).**

Schematic diagram of targeting strategy to generate SENP1<sup>fl</sup> mice. The targeting vector contains intron 3 at the 5' arm, exons 5/6 in the targeting region, and intron 5 at the 3' arm. The *neo* cassette is located between LoxP2 and LoxP3.

To our knowledge the remaining *neo* cassette is the only difference between WT and SENP1<sup>fl</sup> mice, leading to the hypothesis that *neo* somehow causes a hypomorphic SENP1 allele causing the observed phenotypes. Effects of *neo* insertions have been previously reported (Pham et al., 1996). By logic, the *neo* cassette cannot lead to a full loss-of-function mutation of the gene, as a complete knockout of SENP1 is embryonically lethal (Yamaguchi et al., 2005; Yu et al., 2010). However, due to the observed phenotype the conclusion is near, that protein expression or function is substantially hampered.

Interestingly, only a very mild phenotype was observed in other cell types, namely a mild but significant increase in CD4 and CD8 effector T cells (data not shown). All other organs seem to develop and function normal. Even the testicles, which express high amounts of SENP1 (Xu and Au, 2005), show no abnormality in respect to size and cell count. Reproduction of SENP1<sup>fl</sup> CD19-Cre and SENP1<sup>fl</sup> is normal and genotype distribution is according to Mendelian rules. Hence, it was decided to further analyse SENP1<sup>fl</sup> CD19-Cre and SENP1<sup>fl</sup> mice, albeit the unknown origin of the SENP1<sup>fl</sup> phenotypes. To fully exclude the influence of the hypomorphic SENP1 allele from other cell types than B cells, mixed bone marrow chimeras were generated for all further *in vivo* experiments.

### 3.1.2 Transcriptional network in naive *SENP1<sup>ff</sup>* CD19 B cells

One of the main functions of SUMOylation is the regulation of transcription factors and the regulation of cell cycle (David et al., 2002; Johnson and Blobel, 1999) and apoptosis (Buschmann et al., 2000; Zhong et al., 2000). In Figure 3-7 we aimed to investigate the mRNA expression of several components of the SUMOylation pathway as well as the transcriptional network responsible for early B cell development, GC and PC development in B cells from naive *SENP1<sup>ff</sup>* CD19-Cre mice and control mice. Further analysed were factors important in cell cycle regulation and apoptosis.

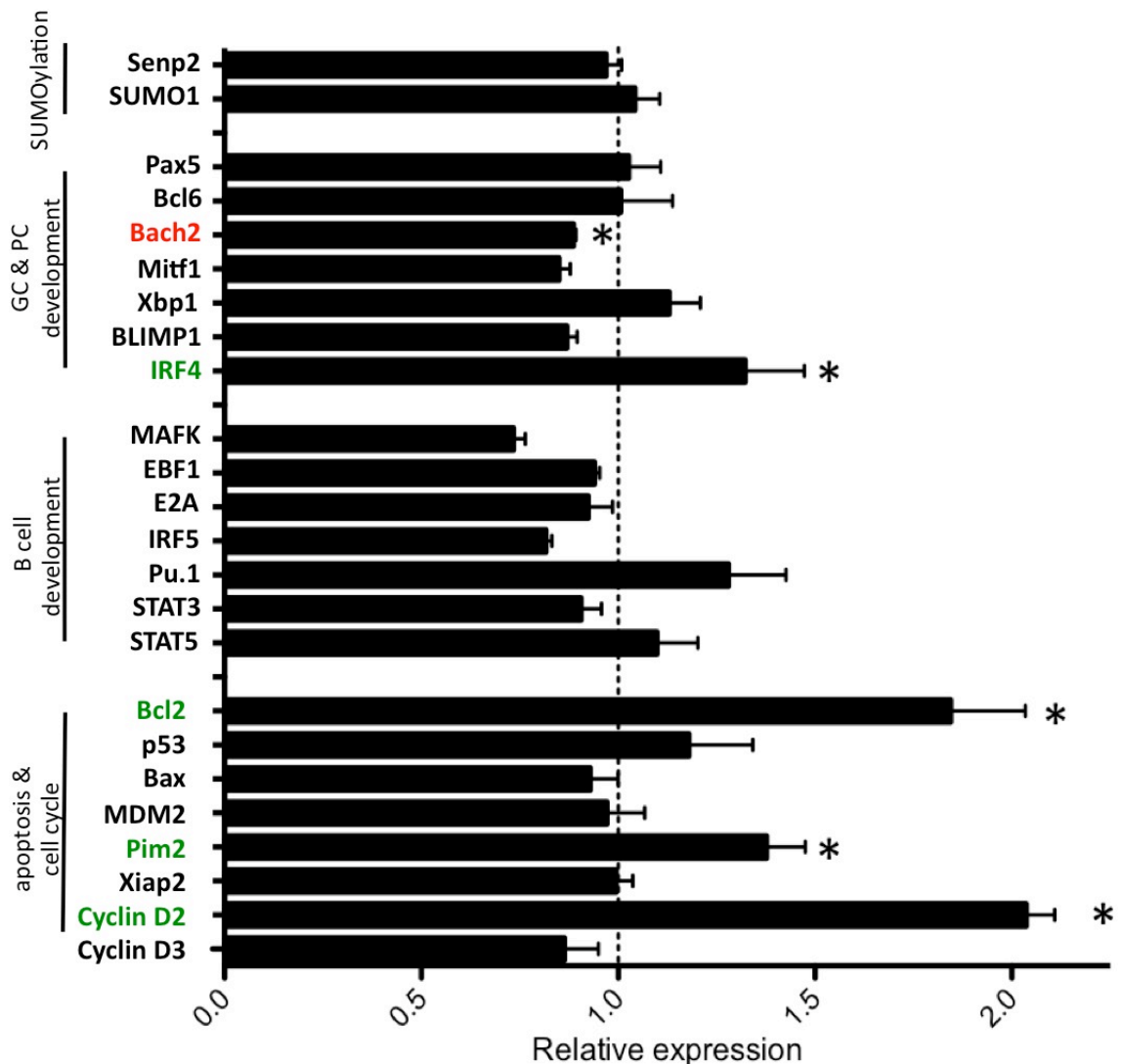


**Figure 3-7: quantitative real-time RT-PCR analysis of B cell, apoptosis and cell cycle relevant genes.** MACS purified splenic B cells from *SENP1<sup>ff</sup>* CD19-Cre mice were analysed. Results compared to HPRT are normalised to CD19-Cre control cells, indicated by the dotted line. Significantly upregulated genes are marked in green, downregulated genes in red. n=3; \* p<0,05, \*\* p<0,01, \*\*\* p<0,001

SENP1 regulates SUMO on a posttranslational level by cleaving the C terminal tail, leading to SUMO maturation (Muller et al., 2001). This regulation is not based on transcriptional activity, hence no change in SUMO mRNA expression is observed (Figure 3-7). As it is thought that SENP2 can compensate for the loss of SENP1, also SENP2 expression was analysed. It could be shown that no compensational upregulation of SENP2 is apparent in the SENP1<sup>ff</sup> CD19-Cre cells (Figure 3-7).

As the analysed cells were derived from the spleen all cells were matured past the immature B cell stage, and therefore no differences were expected and observed in transcription factors that are responsible for early lymphocyte and B cell development (Figure 3-7).

Figure 3-4 displays an increase, albeit non-significant, in GC B cells in the PP of the SENP1<sup>ff</sup> CD19-Cre mice. To investigate if this is caused by altered expression levels of the GC and plasma cell transcriptional network several important genes of this network were analysed for their mRNA expression level. Pax5, Bcl6, Bach2 and Mitf1 are essential for the maintenance of the GC reaction and suppress further development into PCs and memory B cells by suppressing Xbp1, Blimp1 and Irf4 (Nutt et al., 2011). All of these mentioned transcription factors except Bcl6 and Irf4 are known to be SUMOylated (Bertolotto et al., 2011; Chen and Qi, 2010; Jiang et al., 2012; Kono et al., 2008; Kurahashi et al., 2011; Miller et al., 2005; Murakami and Arnheiter, 2005; Shimshon et al., 2011; Tashiro et al., 2004; Ying et al., 2012).

Only Bach2 and IRF4 expression were significantly changed compared to CD19-Cre control B cells, whereas Bach2 expression was decreased and IRF4 expression increased (Figure 3-7) It has to be kept in mind that the analysed cells were naïve *ex vivo* B cells, where only a minor fraction is undergoing a GC reaction in the steady state. So no large differences are expected in the GC and PC transcriptional network. Non the less increased IRF4 levels and decreased Bach2 levels might make SENP1<sup>ff</sup> CD19-Cre B cells more prone to PC differentiation once appropriate stimulation occurs.

Up to this point the strongest phenotype in the SENP1<sup>ff</sup> CD19-Cre mice is the reduction of mature recirculating B cell compartment in the bone marrow and the Fol B cells in the spleen. To elucidate this phenotype in more detail we examined



mRNA expression of important cell cycle regulatory and apoptotic elements (Figure 3-7), as the importance of SUMOylation in cell cycle regulation and apoptosis has been shown by several groups (Gutierrez and Ronai, 2006; Ulrich, 2009; Ulrich et al., 2005; Wan et al., 2012). Interestingly, and against expectations Bcl2, an anti-apoptotic factor, is nearly two fold increased in SENP1<sup>ff</sup> CD19-Cre B cells, however the pro-apoptotic factor Bax, was not altered (Figure 3-7). The question remains now on why Bcl2 is upregulated in a cell compartment that has apparent survival problems.

Several different cellular mechanisms are active in B cell development, activation, GC formation and PC differentiation. One of these mechanisms is the response to DNA strand breaks which occur during B cell development and in response to antigen encounter. DNA strand breaks are induced by RAG1 in the V(D)J rearrangement of the BCR (Johnson, 2004) and later by AID in CSR and SH. These response mechanisms are partially regulated and fine tuned by SUMOylation. MDM2, Pim2 and p53 are all upregulated upon DNA damage response in CSR and additionally MDM2 and p53 are directly regulated by SUMOylation (Bode and Dong, 2004). However, only in Pim2 (Fox et al., 2003), which was also shown to be a potent anti-apoptotic factor that drives early B cell survival after RAG induced DSBs (Bednarski et al., 2012), a significant upregulation was observed in the SENP1 KO cells. This indicates again on the one hand an influence of SUMOylation in the DNA damage response mechanism during BCR maturation and CSR, and on the other hand the need for upregulation of certain anti-apoptotic factors for SENP1 KO B cells to survive.

Cyclins are, with cyclin dependant kinases (CDKs), retinoblastoma proteins (pRBs) and CDK inhibitors, the four major regulators of the cell cycle. Specifically the D-type cyclins D2 and D3 (CCND2, CCND3) play a nonredundant role in GC B cell proliferation (Chiles, 2004; Cooper et al., 2006; Lam et al., 2000; Mataraza et al., 2006). CCND2 deficiencies lead to reduced B cell proliferation (Mohamedali et al., 2003) and compensatory CCND3 overexpression but CCND3 was also shown to be essential for B cell proliferation, maturation and T cell-dependant antibody response. Both cyclins have so far not been reported as SUMO targets, however CCND2 is significantly upregulated two fold in the SENP1 KO B cells whereas

CCND3 shows no change in expression level compared to CD19-Cre control mice (Figure 3-7). The reason for CCND2 upregulation can have several origins and lead to distinct effects in cell cycle progression. Upregulation of CCND2 has been observed in many proliferative B cell diseases such as chronic lymphocytic small/small lymphocytic leukaemia (CLL/SLL) (Delmer et al., 1995; Igawa et al., 2011), however no such malignant phenotypes of any kind have been observed in SENP1<sup>ff</sup> CD19-Cre mice. As the observed mice were analysed at an age of six to nine weeks, they might have been too young for any B cell malignancies to be seen. For this older mice would have to be analysed. CCND2 was also observed to be upregulated upon CCND3 inhibition (Peled et al., 2010). This would have to be clarified on a protein basis.

### *3.1.3 Impaired survival after in vitro stimulation due to activation induced cell death (AICD)*

As B cell numbers are decreased in SENP1<sup>ff</sup> CD19-Cre spleens and the percentage of GC B cells in the Peyer's patches was increased it was hypothesized that SENP1 KO B cells harbour either survival and/or proliferation defects. To investigate survival and proliferation capacities of SENP1 KO B cells, total splenocytes were isolated and cultured in medium alone or enriched with LPS and IL4 to induce proliferation, class switch recombination and plasma cell differentiation. Cells were cultured for up to five days and monitored daily by cell counting and FACS analysis. As seen in Figure 3-8A from day three on cell numbers of SENP1<sup>ff</sup> CD19-Cre mice were significantly reduced and stagnated until day five. In cells of SENP1<sup>ff</sup> mice a significant reduction compared to WT cells was observed from day four on.

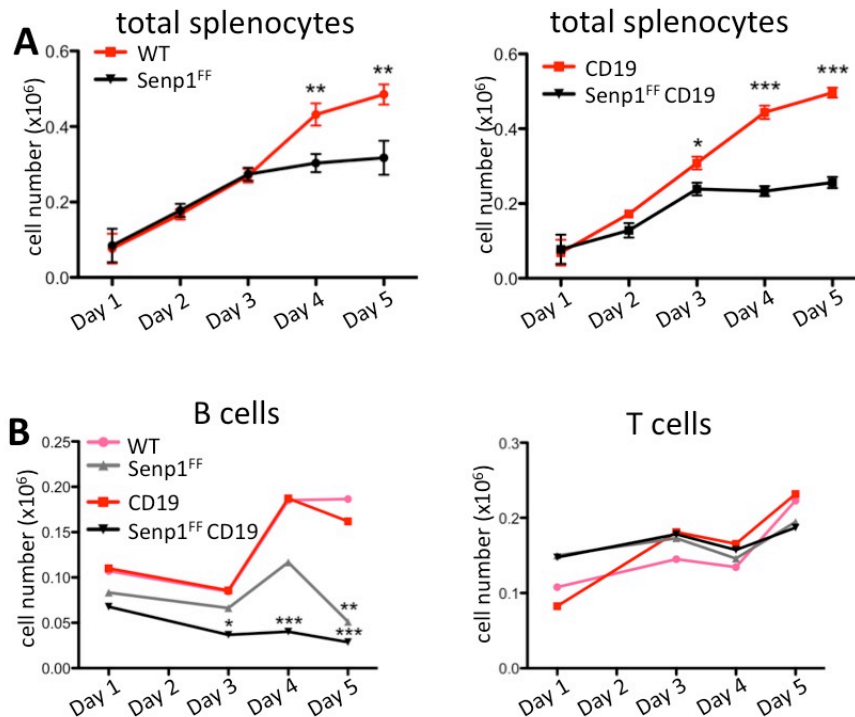


**Figure 3-8: *in vitro* stimulation of total splenocyte culture.** (A) Cell count of live cells of LPS (50 $\mu$ g/ml) and IL4 (20ng/ml) stimulated total splenocyte cultures at indicated time points. Left graph: splenocytes isolated from WT and SENP1<sup>ff</sup> mice; right graph: splenocytes isolated from CD19-Cre and SENP1<sup>ff</sup> CD19-Cre mice. (B) Left graph shows total cell count of live B cells and right graph of live T cells of LPS (50 $\mu$ g/ml) and IL4 (20ng/ml) stimulated total splenocyte cultures at indicated time points. Cell count was calculated by FACS analysis of B220 positive B cells and CD4 & CD8 positive T cells. Both graphs show combined results of WT, SENP1<sup>ff</sup>, CD19-Cre and SENP1<sup>ff</sup> CD19-Cre mice. For each group n=3; \* p<0,05, \*\* p<0,01, \*\*\* p<0,001

When comparing B and T cell survival it can be seen in Figure 3-8B that T cells were not affected by the SENP1 KO, nor by the SENP1 hypomorph. Interestingly, B cells were significantly reduced from day three on in SENP1 KO and at day five in SENP1 hypomorph. This implies that even though SUMOylation is a ubiquitous mechanism, important in every cell of an organism, SUMOylation is crucial for B cell survival and/or development.

Next, we determined the ability of CD19<sup>+</sup> purified SENP1 KO and hypomorph B cells to undergo cell cycle after LPS and IL4 stimulation (Figure 3-9). B cells were cultured under normal conditions and labelled with bromdesoxyuridin (BrdU) for one hour prior to harvest. BrdU is a synthetic analogue of thymidine which incorporates into the newly synthesised DNA during S-phase replication. By the

amount of BrdU incorporation in respect to 7AAD binding, information about the cell cycle stage of a cell can be gained.

On day one of culture with LPS and IL4 supplemented medium twice as many SENP1 KO B cells were undergoing S-Phase (7AAD<sup>high</sup>BrdU<sup>high</sup>) compared to CD19-Cre B cells (4% CD19-Cre B cells; 8% SENP1<sup>ff</sup> CD19-Cre B cells) (Figure 3-9B), indicating a quicker onset of stimulation and a higher proliferation rate, whereas on day two S-Phase SENP1 KO B cells are significantly reduced by 30% compared to control cells (SENP1 KO B cells 17%, CD19-Cre B cells 27%). What can also be seen in this graph is that despite the early increased proliferation on day one, the rate of proliferation towards day two is markedly decreased in the SENP1<sup>ff</sup> CD19-Cre mice. This is similar, however not as strong in the SENP1<sup>ff</sup> mice compared to WT (Figure 3-9B).

Additionally, apoptotic cells (7AAD<sup>+</sup>BrdU<sup>-</sup>) are significantly increased in SENP1 KO B cells on day two (Figure 3-9C), giving the notion that after fast proliferation in the first 24 hours cells undergo activation induced cell death (AICD) after day one.

As AID induced CSR is occurring during G1 Phase of the cell cycle it is interesting to note that except for a small but significant decrease of SENP1 KO B cells on day one, compared to CD19-Cre control cells, no change is measured in the percentage of G1 phase B cells (data not shown). However, G2/M phase cell are significantly increased two fold in SENP1<sup>ff</sup> CD19-Cre B cells on day one and day two after LPS & IL4 stimulation (Figure 3-9D).

SENP1 hypomorphic cells show only a mild phenotype, as seen in Figure 3-9. Only the percentage of apoptotic cells is increased on day one and two.

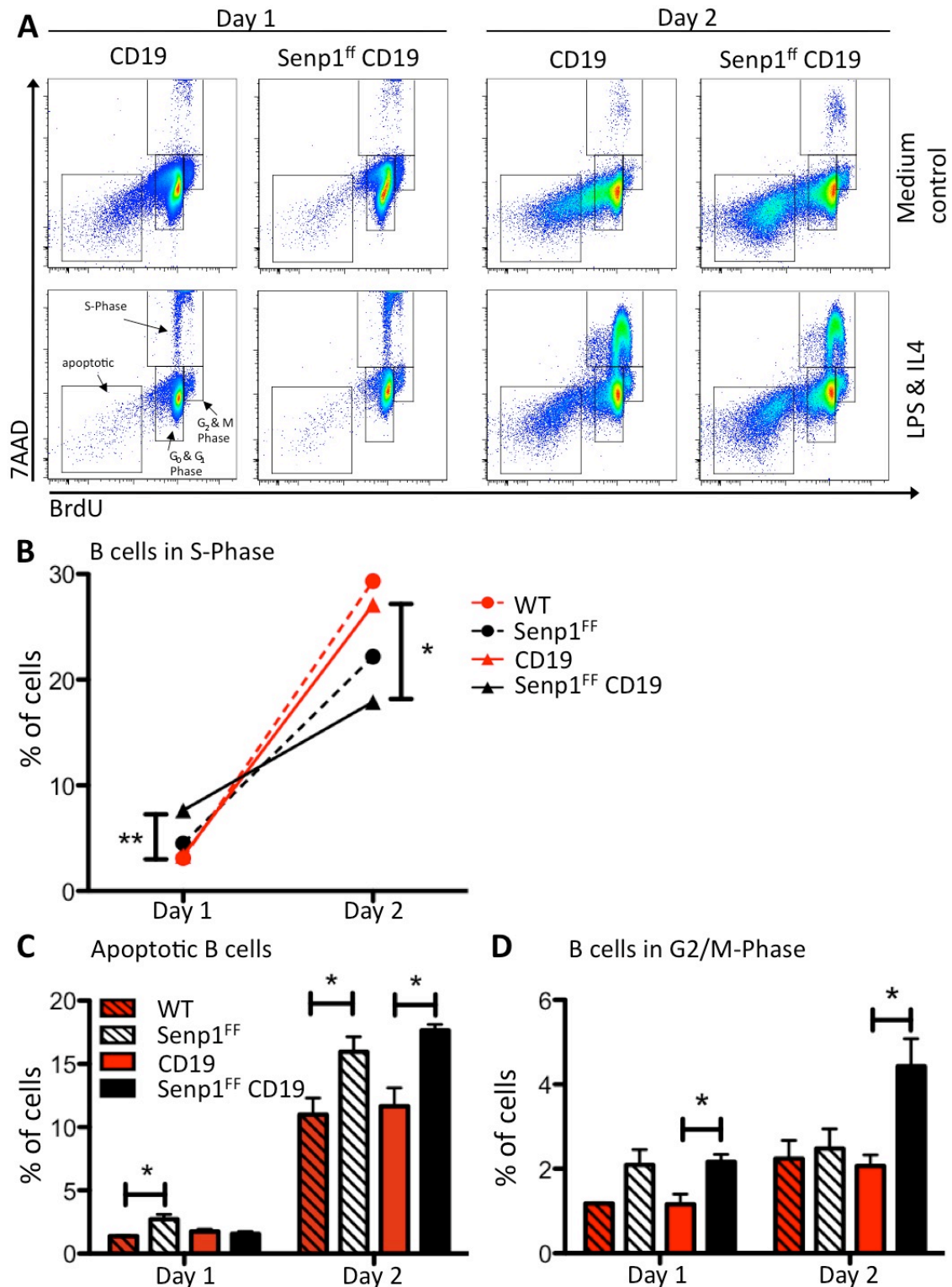


**Figure 3-9: Cell cycle analysis.** (A) FACS analysis of CD19 MACSed BrdU pulsed B cells of indicated genotypes after LPS (50 $\mu$ g/ml) and IL4 (20ng/ml) stimulation. Cells were analysed for BrdU and 7AAD incorporation on day 1 and day 2. (B) Statistical evaluation of cells in S Phase, (C) apoptotic B cells (D) and in G2/M Phase. For each group n=3; \* p<0,05, \*\* p<0,01, \*\*\* p<0,001

After investigating the cell cycle we wanted to look at the overall proliferative capacity of SENP1<sup>ff</sup> CD19-Cre B cells over a course of four days. Therefore, cells were labelled with CellTrace™ Violet and cultured again with LPS and IL4 for four days. CellTrace™ Violet is a fluorescent cell staining dye that incorporates into the cell membrane. The amount of the fluorescent dye is halved with each cell division. By measuring the fluorescence intensity of a given cell the proliferation rate can be calculated. However, by looking at Figure 3-10, it can be seen that SENP1 KO B cells that survive until day four do proliferate normal (Figure 3-10B), albeit the overall cell number is markedly reduced (Figure 3-10A).

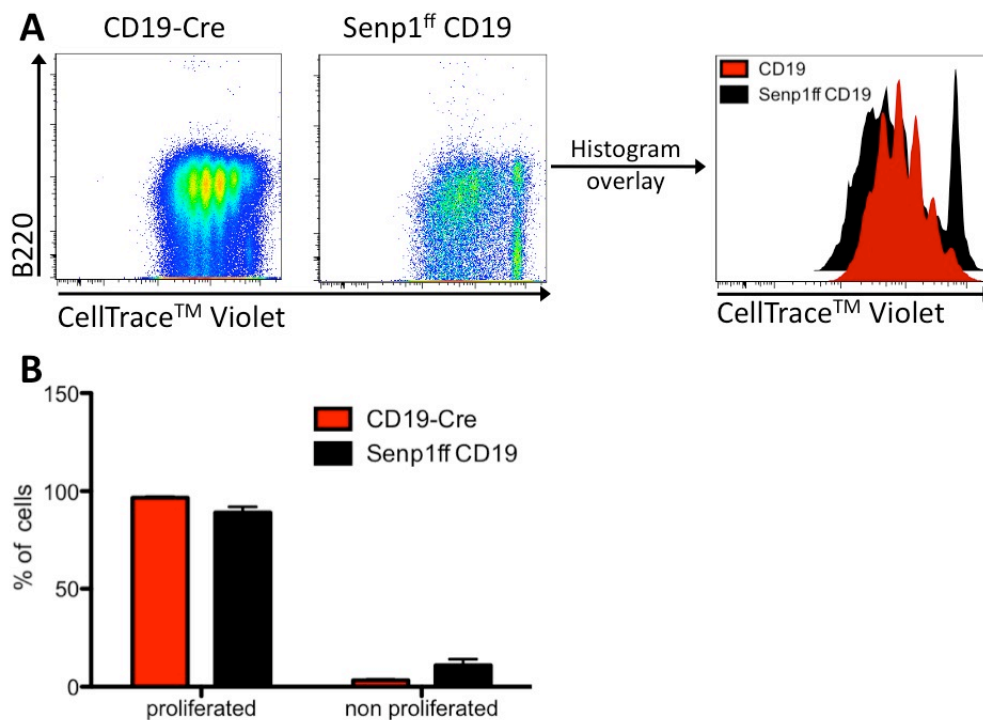


**Figure 3-10: *in vitro* proliferation assay.** CD19<sup>+</sup> purified B cells were labelled with the proliferation dye CellTrace™ Violet and stimulated with LPS (50µg/ml) and IL4 (20ng/ml) for four days. (A) FACS analysis of indicated genotypes. Cells were analysed for the expression of B220 and the incorporation of Violet Cell Trace after pre-gating on popro1<sup>-</sup> cells. (B) Statistical evaluation of proliferation. For each group n=3.

### 3.1.4 *In vitro* class switch recombination and plasma cell differentiation

As mentioned before, SUMOylation was shown to be an important regulator in several cellular mechanisms involved in CSR. It regulates several relevant transcription factors, DNA damage response systems induced during CSR, survival, proliferation, and differentiation mechanisms. To see whether CSR and PC

differentiation is affected in the SENP1<sup>ff</sup> CD19-Cre mice compared to controls we stimulated CD19<sup>+</sup> purified splenic B cells *in vitro* with LPS and IL4, a TLR4 antagonist and T<sub>H</sub>2 T cell derived cytokine, respectively, in order to drive Ig switch from IgM to IgG1 and plasma cell differentiation.

In Figure 3-11A and B we observed, similar to Figure 3-8, a general reduction in total B cell numbers in the SENP1<sup>ff</sup> CD19-Cre B cells and in IgG1 switched B cells. At day five hardly any B cells from SENP1<sup>ff</sup> CD19-Cre mice were still alive.

On day five of culture we could observe 30% IgG1 positive CD19-Cre control B cells, whereas only 20% SENP1<sup>ff</sup> CD19-Cre B cells switched for IgG1 (Figure 3-11). The reduction is even stronger when investigating the total cell number of IgG1 switched cells. There, a 60% reduction can be seen in the IgG1 switched B cells of the SENP1<sup>ff</sup> CD19-Cre mice compared to the CD19-Cre controls.

When we examined PC differentiation in SENP1<sup>ff</sup> CD19-Cre mice the percentual amount of CD138<sup>pos</sup> PCs on day three, four and five were in average four fold increased compared to CD19-Cre controls (Figure 3-11). And albeit the reduced total number of B cells in culture, the total amount of PCs is slightly increased, however not significant.

It seems that SENP1 deficiency in LPS and IL4 stimulated B cells on the one hand hamper the switching capacity to IgG1 but on the other hand highly increase PC differentiation and survival. This goes in hand with the observed increase of IRF4 in naïve splenic B cells from Figure 3-7.

In order to investigate the activation state of the stimulated B cells isolated from SENP1<sup>ff</sup> CD19-Cre mice we looked at MHC II expression (Figure 3-12), which is upregulated upon LPS stimulation, hence serves as an marker for activation. MHC II expression is nearly at 100% at day three and drops to about 30% and 12% at day four and five, respectively, in the CD19-Cre control cells. In the SENP1<sup>ff</sup> CD19-Cre cells, however, MHCII expression stays at around 95% to 90%, indicating a constant high state of activation.

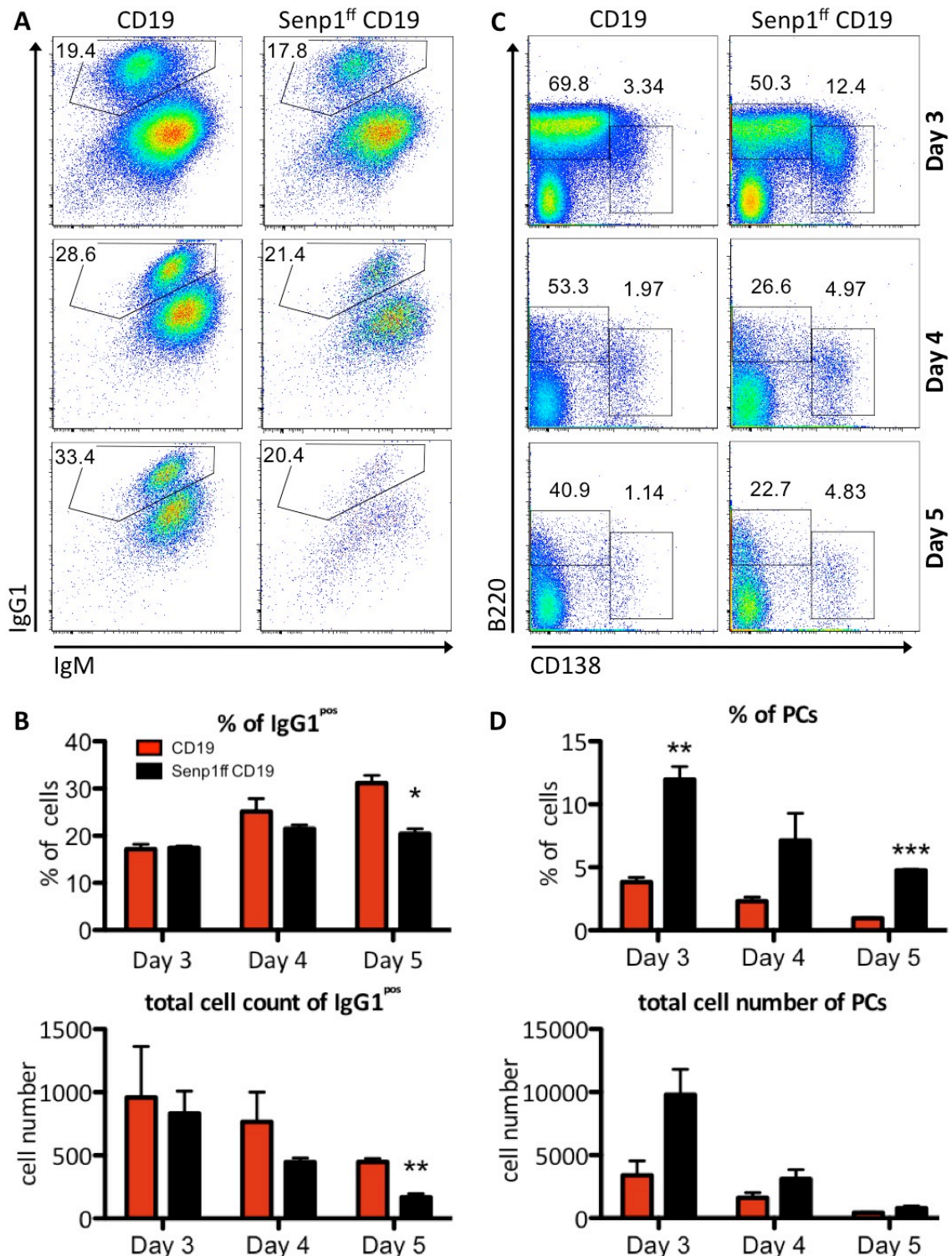


**Figure 3-11: *in vitro* CSR and PC differentiation of total splenocyte culture.** Total splenocytes after erythrocyte lysis of indicated genotypes were stimulated with LPS and IL4 to induce class switch recombination (CSR) and plasma cell (PC) differentiation and were analysed on day three, four and five. (A) FACS analysis of class switched cells. Cells were surface stained for IgG1, IgM and popro1. (B) Statistical evaluation of IgG1 switched cells. Top: percentage of cell population; bottom: number of cells per population. (C) FACS analysis of differentiated PCs. Cells were surface stained for B220, CD138 and popro1. (D) Statistical evaluation of PCs. Top: percentage of cell population; bottom: number of cells per population. For each group n=3; \* p<0,05, \*\* p<0,01, \*\*\* p<0,001



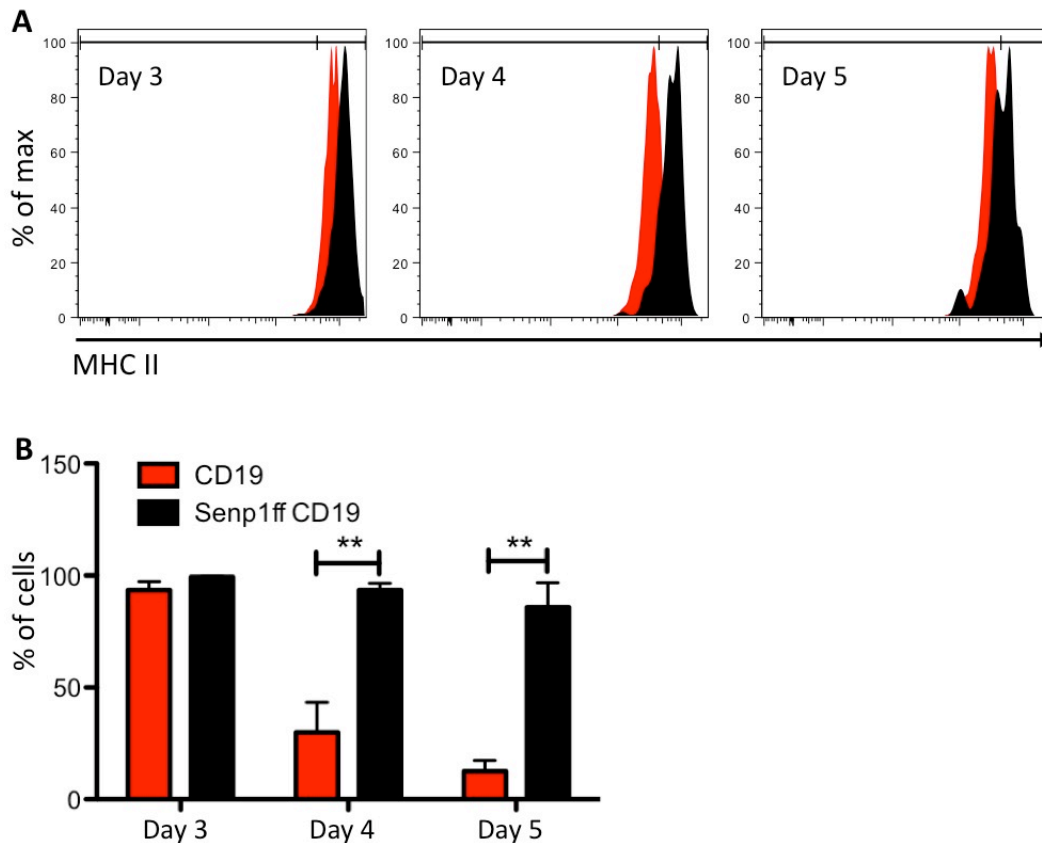


**Figure 3-12: MHC II expression after *in vitro* stimulation.** CD19 MACS isolated B cells of indicated genotypes were stimulated with LPS (50 $\mu$ g/ml) and IL4 (20ng/ml) and were analysed on day three, four and five. (A) FACS analysis of class switched cells. Cells were surface stained for MHC II and pregated on B220<sup>+</sup>popro1<sup>-</sup> cells (B) Statistical evaluation of MHC II expression. For each group n=3; \* p<0,05, \*\* p<0,01, \*\*\* p<0,001

Taken together, our data demonstrated in Figure 3-8 to Figure 3-12 that upon LPS and IL4 stimulation SENP1 deficiency increases apoptosis in B cells, either by positively upregulating pro-apoptotic factors or by dysfunctional anti-apoptotic pathways in response to activation. Altogether, we observed that after a first burst of proliferation SENP1 KO cells as well as SENP1<sup>ff</sup> cells have a decreased survival capacity. SENP1 KO or hypomorph cells undergo 10% more apoptosis on day two after stimulation. From day three on we observed a significant reduction in total cell number of SENP1 KO B cells, in SENP1 hypomorphs from day four on. However, the B cells that survived do proliferate as WT when analysed by cell proliferation dye over a course of four days.

SENP1 KO and hypomorph B cells develop stronger into PCs and less into IgG1 positive B cells (Figure 3-11). However, the question still remains on the origin of

these PCs. As SENP1 hypomorph cells also produce more PCs it is likely that the phenotype comes from B cells that survive a SENP1 KO or SENP1 hypomorph. These cells are then more prone to PC development. To test these hypotheses we crossed the SENP1<sup>ff</sup> CD19-Cre line to an RFP reporter mouse line, which will enable us to observe the Cre activity and therefore the knock-out and escapee rate of SENP1 in any CD19 expressing cell type.

### *3.1.5 Reduction of B cell subsets in naive JHT<sup>-/-</sup>/SENP1<sup>ff</sup>RFP CD19-Cre mixed bone marrow chimeras*

As cells harbouring the hypomorphic SENP1<sup>flox</sup> allele exhibit a knockout-like phenotype in B cells, and as SUMOylation is a ubiquitous cellular regulatory mechanism, consequences in other cell types and organs can be expected. To exclude these effects and to solely investigate a B cell specific SENP1 knockout we generated mixed BM chimeras (Figure 3-13).

B cell deficient JHT<sup>-/-</sup> mice with a disruption in V<sub>H</sub>-D<sub>H</sub>-J<sub>H</sub> recombination were selected as hosts. JHT<sup>-/-</sup> mice harbour a deletion of the J<sub>H</sub> gene for antibody heavy chain production (Gu et al., 1993). This mutation disrupts proper BCR production as V<sub>H</sub>-D<sub>H</sub>-J<sub>H</sub> somatic recombination is non-functional, therefore B cell development is stopped at the pre-pro B cell stage, making these mice an excellent model for B cell deficiency.

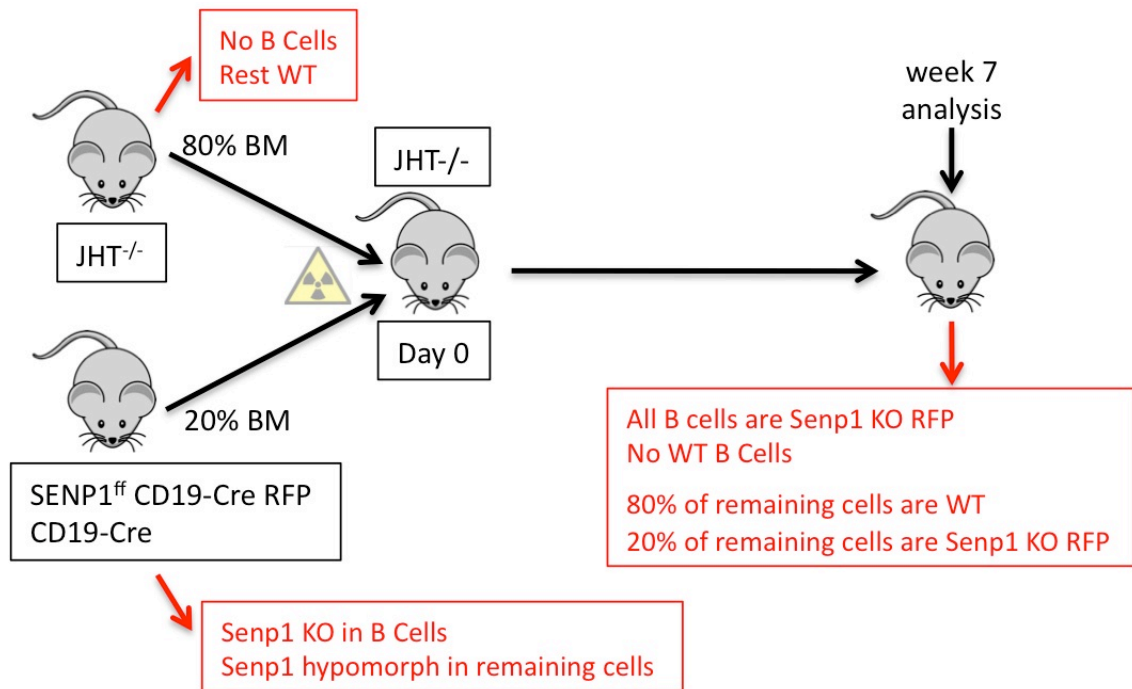


**Figure 3-13: Schematic of mixed bone marrow chimera generation.** Bone marrow (BM) of donor mice was isolated and mixed in a 80:20 ratio of JHT<sup>-/-</sup> and SENP1<sup>ff</sup> RFP CD19-Cre BM (and respective control). Host mice were lethally irradiated with 9,5 Gy and i.v. injected with the donor BM mix. Seven weeks post transfer mice were analysed.

For this, the SENP1<sup>ff</sup> CD19-Cre mouse strain was crossed to a ROSA-RFP strain, which expresses the RFP behind a loxP flanked stop cassette after the ROSA gene promoter. Upon Cre-mediated recombination the stop cassette is excised and RFP will be constitutively expressed. By facilitating this system the Cre recombination activity on the SENP1<sup>lox</sup> locus will be reported and Cre escapees can be detected. The BM chimeras were generated from isolated BM from JHT<sup>-/-</sup> mice and SENP1<sup>ff</sup> RFP CD19-Cre, with the respective CD19-Cre controls.

BM was mixed in an 80% to 20% ratio (JHT with SENP1<sup>ff</sup> RFP CD19-Cre or JHT with CD19-Cre) and a total of  $5 \times 10^6$  cells were i.v. injected into previously irradiated JHT<sup>-/-</sup> host mice (Figure 3-13). Mice were analysed between week seven and eight after reconstitution. All B cells of the reconstituted mice were SENP1<sup>ff</sup> RFP CD19-Cre or if they escaped Cre mediated recombination they were RFP negative SENP1<sup>ff</sup> escapees with the hypomorphic SENP1 phenotype. However, only 20% of the remaining cell populations harboured the hypomorph, whereas 80% were WT of the JHT<sup>-/-</sup> origin. The 20% of SENP1<sup>ff</sup> BM cells generate no

measurable phenotype in the non-B cell myeloid cell compartment (data not shown).

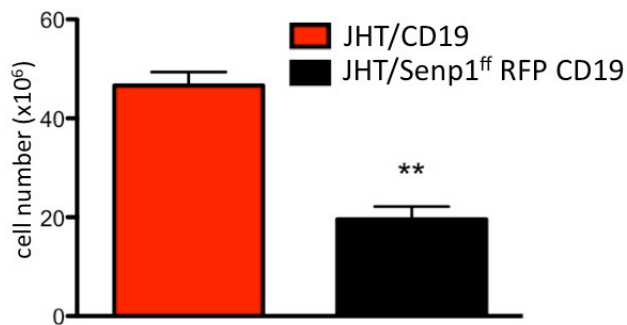


**Figure 3-14: Total cell number of splenocytes in JHT/SENP1<sup>ff</sup> RFP CD19 bone marrow chimeras 8 weeks after reconstitution.** For each group n=4; \* p<0,05, \*\* p<0,01, \*\*\* p<0,001

The 80% to 20% ratio of BM mix was chosen as in mice reconstituted with a 90% to 10% ratio no SENP1<sup>ff</sup> RFP CD19-Cre could be reconstituted and in the respective CD19-Cre controls only a small amount of B cells was observed (data not shown) As the 80% to 20% ratio produced higher and more reliable B cell numbers this protocol was chosen for further experiments. Reconstituted mice will be termed JHT/SENP1<sup>ff</sup> RFP CD19-Cre for the 80% JHT with 20% SENP1<sup>ff</sup> RFP CD19-Cre mix and JHT/CD19-Cre for the 80% JHT with 20% CD19-Cre mix.

Figure 3-14 shows the total number of splenocytes, eight weeks after BM chimera generation. Total splenocyte numbers were significantly reduced by approximately 60%. By FACS analysis we could show that this reduction is caused by an 8 fold reduction in the total B cell population and a 30% reduction of the total T cell population (Figure 3-15). In percentage as well as in total.

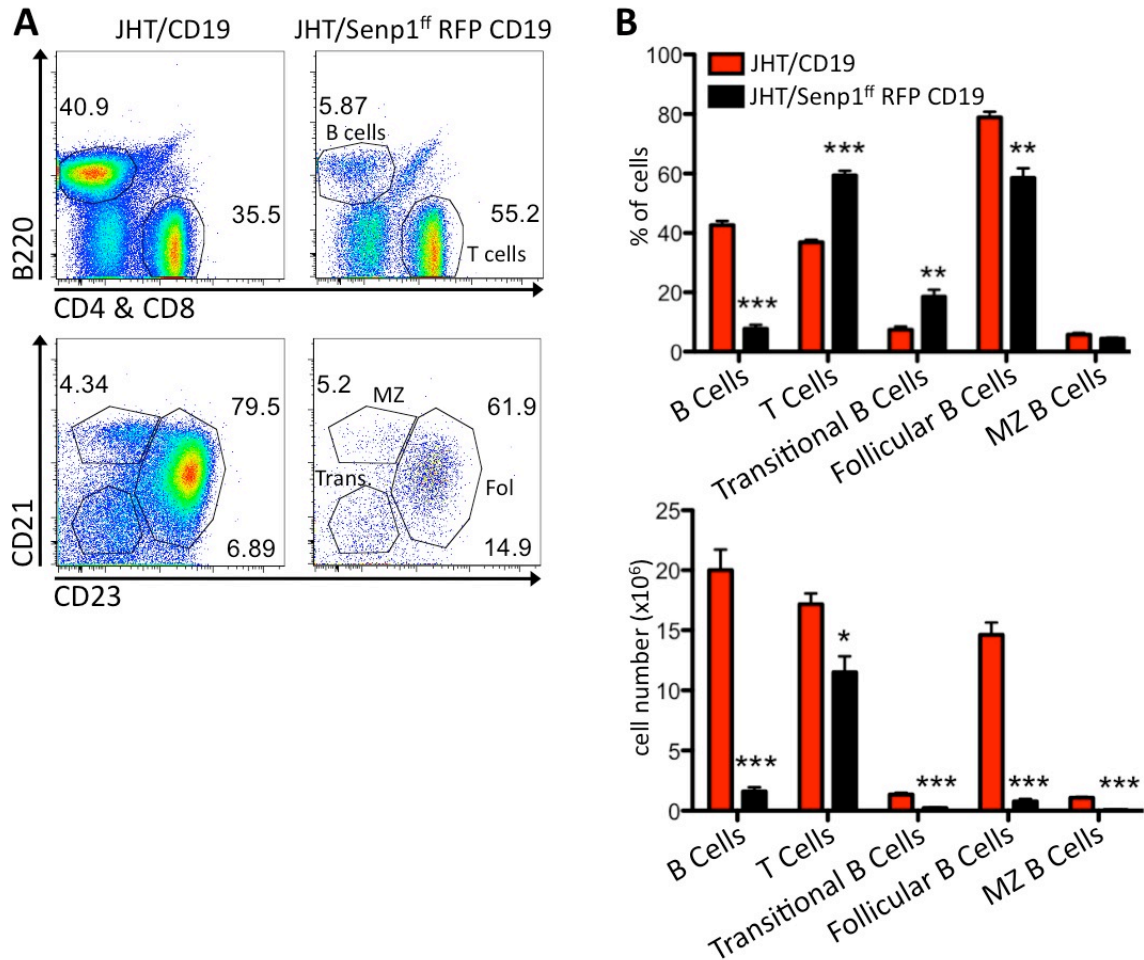


**Figure 3-15: B cell subsets in the spleen of JHT/SEN1<sup>ff</sup> RFP CD19 bone marrow chimeras 8 weeks after reconstitution.** (A) FACS analysis of naive splenocytes of indicated genotypes. Cells were analysed for the expression of B220 and CD4 & CD8, as well as CD21 and CD23 surface markers after pre-gating on popro1<sup>-</sup> and B220<sup>+</sup>popro1<sup>-</sup> cells, respectively. (B) Statistical evaluation of splenic B cell subsets. Left, percentage of cell population, right, number of cells per population. For each group n=4; \* p<0,05, \*\* p<0,01, \*\*\* p<0,001

As seen in the FACS blots and the statistical analysis of the B cell populations in Figure 3-15 only few B cells are remaining in the spleen of the JHT/SEN1<sup>ff</sup> RFP CD19-Cre mice, most of them representing follicular B cells. The percentage of B cell subsets in the spleen is similar to that seen in naïve SEN1<sup>ff</sup> CD19-Cre mice (Figure 3-3). The percentage of transitional B cells is significantly increased and of follicular B cells significantly decreased, whereas the ratio of MZ B cells is not changed compared to the JHT/CD19-Cre control. In naïve SEN1<sup>ff</sup> CD19-Cre mice  $2 \times 10^6$  transitional B cells,  $12 \times 10^6$  follicular B cells and  $2 \times 10^6$  MZ B cells remain in the spleen, whereas in the JHT/SEN1<sup>ff</sup> RFP CD19-Cre only  $2 \times 10^5$  transitional B cells,  $7.5 \times 10^5$  follicular and  $5 \times 10^4$  MZ B cells can be found (Figure 3-15). This

general reduction of B cells in the JHT/SEN1<sup>ff</sup> RFP CD19-Cre compared to the naïve SEN1<sup>ff</sup> CD19-Cre can be explained by the general survival problem of the SEN1<sup>ff</sup> RFP CD19-Cre B cells, which on one hand might have problems in surviving the procedure of the transfer and on the other hand will die after the transfer.

Figure 3-16 and Figure 3-17 investigate B cell subsets in more detail. The gating strategy applied here is adapted from Allman and Pillai (2008). Here can be seen that the total cell number of all B cell subsets is drastically reduced, between five fold in transitional T2 B cells (AA4.1<sup>+</sup> CD23<sup>+</sup> IgM<sup>+</sup>), and 40 fold in follicular I B cells (B220<sup>+</sup> AA4.1<sup>-</sup> CD21<sup>low</sup> IgM<sup>+</sup> IgD<sup>+</sup>). The percentages of all subsets except immature B cells (B220<sup>+</sup> AA4.1<sup>+</sup>), MZ precursor B cells (B220<sup>+</sup> AA4.1<sup>-</sup> CD21<sup>+</sup> IgM<sup>+</sup> CD23<sup>+</sup>) MZ B cells (B220<sup>+</sup> AA4.1<sup>-</sup> CD21<sup>+</sup> IgM<sup>+</sup> CD23<sup>-</sup>), follicular II (B220<sup>+</sup> AA4.1<sup>-</sup> CD21<sup>low</sup> IgM<sup>low</sup> IgD<sup>+</sup>) and transitional T1 (B220<sup>+</sup> AA4.1<sup>+</sup> CD23<sup>-</sup> IgM<sup>+</sup>) and transitional T2 (B220<sup>+</sup> AA4.1<sup>+</sup> CD23<sup>+</sup> IgM<sup>+</sup>) B cells are significantly decreased. The increase in the latter can be explained by three factors: a developmental block at these cell stages, a stronger rate of apoptosis in the subsequent cell populations, or it might be due to an artefact that is generated through the drastic shift in cell number and ratio between the cell populations. With such a drastic reduction in total cell numbers throughout all B cell subsets the significant changes in ratios between the different subsets is not convincing.

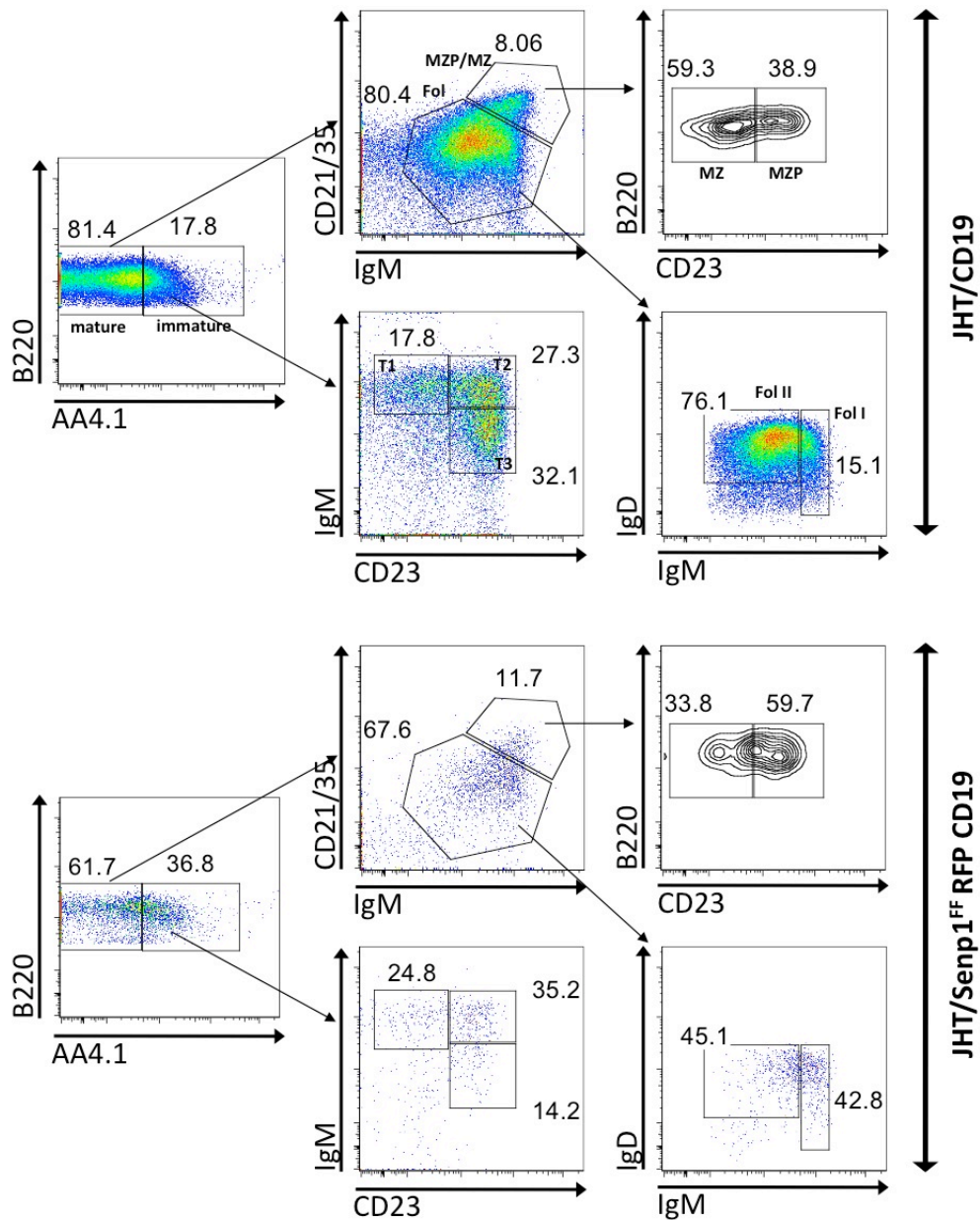


**Figure 3-16: B cell subsets in the spleen of JHT/SEN1<sup>ff</sup> RFP CD19 bone marrow chimeras 8 weeks after reconstitution.** FACS analysis of naive splenocytes of indicated genotypes. Cells were pregated on B220<sup>+</sup>popro1<sup>-</sup> cells and further as indicated in graph. Respective statistical analysis is shown in **Figure 3-17**. For each group n=4

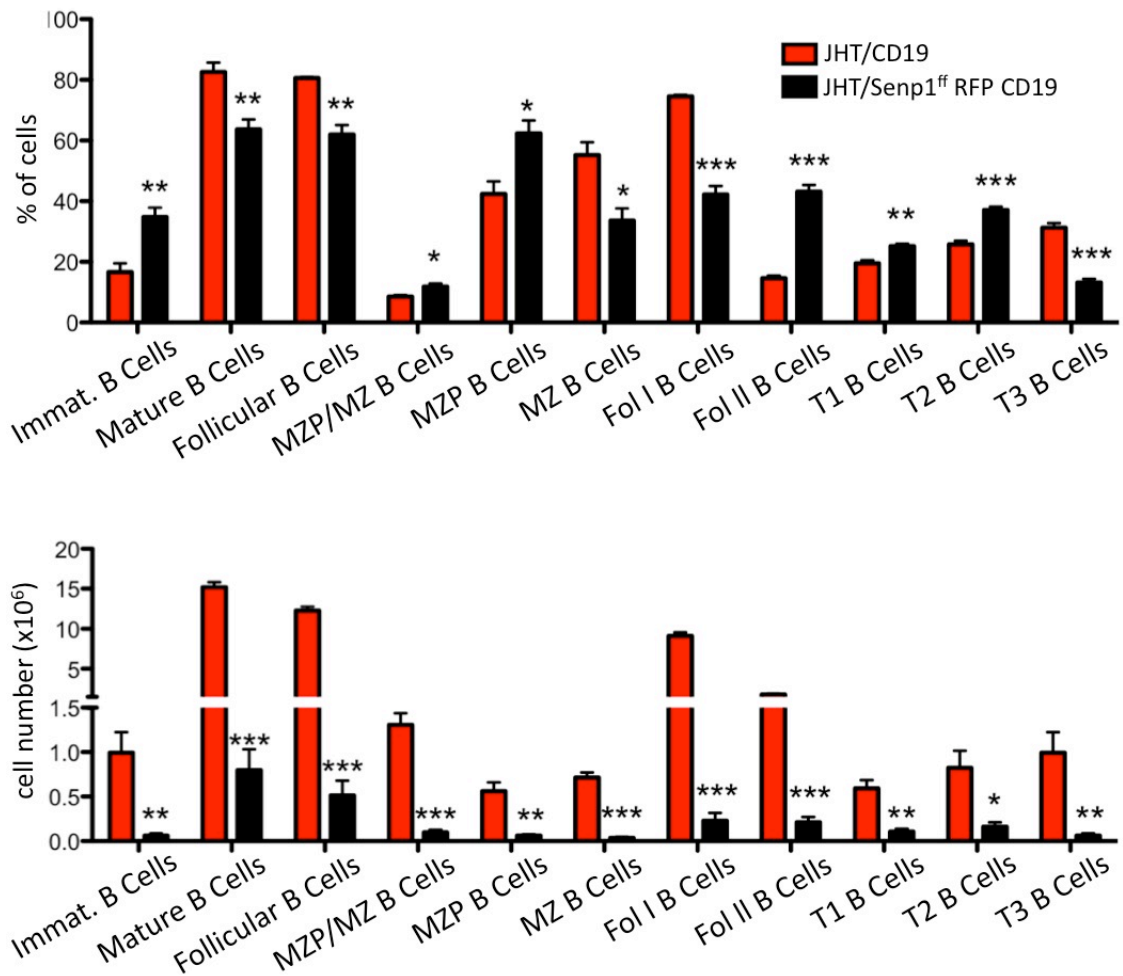


**Figure 3-17: Statistical analysis of B cell subsets in the spleen of JHT/SEN1<sup>ff</sup> RFP CD19 bone marrow chimeras 8 weeks after reconstitution, as depicted in Figure 3-16. Upper panel, percentage of cell population, lower panel, number of cells per population. For each group n=4; \* p<0,05, \*\* p<0,01, \*\*\* p<0,001**

About 95% of lymph node (LN) B cells in wild type mice are fully matured, therefore express besides IgM also IgD and have lost the surface expression for AA4.1 (also known as CD93), an adhesion protein. In JHT/SEN1<sup>ff</sup> RFP CD19-Cre mice, however, the percentage of immature B cells is nearly triple of that of the JHT/CD19-Cre controls (Figure 3-18). Usually B cells leave the BM in a naive immature stage and fully develop in the spleen (Johnson et al., 2005). But high numbers of immature B cells in the LN indicate that either B cell maturation is slower than in WT or that there is some sort of developmental blockage, albeit mild, as full maturation can be achieved.



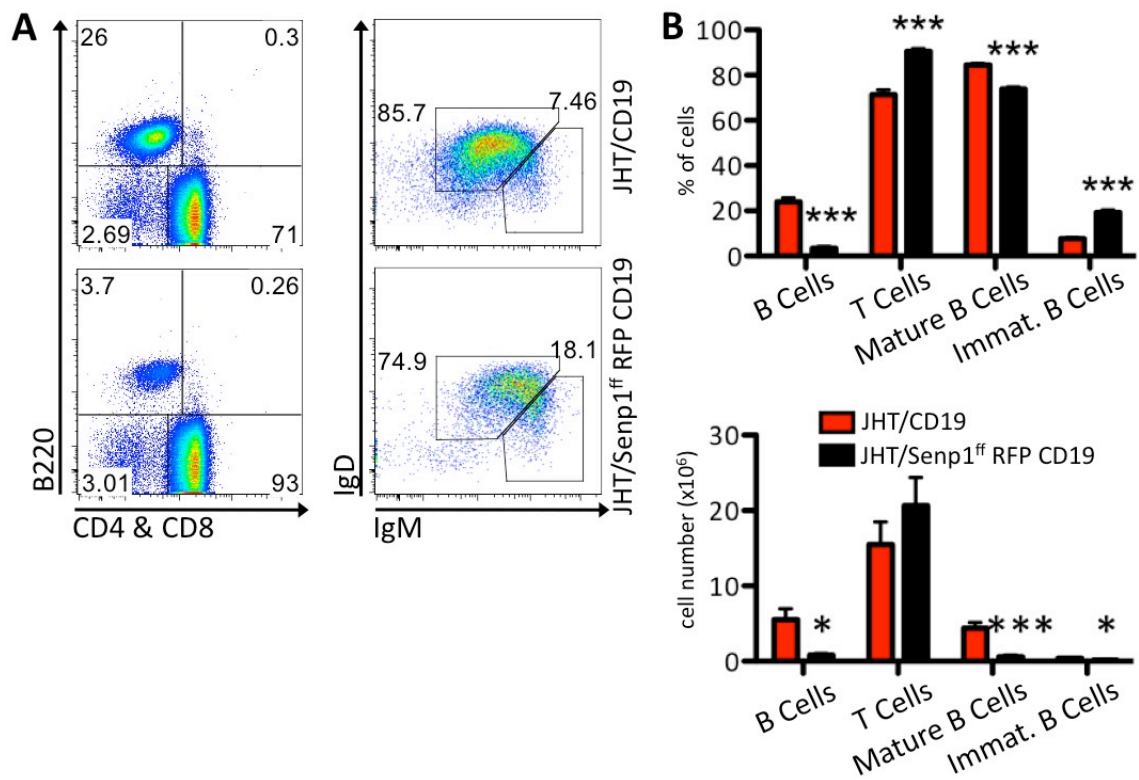


**Figure 3-18: B cell subsets in the lymph nodes (LN) of JHT/SEN1<sup>ff</sup> RFP CD19 bone marrow chimeras 8 weeks after reconstitution.** (A) FACS analysis of LN of indicated genotypes. Cells were analysed for the expression of B220 and CD4 & CD8, as well as IgM and IgD surface markers after pre-gating on popro1<sup>-</sup> and B220<sup>+</sup>popro1<sup>-</sup> cells, respectively. (B) Statistical evaluation of B cell subsets. Left, percentage of cell population, right, number of cells per population. For each group n=4; \* p<0,05, \*\* p<0,01, \*\*\* p<0,001

Interestingly, in the PP and the peritoneal cavity (PC) of JHT/SEN1<sup>ff</sup> RFP CD19-Cre mice B cells were completely absent (Figure 3-19). Both organs, the PP on the epithelium of the small intestine, and the PC, enclosing all intestinal organs, contain large amounts of foreign antigen leading to B cell activation. This antigen encounter may lead to AICD as already shown *in vivo* in Figure 3-9.

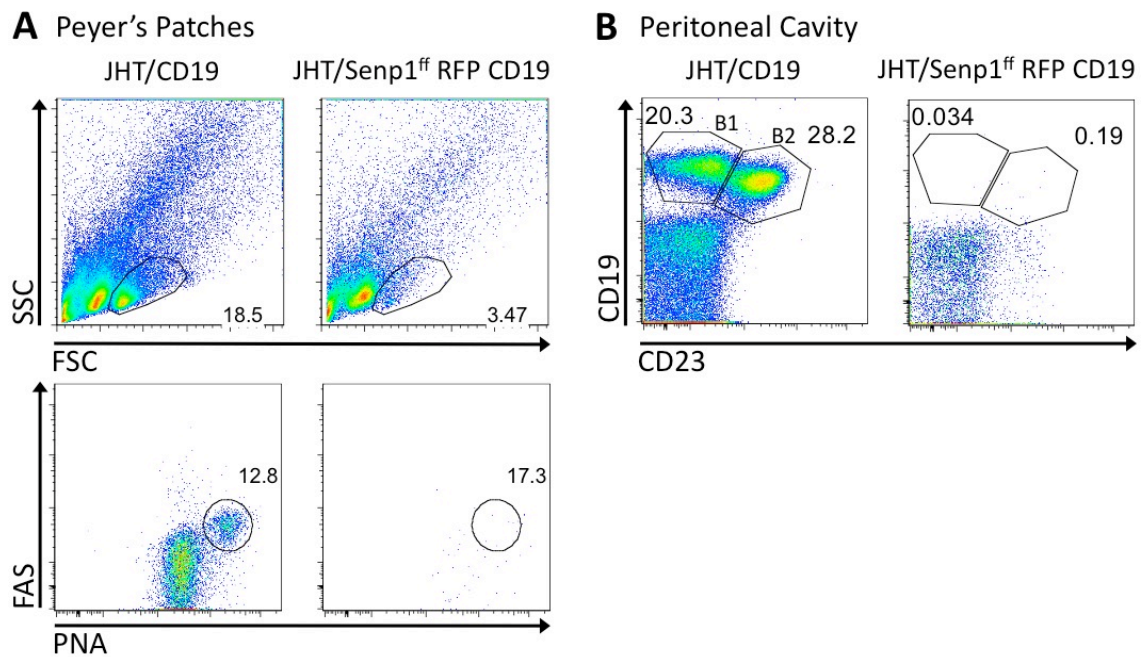


**Figure 3-19: B cells in the Peyer's patches (PP) and peritoneal cavity (PC) of naive JHT/SEN1<sup>ff</sup> RFP CD19 bone marrow chimeras 8 weeks after reconstitution.** (A) FACS analysis of PP of indicated genotypes. Cells were analysed for the forward and side scatter and expression of Fas and PNA surface markers after pre-gating on B220<sup>+</sup>popro1<sup>-</sup> cells. (B) FACS analysis of PC of indicated genotypes. Cells were analysed for the expression of CD19 and CD23 surface markers after pre-gating on popro1<sup>-</sup> cells. For each group n=4; \* p<0,05, \*\* p<0,01, \*\*\* p<0,001

Crossing the SENP1<sup>ff</sup> CD19-Cre mouse to a RFP reporter mouse strain gave the opportunity to analyse the ratio of SENP1 KO cells in a given population. As Rickert et al. (1997) reported, the efficiency of the CD19-Cre is 75-80% in BM-derived pre-B cells and 90-95% in splenic B cells. The remaining cells still have the floxed WT alleles, in the case of the SENP1<sup>ff</sup> RFP CD19-Cre mouse the Cre escapees will have the SENP1 hypomorph phenotype. As shown in various previous experiments SENP1<sup>ff</sup> CD19-Cre mice and SENP1<sup>ff</sup> mice have reduced B cell numbers, due to so far unknown reasons. By analysing the RFP expression in the SENP1<sup>ff</sup> RFP CD19-Cre mice it can be investigated how many B cells actually survive of SENP1 knock out B cells.

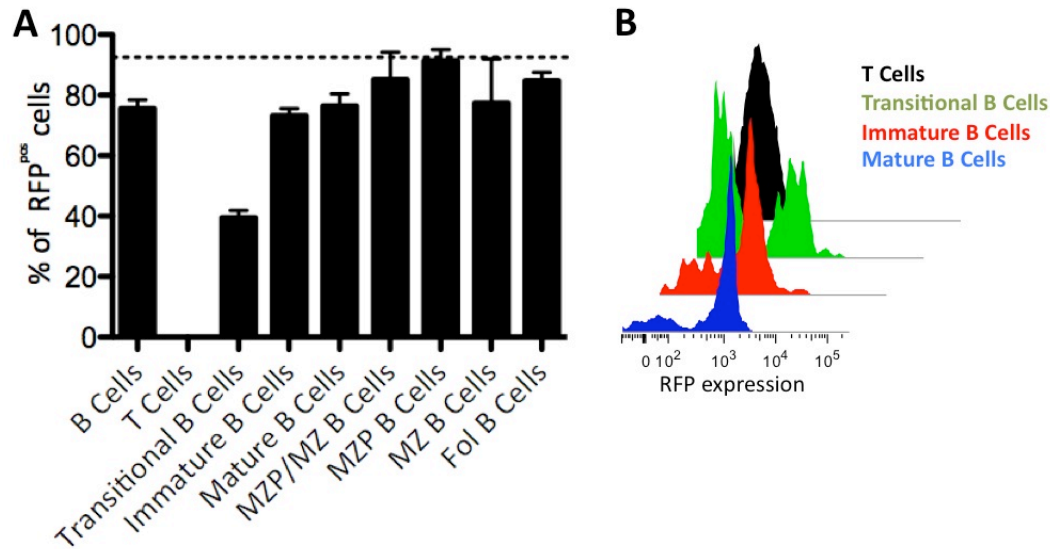


**Figure 3-20: Analysis of RFP expression in splenic B cells of naive JHT/SENP1<sup>ff</sup> RFP CD19 bone marrow chimeras 8 weeks after reconstitution.** (A) Statistical analysis of RFP expression, dotted line represents 92,4% Cre efficiency in WT (B) FACS analysis of RFP expression in B cell populations of indicated genotypes. Cells were analysed for RFP expression after gating on B220 and CD4 & CD8 as well as AA4.1 surface markers for the different B and T cell populations and after pregating on popro1<sup>-</sup> cells. For each group n=4; \* p<0,05, \*\* p<0,01, \*\*\* p<0,001

Figure 3-20 shows the expression levels of RFP in various subpopulations of splenic B cells. The dotted line in each bar graph represents the average Cre efficiency of WT splenic B cells (92,4%, Rickert *et al.*, 1997). As expected, T cells express no RFP, stating that the CD19-Cre is B cell specific.

It is important to note, when comparing RFP positive to RFP negative cells in Figure 3-20, that the RFP negative Cre escapee cells represent SENP1 hypomorphic cells and not CD19-Cre WT cells.

Observing the different B cell subsets in detail, it can be seen that transitional B cell in the spleen, which just arrived from the BM and have not further developed to Fol B cells or MZ B cells show RFP expression of 40% (Figure 3-20). This is about half of the expected Cre efficiency that has been shown by Rickert *et al.* (1997) for WT BM B cells. This indicates that early SENP1 KO B cells in the BM and spleen are under strong selection pressure compared to the SENP1 hypomorphic cells, meaning that cells that escape the Cre mediated recombination have a survival and proliferation advantage. However, when looking at subsequent B cell developmental stages it can be observed that RFP expression is increasing.

Immature and mature JHT/SENP1<sup>ff</sup> RFP CD19-Cre B cells express 75% and 80% RFP, respectively, and MZ and Fol B cell in average around 90% RFP. This indicates that SENP1 KO B cells, which survive the early stages of B cell development have either a survival advantage or increased proliferation compared to the SENP1 hypomorphic RFP negative Cre escapee cells.

### 3.1.6 *SENP1<sup>ff</sup> CD19-Cre mice experience a higher B cell turnover*

*In vivo* experiments so far show significantly reduced B cell numbers specifically in Fol B cells (Figure 3-3 & Figure 3-15). To investigate whether this is caused by an increased rate of apoptosis, as indicated in *in vitro* experiments (Figure 3-9) or a failure to differentiate into Fol B cells, mice were *in vivo* labelled with BrdU. BrdU is a synthetic analogue of thymidine, which incorporates into the newly synthesised DNA during S-phase replication. BrdU is passed on to the daughter cell and accumulates with every cell division. Therefore, the more BrdU is integrated in a given cell, the more cell cycles has a cell undergone. In this way, cell proliferation and turnover rate can be measured, which indirectly gives clues about the apoptosis rate of a cell population

BrdU was applied through the drinking water to SENP1<sup>ff</sup> CD19-Cre mice and CD19-Cre controls for the duration of one week. The ratio of BrdU positive cells in the spleen is measured by FACS analysis eight days after first feeding.

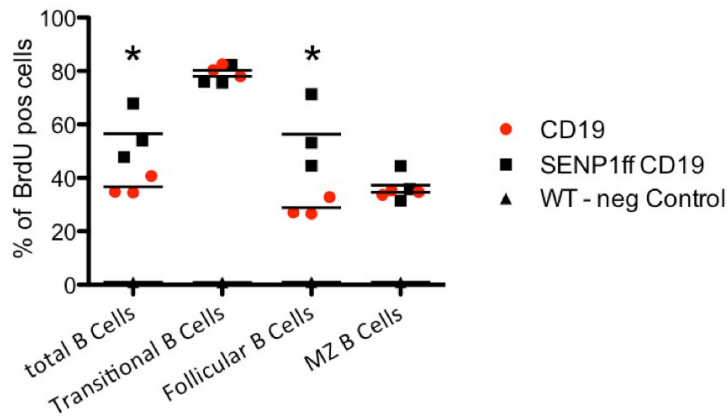


**Figure 3-21: *in vivo* BrdU incorporation indicates increased B cell turnover.** FACS analysis of BrdU incorporation in B cells after feeding BrdU in drinking water for eight days. For each group n=3; \* p<0,05, \*\* p<0,01, \*\*\* p<0,001

As seen in Figure 3-21, SENP1<sup>ff</sup> CD19-Cre B cells incorporate 1,5 fold more BrdU into their DNA than the CD19-Cre controls. Looking at further B cell subsets it was observed that Fol B cells incorporate in average even two fold more BrdU compared to controls. Ratios for transitional and MZ B cells were similar. This leads to the conclusion that Fol B cells have a decreased half-life and an increased rate of cell turnover. As Fol B cell numbers in naïve and in BM chimeric mice are significantly reduced (Figure 3-3 & Figure 3-15), but also show an increased BrdU uptake, therefore turnover, this data supports the hypothesis that reduced B cell numbers come from a increased rate of apoptosis and not from an inability to form Fol B cells.

### 3.1.7 Block of de novo B cell generation through *IL7R* treatment results in B cell reduction

B cells are generated in the BM and migrate into the periphery after maturation. The peripheral B cell pool needs constant replenishing by a continuous stream of B cells out of the BM. To further test the survival capacity of SENP1<sup>ff</sup> CD19-Cre B cells after Cre mediated deletion mice were treated with an antagonistic antibody treatment with monoclonal  $\alpha$ IL7R antibodies. IL7R is crucial for early B cell survival and subsequent development in the BM. Without IL7R signalling no new B cells can be formed and the survival capacity of the remaining peripheral B cells can be measured.

JHT/SEN1<sup>ff</sup> CD19-Cre BM chimeric mice and the respective JHT/CD19-Cre control mice were injected every second day with  $\alpha$ IL7R for 14 days and were analysed on day 16. After two weeks of treatment a substantial loss of peripheral B cell populations compared to the untreated controls was measurable (Figure 3-22), showing once more the reduced survival capacities of all B cells with impaired deSUMOylation in SEN1<sup>ff</sup> CD19-Cre mice.

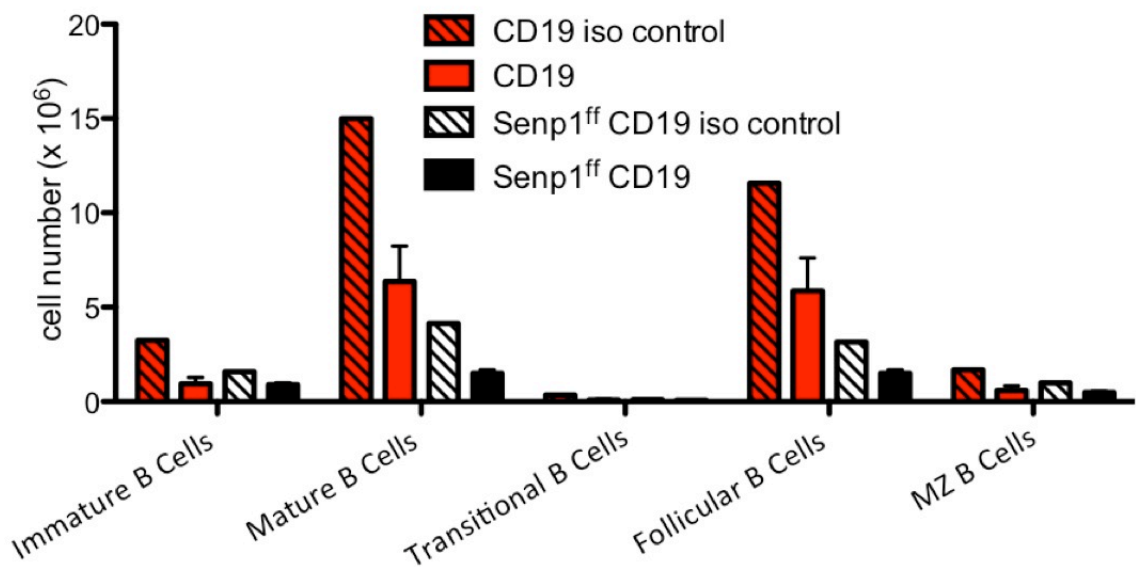


**Figure 3-22: Block of *de novo* B cell generation through *in vivo*  $\alpha$ IL7R treatment.** FACS analysis of different splenic B cell subsets in mice of indicated genotypes 16 days after  $\alpha$ IL7R treatment or isotype control treatment (striped bars). For each group of the  $\alpha$ IL7R treated mice n=3, For each group of the isotype control treated mice n=1; \* p<0,05, \*\* p<0,01, \*\*\* p<0,001

### 3.1.8 Sheep red blood cell immunization of JHT/SEN1<sup>ff</sup> CD19-Cre bone marrow chimeras

To this point the SEN1<sup>ff</sup> CD19-Cre mouse strain has been investigated under several different *in vivo* and *in vitro* aspects. In the following experiment we assessed the immune response of SEN1 KO B cells to a T cell dependant immunization with sheep red blood cells (SRBC). The SRBC immunization was undertaken in the mixed BM chimera model that was introduced in chapter 3.1.5 with the exception that SEN1<sup>ff</sup> CD19-Cre mice did not contain the ROSA-RFP reporter gene (Figure 3-23). The process of BM chimera generation was as

described above. Fully reconstituted mice were immunized with SRBC in week 7 and sacrificed 14 days post immunization.

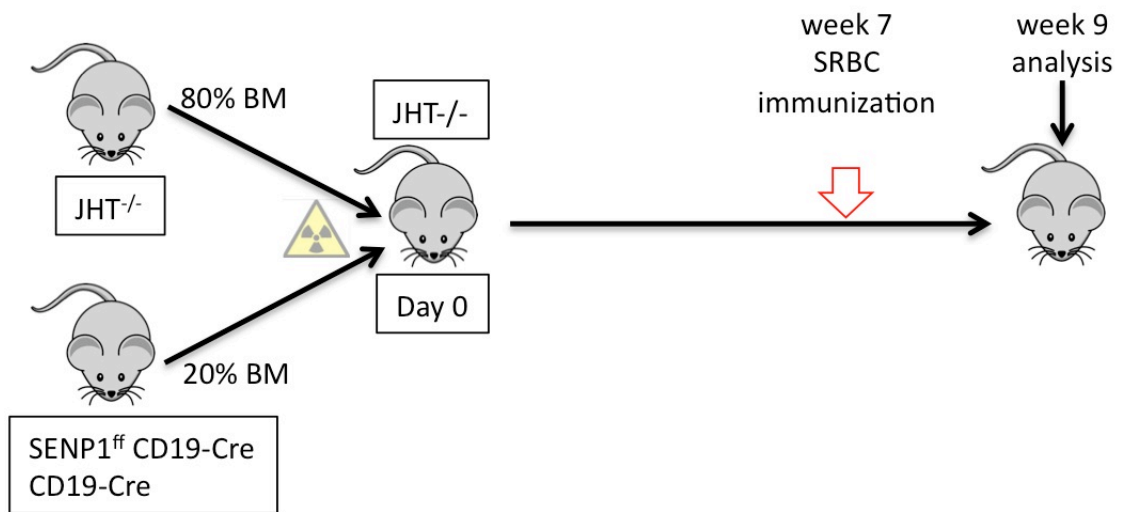


**Figure 3-23: Schematic of mixed bone marrow chimera generation.** Bone marrow (BM) of donor mice was isolated and mixed in a 80:20 ratio of  $JHT^{-/-}$  and  $SENP1^{ff} CD19-Cre$  BM (and respective control). Host mice were lethally irradiated with 9,5 Gy and i.v. injected with the donor BM mix. Seven weeks post transfer mice were immunized with  $1 \times 10^8$  Sheep red blood cells (SRBC) and analysed 14 days post immunization

The model of SRBC immunization enables the investigation of B cell response to foreign antigens by overloading the immune system with the latter. The whole primary humoral immune response can be observed, whereas our particular interest is the formation of germinal centres in the spleen, IgG1 CSR and subsequent short lived plasma cell development. Within the timeframe of this experiment no changes in long lived plasma cells in the BM can be observed, as long lived PC development takes longer than 14 days.

Figure 3-24 depicts the total cell count of BM and spleen cells of  $JHT/SENP1^{ff} CD19-Cre$  mice compared to  $JHT/CD19-Cre$  control mice. BM cell numbers were slightly reduced in  $JHT/SENP1^{ff} CD19-Cre$  mice, whereas again the splenic cell count was significantly reduced by about 25% compared to the  $CD19-Cre$  control.

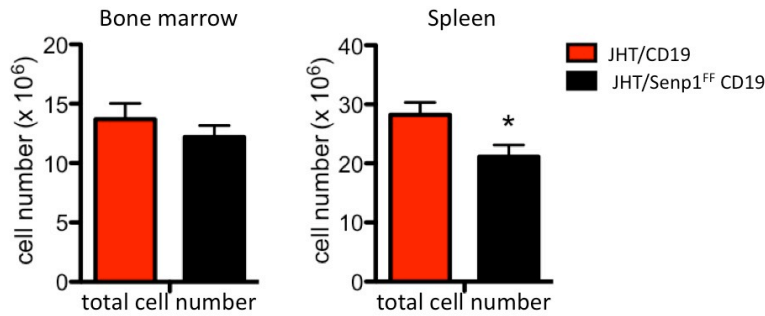


**Figure 3-24: Total cell number of all bone marrow and spleen cells in JHT/SENP1<sup>ff</sup> CD19-Cre mice after SRBC immunization.** Bone marrow numbers represent the cellular content of one femur and splenic cell numbers represent a whole spleen, both after erythrocyte lysis. For each group n=4; \* p<0,05, \*\* p<0,01, \*\*\* p<0,001

As shown now in different experiments splenic B cell numbers are significantly reduced. In the case of the BM in Figure 3-25A & B a significant reduction by 50% can be observed for the mature recirculating B cell population in the JHT/SENP1<sup>ff</sup> CD19-Cre mice, by percentage and total cell number. This population has homed back to the BM after having matured in the periphery. Pro, Pre and naive B cell populations are not significantly changed. SENP1 KO starts at the pro B cell stage, with first expression of CD19, however due to fast proliferation throughout the early B cell stages, Cre activity and therefore SENP1 absence is only fully achieved in the spleen. As shown in Figure 3-20 60% of the immature B cell population are SENP1<sup>ff</sup> hypomorph Cre escapees with a selective survival advantage over the SENP1<sup>ff</sup> KO cells.

As mentioned above, no change in the very small population of long lived plasma cells can be observed in the BM (Figure 3-25C & D). As JHT mice lack all B cell populations from the pro B cell stage on, they do not have any plasma cells. The timeframe for the transferred SENP1<sup>ff</sup> CD19-Cre cells to differentiate into long lived plasma cells and home to the BM is too long for the scope of this experiment. Hence, no long lived PCs can be expected in the BM at time of sacrifice.



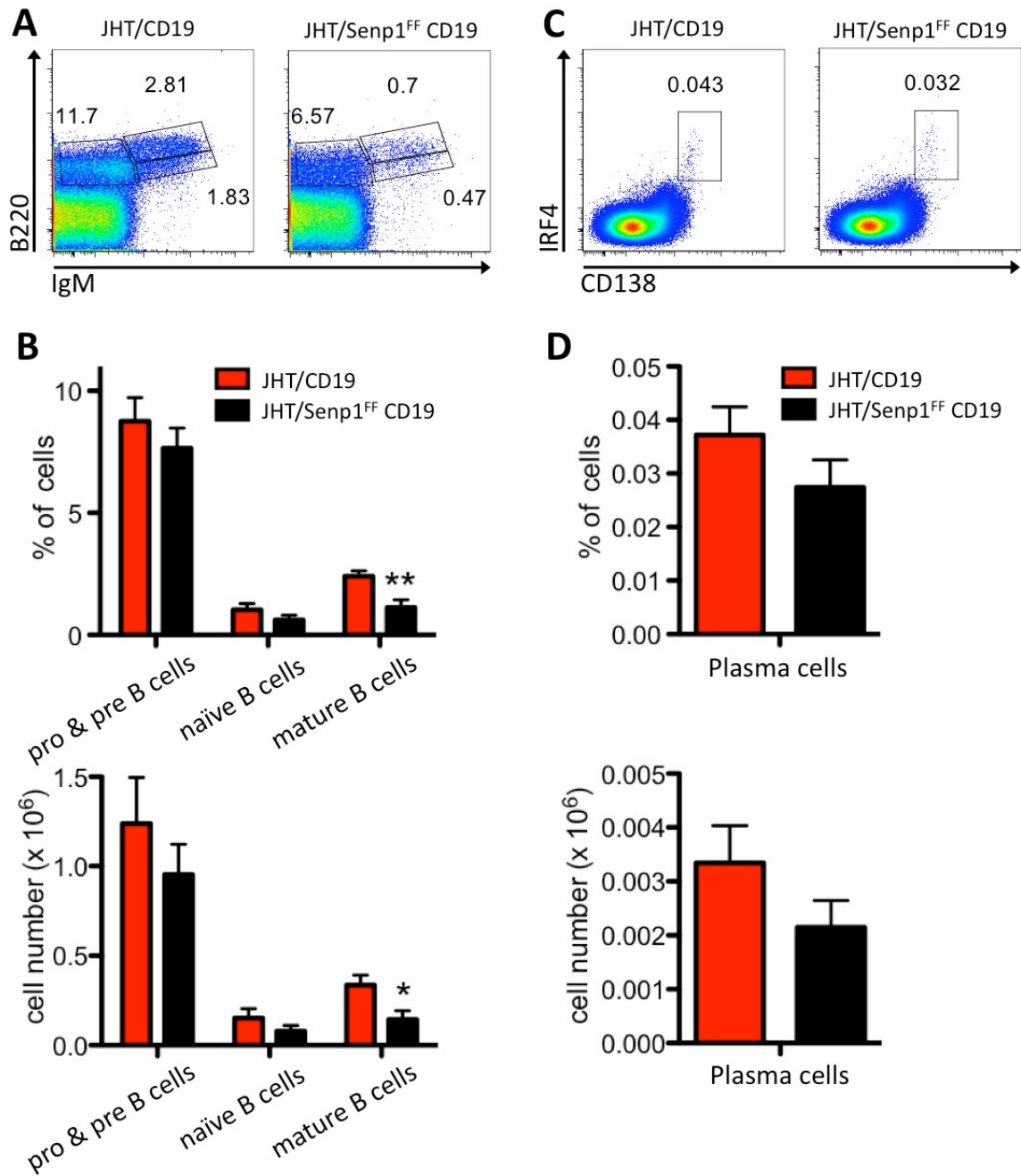


**Figure 3-25: B cell subsets in the BM of JHT/SEN1<sup>ff</sup> CD19 bone marrow chimeras after SRBC immunization.** FACS analysis of BM B cell subsets in SRBC immunized mice of indicated genotypes. Cells were pregated on B220<sup>+</sup>popro1<sup>-</sup> (A) and B220<sup>+</sup>fixable viability dye<sup>®</sup>- and further as indicated in graph. A & B show analysis of the pro and pre B cell population (B220<sup>+</sup>IgM<sup>-</sup>), the subsequent naïve population (B220<sup>+</sup>IgM<sup>+</sup>) and the recirculating mature B cells (B220<sup>+</sup>IgM<sup>high</sup>), that have returned from the periphery. C & D show the analysis on long lived BM plasma cells by intracellular staining for IRF4. For each group n=4; \* p<0,05, \*\* p<0,01, \*\*\* p<0,001

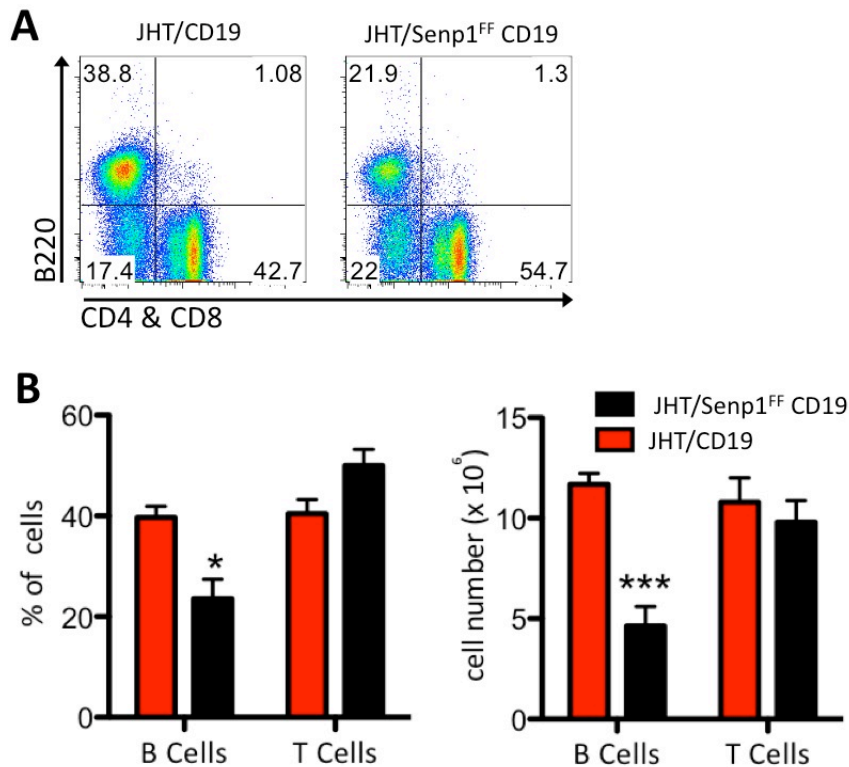


**Figure 3-26 Splenic B cell populations in SRBC immunized JHT/SEN1<sup>ff</sup> CD19-Cre BM chimeras.** FACS analysis of B/T cell ration in the spleen of SRBC immunized JHT/SEN1<sup>ff</sup> CD19-Cre BM chimeras of indicated genotypes. Cells were analysed for B220 and CD4 & CD8 surface markers after pre-gating on popro1-cells. (B) Statistical analysis, left, percent of population, right, total cell count of population. For each group n=4; \* p<0,05, \*\* p<0,01, \*\*\* p<0,001

In the spleen of the JHT/SEN1<sup>ff</sup> CD19-Cre BM chimeras the overall B cell population is significantly reduced by approximately half in terms of percentage and by two thirds in total cell number (Figure 3-26). T cell populations of JHT/SEN1<sup>ff</sup> CD19-Cre BM chimeras behave as CD19-Cre controls. When observing the different B cell subpopulations in the JHT/SEN1<sup>ff</sup> CD19-Cre BM chimeras the ratios compared to WT are as in the naïve unimmunized BM chimeras (Figure 3-17). All cell populations were reduced except immature B cells, Fol II B cells and transitional T1 B cells (Figure 3-27 & Figure 3-28). The difference to the naïve state is that in the immunized mice the ratio of the CD23<sup>-</sup> MZ B cells is increased instead of the CD23<sup>+</sup> MZ precursor B cells as seen in the naïve BM chimeras (Figure 3-27 & Figure 3-28).

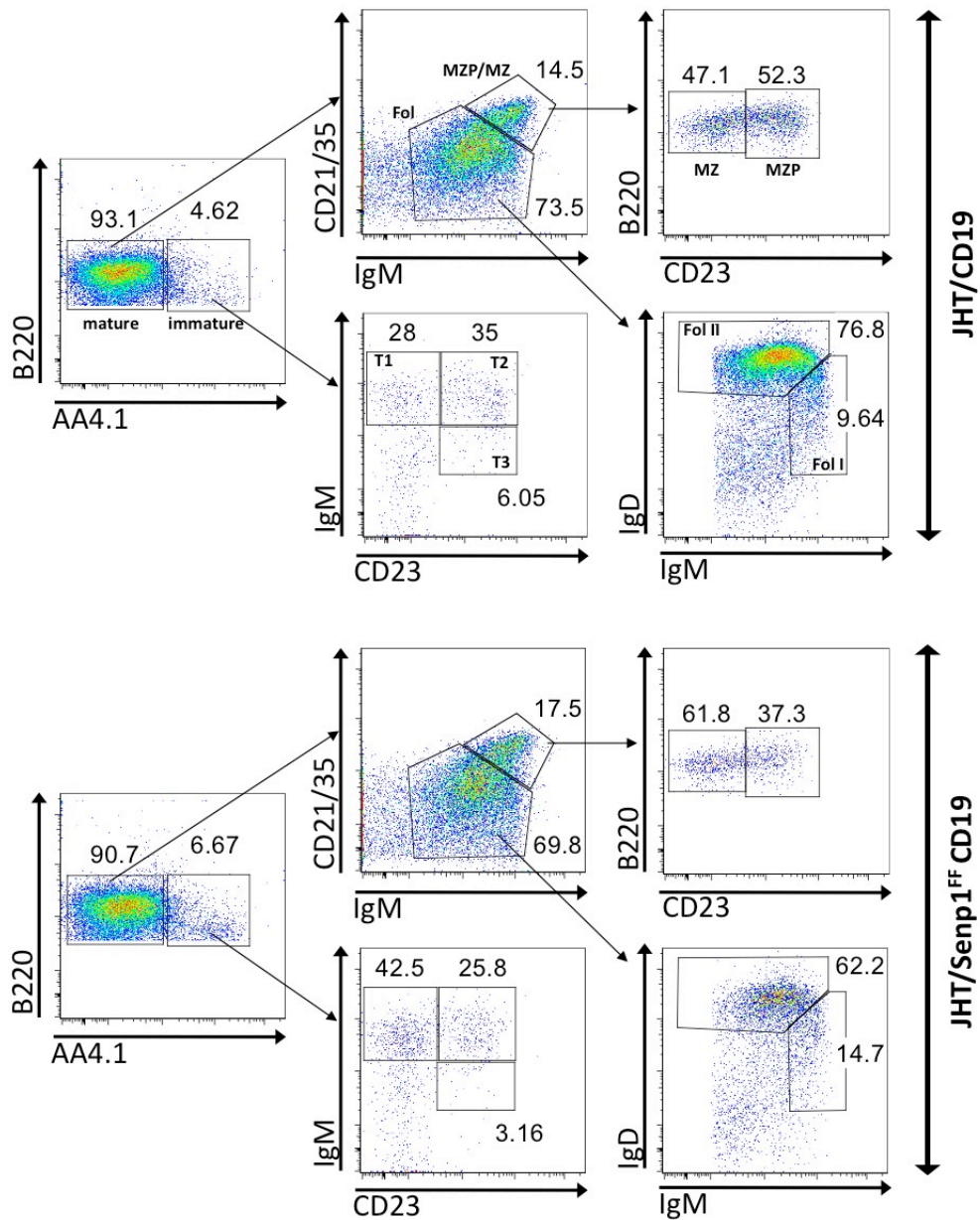


**Figure 3-27: Splenic B cell populations in SRBC immunized JHT/SENp1<sup>ff</sup> CD19-Cre BM chimeras.** FACS analysis of various B cell subpopulations in the spleen of SRBC immunized JHT/SENp1<sup>ff</sup> CD19-Cre BM chimeras of indicated genotypes. Cells were analysed for various surface markers after pre-gating on popro1<sup>-</sup> cells. For each group n=4

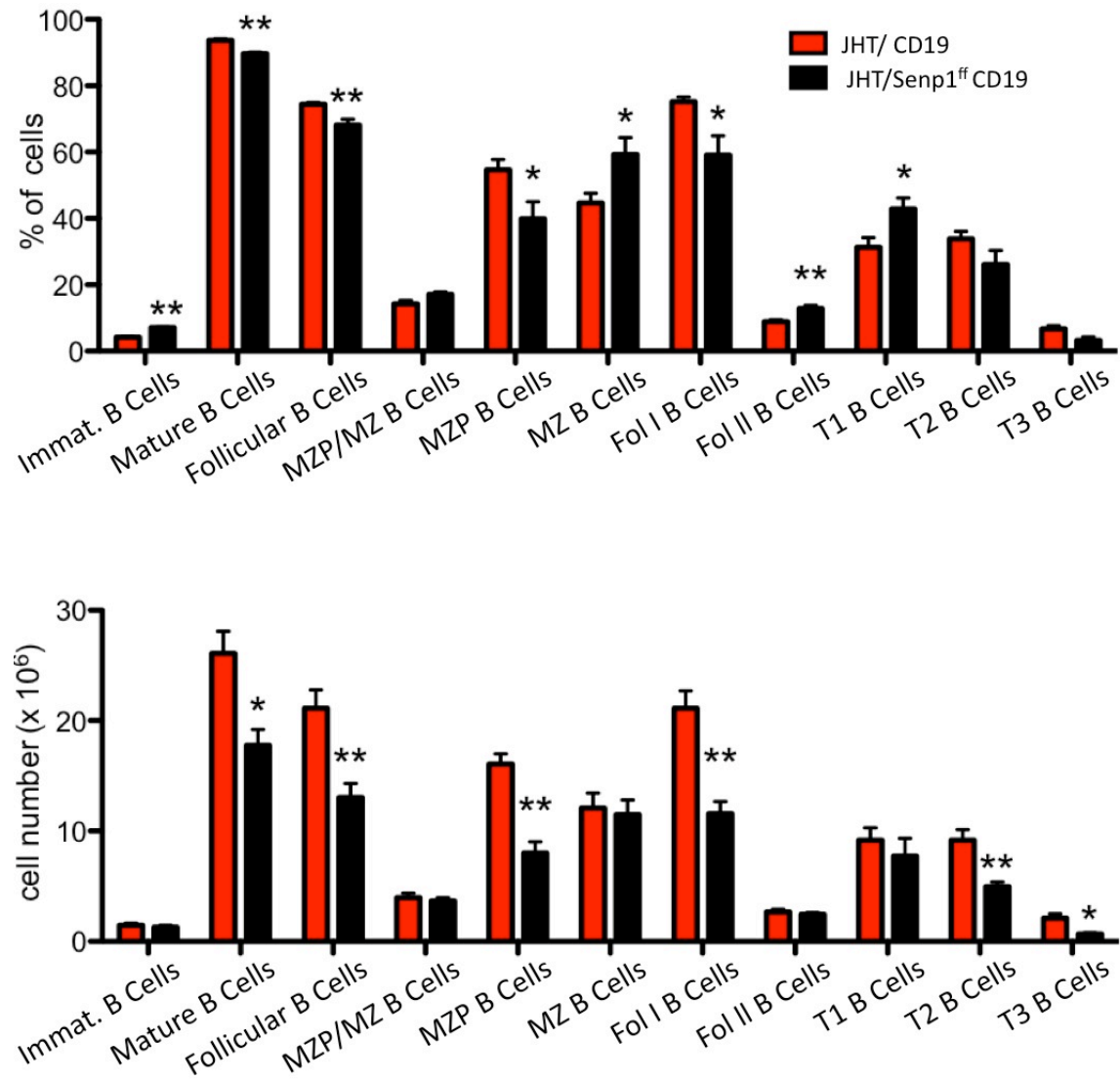


**Figure 3-28: Statistical analysis of splenic B cell populations in SRBC immunized JHT/SEN1<sup>fl</sup> CD19-Cre BM chimeras.** FACS analysis of various B cell subpopulations in the spleen of SRBC immunized JHT/SEN1<sup>fl</sup> CD19-Cre BM chimeras of indicated genotypes. Statistical analysis corresponds to FACS analysis of **Figure 3-27**. For each group n=4; \* p<0,05, \*\* p<0,01, \*\*\* p<0,001

Through SRBC immunisation a T cell dependant immune response is triggered that induces the formation of GC within the follicles of the spleen. In the GC activated B cells undergo CSR and SHM to change the antibody isotype and increase the antibody specificity through affinity maturation. Through SRBC immunisation class switch is mainly induced to switch from IgM and IgD to IgG1, as is the case for *in vitro* LPS & IL4 stimulation.

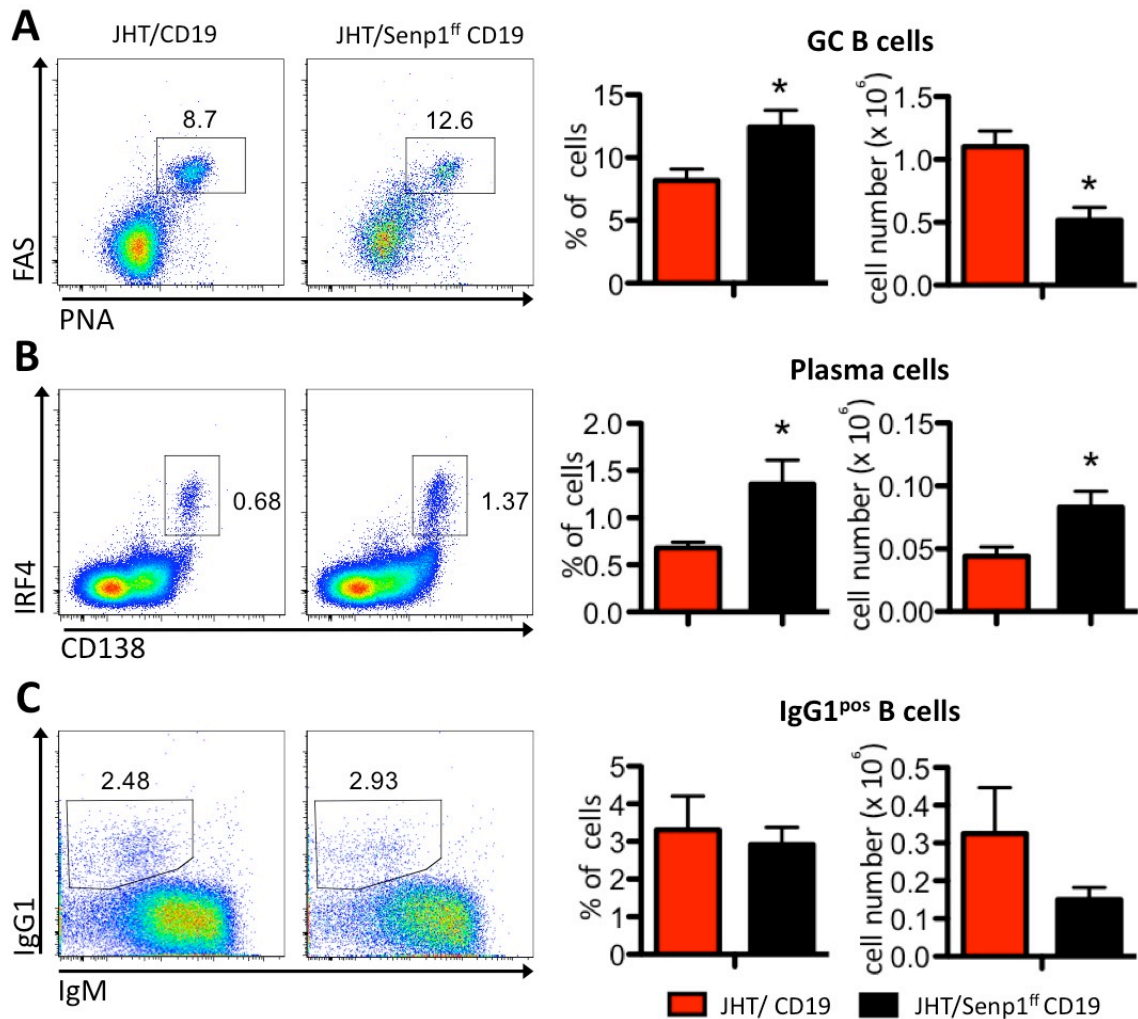


**Figure 3-29: Analysis of CSR and plasma cell differentiation in SRBC immunized JHT/SEN1<sup>ff</sup> CD19-Cre BM chimeras.** FACS analysis of germinal centre B cells, plasma cell differentiation and IgG1 expression in the spleen of SRBC immunized JHT/SEN1<sup>ff</sup> CD19-Cre BM chimeras of indicated genotypes. Cells were analysed for indicated surface markers after pre-gating on popro1<sup>-</sup> cells. For each group n=4; \* p<0,05, \*\* p<0,01, \*\*\* p<0,001

As indicated in Figure 3-29A we observe a significant increase in the percentage of GC B cell formation in JHT/SEN1<sup>ff</sup> CD19-Cre BM chimeras by about 25%. The total cell number of GC B cells in JHT/SEN1<sup>ff</sup> CD19-Cre is significantly decreased as expected (Figure 3-29A). Despite the drastic reduction in GC B cells, PC formation is two fold increased in the percentage. PC cell numbers are at such a high level that also by total cell count nearly double as many PCs can be measured as in the controls (Figure 3-29B). By FACS analysis we did not observe any differences in the surface expression of IgG1 (Figure 3-29C). However, when analysing the IgM expression on IRF4 and CD138 positive PC a significant increase of IgM can be seen compared to the JHT/CD19-Cre controls. This indicates that B cells of JHT/SEN1<sup>ff</sup>

CD19-Cre mice can either not switch as efficiently as WT B cells or only the IgM positive PC compartment is drastically increased. Furthermore, when analysing the serum of these mice on day 0 and 14 after immunization by ELISA (Figure 3-31), a decrease in secreted IgG1 is measured and an increase in IgM on day 14 after SRBC immunisation. All other Ig show no difference. On day 0 no difference can be seen in any of the observed Ig's.

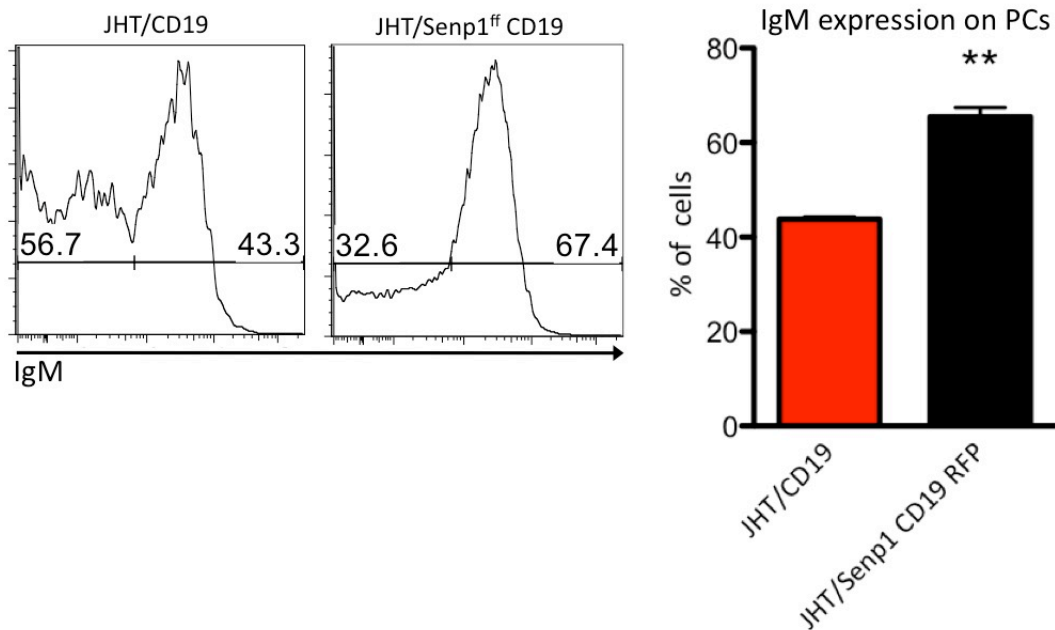


**Figure 3-30: IgM expression on plasma cells.** FACS analysis of IgM expression on IRF4<sup>+</sup>CD138<sup>+</sup> plasma cells in the spleen of SRBC immunized JHT/SEN1<sup>ff</sup> CD19-Cre (n=5) BM chimeras and the respective JHT/CD19-Cre controls (n=3). Cells were pregated on popro1<sup>-</sup> live cells; \* p<0,05, \*\* p<0,01, \*\*\* p<0,001

From these results we conclude that SRBC immunization in JHT/SEN1<sup>ff</sup> CD19-Cre BM chimeras leads to an increase in total cell number (Figure 3-28) compared to unimmunized mice (Figure 3-17), however cell numbers of JHT/SEN1<sup>ff</sup> CD19-Cre BM mice are still significantly decreased compared to the JHT/CD19-Cre control mice (Figure 3-28). Immunization of JHT/SEN1<sup>ff</sup> CD19-Cre BM mice led to an increase of GC formation and PC differentiation. However, even though PC numbers are increased the amount of class switched IgG1 positive B cells and PCs is decreased. These results go in line with the results gained from *in vitro* stimulation, further strengthening the hypothesis that upon stimulation, a part of SENP1 KO B cells undergo apoptosis, whereas the surviving SENP1 KO B cells proliferates into PCs with a decreased rate of CSR.

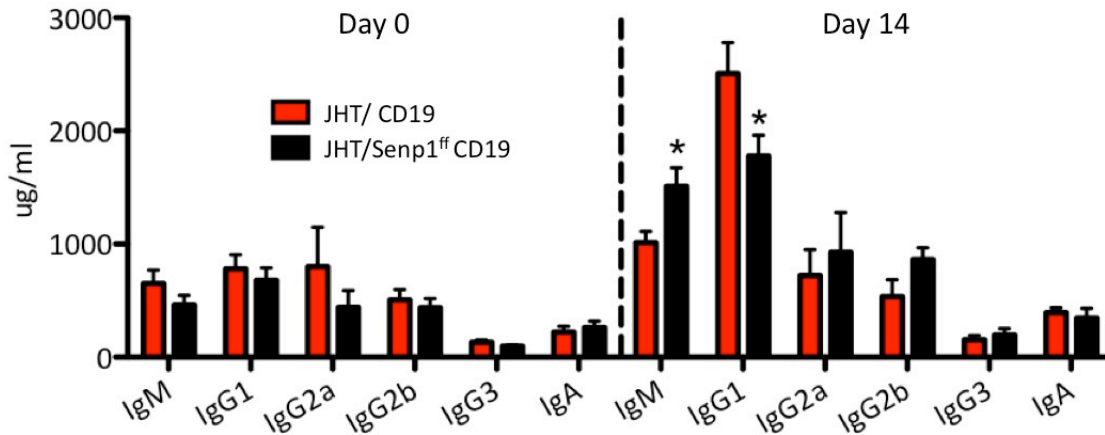


**Figure 3-31: Immunoglobulin ELISA from serum of SRBC immunized JHT/SEN1<sup>ff</sup> CD19-Cre mice.** Serum was taken before and 14 days after immunization with SRBC. For each group n=4; \* p<0,05, \*\* p<0,01, \*\*\* p<0,001

### 3.2 Generation of SENP2<sup>flox</sup> mice

As SUMO-1 is also deSUMOylated by SENP2 it was decided to generate a SENP2 conditional knockout mouse by creating a gene targeted floxed version of exon 3. SENP2 consists of 17 exons and the catalytic domain is located in the last exon. Exon 3 was selected for the targeting due to its small size of 134bp. By conditionally knocking out exon 3 with the Cre/lox system, an out-of-frame transcript is generated which leads to a transcriptional stop.

Standard gene targeting strategies (Kuhn and Schwenk, 1997) were used to generate the SENP2<sup>FL/FL</sup> mice following the strategy shown in Figure 3-32. The targeting vector was generated by inserting the left and right arm of homology and exon 3 into the pRAPIDflirt vector (A. Bruehl and A. Waisman, unpublished data). The pRAPIDflirt vector contained the *loxP* sites, the *FRT* flanked *neomycin* resistance gene and the *thymidine kinase (TK)* gene from *Herpes simplex* as a negative selection marker. The gene sequences were cloned from a bacterial artificial chromosome (BAC) vector and were inserted using the phusion flash<sup>®</sup> cloning kit. The complete vector is shown in Figure 3-33.

All PCR fragments and plasmids were verified by restriction analysis and sequencing. V6.5 (129Sv x C57BL/6) ES cells (Eggan et al., 2002) were electroporated with the *Senp2* targeting vector and incubated with G418 and for positive selection.

Nine days after electroporation, 1000 colonies were isolated as single clones, grown and subjected to Southern blot analysis. Out of these 1000 G418 resistant colonies, four were identified through Southern blot analysis of the right arm of homology as homologous recombinants (Clone 6.7F, 6.11c, 6.12A & 7.5F; Figure 3-34). Unfortunately, due to too many repetitive sequences 5' of exon 1 of the SENP2 locus, no probe for the left arm of homology could be developed to give a signal for the wild type or the transgenic band.

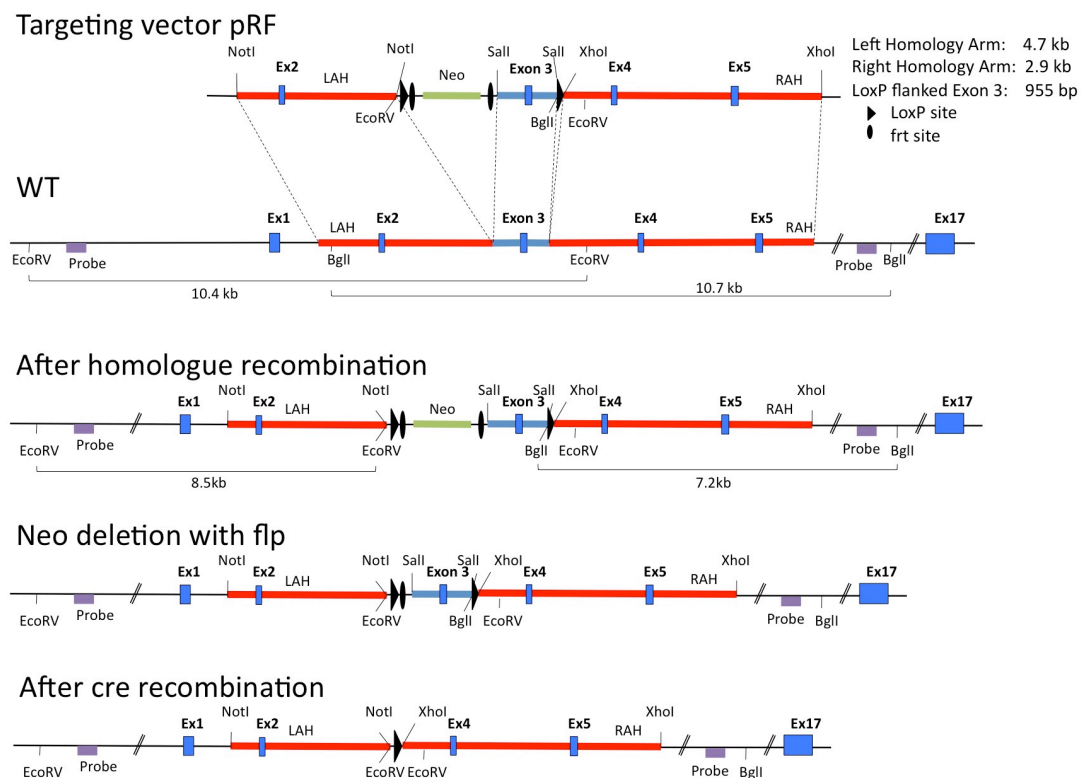


**Figure 3-32: Schematic representation of targeting strategy.** On top the generated targeting vector is shown with the included with the left and right arms of homology and the loxP flanked exon 3. The second panel shows the wild type *senp2* gene, then the gene after homologue recombination with the integrated floxed exon 3. The fourth panel depicts the *senp2* gene after recombination with flp, excising the *neo* cassette. The lower panel then shows the gene after *cre* mediated deletion of exon 3, which subsequently will lead to a frame shift and a knockout. Blue rectangles, exons; red rectangles, arms of homology; black triangles, loxP sites; black ovals, frt sites.

As integration could not be verified for the left arm of homology, functionality of the Cre/lox system was tested. Therefore, the four positive clones were electroporated with a Cre expression vector (pGK-Cre, Kurt Fellenberg, Institute for Genetics, Cologne 1997). One hundred colonies per clone were subsequently



picked in duplicates and one half of the clones was treated with G418. 30% of the treated colonies died upon treatment, indicating a functional integration of the neo cassette into the genome. To further verify correct integration Southern blot probes for exon 3 and neo were designed, however these probes were also not functioning. Due to the functionality of the Cre/lox system and the correct integration of the 3' right arm of homology it was decided to continue with the subsequent steps. Therefore, ES cells of the clone 6.11c and 6.12A were injected into tetraploid blastocysts generating two female chimeras (Figure 3-35). These females were crossed to C57BL/6 which produced 57 offsprings. All animals were typed by PCR, however non of them carried the  $SEN2^{fllox}$  allele.

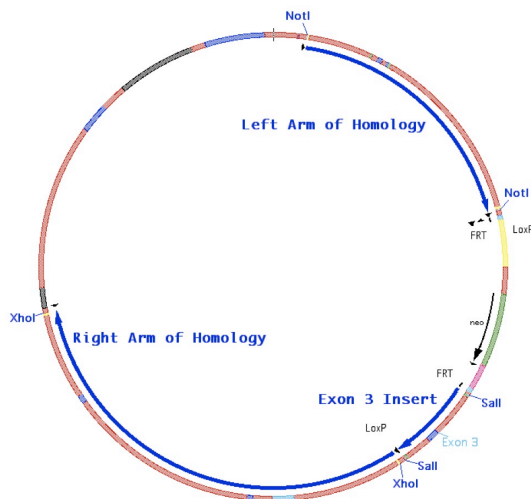


**Figure 3-33: Schematic representation of targeting vector.** The vector consists of the pRAPIDflirt vector backbone and the inserted arms of homology and exon 3, indicated as blue arrows

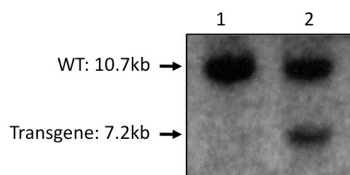


**Figure 3-34: Southern blot analysis of *BglI* digested ES cell DNA.** A  $^{32}P$ -radiolabeled DNA probe was used to confirm homologous recombination of right arm of homology. (1) wild type clone; (2) transgenic clone.

Short after blastocyst injection it was revealed that the facilitated ES cells from the V6.5 line were trisomic for chromosome 8. This was confirmed for all positive clones by an external analysis at Chrombios Molecular Cytogenetics GmbH (Figure 3-35).

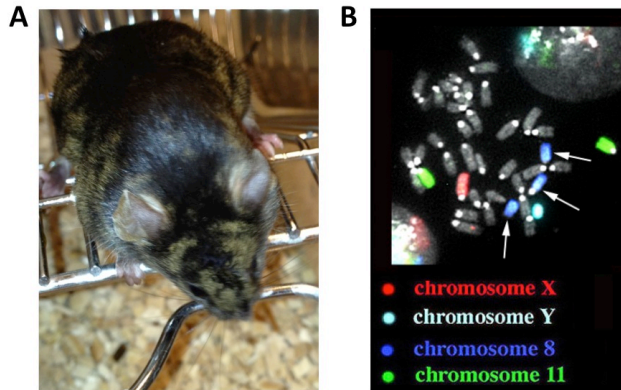


**Figure 3-35: (A) Picture of chimeric mouse after blastocyst ES cell injection. (B) Results of chromosome counting in metaphase.** Hybridisation of clone 6.7F. X chromosome is coloured red, Y is aqua, chromosome 8 is blue, chromosome 11 is green. Arrows point to the three chromosomes 8.

A second attempt to generate a SENP2 conditional knockout mouse was undertaken with JM8 ES cells (Pettitt et al., 2009) and V6.5 ES cells of different origin and confirmed to be non-trisomic. Two positive clones could be found in the transfected JM8 cells by Southern blot analysis with the *Bgl*I probe of the 3' arm of homology. However, confirmation for the 5' arm of homology and exon 3 is still in progress.

## 4. Discussion

SUMOylation is a highly dynamic and reversible posttranslational protein modification closely related to ubiquitination (Hoeller et al., 2006). SUMOylation regulates a vast array of different cellular functions, such as cell cycle, nuclear transport, DNA damage response, proliferation and transcriptional activation (Melchior, 2000). SUMO deconjugation from the lysine residue of the modified target protein is regulated by a group of six SUMO proteases (SENPs) (Li and Hochstrasser, 1999, 2000; Muller et al., 2001).

Several groups have shown in *in vitro* studies how important SUMOylation is for early B cell development and survival (Van Nguyen et al., 2012) as well as for later plasma cell (PC) differentiation (Shimshon et al., 2011; Ying et al., 2012). Of the four SUMO isoforms particular SUMO1, which is mainly regulated by SENP1 and SENP2, is connected to B cells. This thesis focuses on SENP1 and the effects of its deSUMOylation in B cell development and differentiation. For this a conditional SENP1 knockout mouse model (Yu et al., 2010) was crossed to the CD19-Cre mouse strain to generate a B cell specific SENP1 knockout mouse.

### 4.1 SENP1 in B cell survival

Previous *in vitro* studies suggest a strong regulatory role of SUMO in early B and T cell development (Van Nguyen et al., 2012). Dependant on impaired STAT5 deSUMOylation Van Nguyen *et. al* could show that defective SENP1 regulation of SUMO leads to intrinsic defects in B and T cell maturation. Interestingly, in our conditional SENP1<sup>ff</sup> CD19-Cre mouse model we could show *in vivo* a general impairment of B cell survival, whereas T cell numbers were comparable to control mice. In the bone marrow (BM) of SENP1<sup>ff</sup> CD19-Cre mice we could observe normal numbers of pro-, pre- and naïve B cells. However, the total cell count of mature recirculating B cells in the BM was significantly reduced. CD19 is expressed in B cells at the pro-B cell stage, hence effects of the SENP1 KO and subsequent impaired deSUMOylation of SUMO1 can be observed from this stage on. Furthermore, according to Rickert et al. (1997) Cre efficiency in the BM is 75-80%,

in the fully matured B cell in the spleen Cre efficiency reaches 90-95%. Hence, the full impact of a SENP1 KO can only be expected from the matured B cell stage on.

In the spleen of SENP1<sup>ff</sup> CD19-Cre mice total B cell numbers were significantly reduced. This reduction is solely based on 50% reduction of the follicular B cell compartment (Fol B cells), whereas MZ B cell compartments were unchanged in regards to total cell number. Leading to the hypothesis that mainly Fol B cells are effected by the SENP1 KO and MZ B cells are unaffected.

As the SENP1<sup>ff</sup> mice had not been published after being crossed to a cell type specific Cre line we needed to verify that these mice do not harbour any unexpected phenotypes. To our big surprise the SENP1<sup>ff</sup> mice showed in first preliminary experiments the same phenotypes as the SENP1<sup>ff</sup> CD19-Cre mice, namely reduced total B cell numbers in the spleen. These preliminary results could be reproduced in every subsequent experiment. This circumstance, however, raised the problem that phenotypes caused by the SENP1<sup>ff</sup> alleles may not be B cell specific and therefore phenotypes may also occur in other cell types.

Interestingly, analyses on T cells of SENP1<sup>ff</sup> mice showed a very mild phenotype. Percentages of CD4<sup>+</sup> and CD8<sup>+</sup> T cells were significantly elevated, especially of CD8<sup>+</sup> effector T cells. However, these results were significant, but mild and only partially reproducible. Further, the morphology and cellularity of organs such as liver, kidney, lung and heart were all comparable to WT mice. Even the testis of male mice showed no physiological difference, which is interesting, as the testis are the organ with the highest SENP1 expression (Zhang et al., 2008). These findings are rather striking, as they imply that B cells are especially sensitive to interference in the SUMOylation system and that ubiquitous impairment of SENP1 leads to strong effects only in B cells.

No empiric findings could be made on the origin of the phenotype in SENP1<sup>ff</sup> mice, however, some conclusions could be drawn. As it was shown by Yu *et al.* and Cheng *et al.* (Cheng et al., 2007; Yu et al., 2010) that a full SENP1 knockout is embryonically lethal, SENP1<sup>ff</sup> cells cannot be full knockout cells. The only apparent genetic difference between WT and SENP1<sup>ff</sup> mice is the *neomycin resistance (neo)* cassette 3' of the loxP targeted exons 5 and 6. The *neo* cassette is additionally

flanked by a loxP site at the 3' end. This makes the selective excision of the *neo* cassette very cumbersome and has not been done due to the lack of the appropriate low efficiency deleter-Cre mouse line, that is needed to delete the *neo* cassette. It is now hypothesised that the *neo* cassette in intron 6 generates a hypomorphic SENP1 allele, leading not to a full knockout, as this would be embryonically lethal (Cheng et al., 2007; Yu et al., 2010) rather to a partial knockdown. Furthermore, it has been published by Van Nguyen et al. (2012), that an *in vitro* knockout of SENP1 in early T cells also leads to developmental impairments. This strengthens the hypothesis that B cells are especially sensitive to impairments of the SUMOylation system, compared to other cell types, and therefore knockout-like phenotypes, caused by a SENP1 hypomorph, can only be observed in the SENP1<sup>ff</sup> B cells, and not in other organs and cells.

There are no insights on how the insertion of the *neo* cassette could interfere with normal SENP1 expression. One study by Pham et al. (1996), however, showed the interference of *neo* cassettes on neighbouring genes in a vicinity of 100 kb. They showed that the *neo* insertion into the granzyme B gene resulted in severe reduction of gene expression of 5' genes of the granzyme B cluster. Comparable to that, they presented that *neo* insertion in the  $\beta$ -globulin gene resulted in abolition of expression of several downstream genes. They hypothesise that the *neo* cassette interacts with several control regions surrounding the locus and thereby interferes with normal gene regulation of neighbouring genes. Five genes surround SENP1 in a radius of 100 kb. *Pfkm*, *Tmem106c*, *Al836003*, *Asb8* and *Col2a1*.

*Pfkm* encodes for the 6-phosphofructokinase muscle type protein, which is a rate-limiting enzyme in glycolysis and represents a major control point in the metabolism of glucose. Mutations in *Pfkm* may lead to type VII Tarui's disease and may contribute to non-insulin-dependent diabetes mellitus (NIDDM) (Howard et al., 1996). *Tmem106c* (Transmembrane Protein 106C) is a endoplasmic reticulum membrane protein which is overexpressed in cancer. Its molecular function is unknown (www.genecards.org). No data is available on *Al836003*. *Asb8* is a substrate-recognition component of a E3 ubiquitin-protein ligase complex, mediating the ubiquitination and subsequent proteasomal degradation of target proteins. Its highest levels of expression are in skeletal muscle. It is also expressed

in heart, brain, placenta, liver, kidney and pancreas ([www.genecards.org](http://www.genecards.org)). And last, *Col2a1* which encodes for the Collagen Type II, Alpha 1 protein, a fibrillar collagen found in cartilage and the vitreous humour of the eye. Mutations may lead to a long list of dysfunctions such as achondrogenesis, chondrodysplasia, early onset familial osteoarthritis and spondyloepimetaphyseal dysplasia Strudwick type. In addition, defects in processing chondrocalcin, a calcium binding protein that is the C-propeptide of this collagen molecule, are also associated with chondrodysplasia ([www.genecards.org](http://www.genecards.org)). None of these five genes seem to be involved in any part of B cell development, immune response or PC differentiation and no direct link can be drawn to the observed phenotypes in SENP1<sup>ff</sup> CD19-Cre mice. Furthermore, none of the above listed outcomes of mutations in these genes are observed in the SENP1<sup>ff</sup> CD19-Cre mice.

However, to exclude any possible effects of the *neo* cassette in other cell types than B cells and to generate a system in which only B cells are SENP1 deficient we generated mixed BM chimeras of B cell deficient JHT<sup>-/-</sup> mice and SENP1<sup>ff</sup> RFP CD19-Cre mice. Mice were irradiated and reconstituted with a mix of 80% JHT<sup>-/-</sup> BM and 20% SENP1<sup>ff</sup> RFP CD19-Cre BM. In this system we generated mice in which all B cells were SENP1 deficient whereas all other cell types were 80% wild type and 20% carried the SENP1<sup>ff</sup> alleles. Any effects of the SENP1 hypomorph in the 20% of the remaining cells are expected to be outcompeted by the 80% wild type cells. Before generation of the BM chimeras the SENP1<sup>ff</sup> CD19-Cre mice were further crossed to RFP reporter mice. This will generate a reliable reporter system where SENP1 deletion can be monitored indirectly through RFP expression, as the homologue recombination induced by the Cre will act unrestricted on RFP as well as SENP1.

Naive JHT/SENP1<sup>ff</sup> RFP CD19-Cre BM chimeric mice showed the same basic phenotype then the non-BM chimeric SENP1<sup>ff</sup> CD19-Cre mice – a general reduction of B cells in the BM and in the spleen. However, in contrast to the non-BM chimeric mice, where only Fol B cells were significantly reduced in the naive JHT/SENP1<sup>ff</sup> RFP CD19-Cre BM chimeric all B cell subpopulations were highly reduced. Also the ratios between the B cell subpopulations were very heterogeneous in all the repeated experiments, compared to experiments of the non-BM chimeric SENP1<sup>ff</sup>

CD19-Cre mice. This can be explained in two ways. First, the generation of BM chimeras is highly complex and strenuous for the transferred cells. In this process and in the process of reconstitution in the host mouse the composition of the B cell population may vary. Second, the up to 40 fold reduction in total cell count of some B cell populations may also strongly bias the ratio between populations.

However, it is interesting to note the complete absence of B cells in the Payer's patches (PP) and the peritoneal cavity of naive JHT/SENP1<sup>ff</sup> RFP CD19-Cre BM chimeric mice. It can be hypothesised that, as the PP and the peritoneal cavity are a place of high pathogen abundance, SENP1 deficient B cell may be triggered into activation induced cell death (AICD), as is also observed in *in vitro* stimulated cells. However, this conclusion is not fully convincing, as some mice throughout the various experiments do repopulate B cells in the PP and the peritoneal cavity.

By utilizing the Rosa-RFP reporter locus in the JHT/SENP1<sup>ff</sup> RFP CD19-Cre BM chimeric mice we can indirectly determine the abundance of the SENP1 KO B cells compared to Cre escapees. It is important to note that RFP negative Cre escapee cells resemble the SENP1 hypomorph cells. One of the aims of this experiment was to analyse the difference between RFP<sup>pos</sup> and RFP<sup>neg</sup> cells, SENP1 KO and SENP1 hypomorph, respectively. A high percentage of RFP<sup>neg</sup> cells was expected, due to the observed survival deficits of SENP1 KO cells. However, a surprisingly high amount of an average of 78% RFP<sup>pos</sup> B cells could be observed. And as the B cell population in the JHT/SENP1<sup>ff</sup> RFP CD19-Cre BM chimeric mice was very small to begin with, a further discrepancy between the 80% RFP<sup>pos</sup> cells and 20% RFP<sup>neg</sup> cells rendered no consistent, convincing results.

What can be concluded from the measured RFP expression is that Cre efficiency is not as high as stated in the literature (e.g. 80% in total B cells, 40% in transitional B cells, approx 80% in mature and immature B cells and up to 92% in marginal zone precursor (MZP) B cells) (Rickert et al., 1997). This can either be a real decrease in efficiency or it could indicate that SENP1 KO cells have a slight survival disadvantage compared to the SENP1 hypomorph cells. The latter hypothesis would stand in line with observations that general B cell reduction in SENP1<sup>ff</sup> mice is in most experiments not as strong as in SENP1<sup>ff</sup> CD19-Cre mice, albeit the

difference is not significant. Of note is that RFP expression is increasing with the developmental stage of a B cell. Whereas in a recently homed splenic transitional B cell the RFP expression is 40%, in a mature MZ or Fol B cell the percentage of RFP expression is at around 80%. This would lead to the conclusion that early SENP1 KO B cell stages have stronger survival disadvantages than early SENP1 hypomorph B cells.

The similarity of results in JHT/SENP1<sup>ff</sup> RFP CD19 BM chimeras and the SENP1<sup>ff</sup> CD19 non-BM chimeric mice – reduction in B cells numbers and absence of non-B cell phenotypes – lead to the conclusion that both systems can be used to analyse the conditional SENP1 KO.

Further, to observe survival the capacity of SENP1<sup>ff</sup> KO B cells *in vivo* in SENP1<sup>ff</sup> CD19-Cre mice we blocked new B cell formation in the BM by blocking the IL7 receptor (IL7R). IL7R signalling is essential for early B cell development. In the periphery of the SENP1<sup>ff</sup> CD19-Cre mice a faster depletion of all B cell subsets could be observed compared to the control mice, indicating that survival in SENP1 KO B cells is severely hampered. However, it was not clear at this stage if the reduced B cell numbers are only from a faster apoptosis rate or also from an inability to develop into B cells.

To closer examine the survival abilities of SENP1<sup>ff</sup> CD19-Cre B cells *in vivo*, and to see if the reduction in cell number is caused by an inability to develop into B cells or an increase rate of apoptosis we *in vivo* labelled naïve SENP1<sup>ff</sup> CD19-Cre mice with BrdU. It could be observed, that indeed Fol B cells have a higher turnover rate in the spleen. As in total less Fol B cells are present in the spleen but the proliferation rate is higher than in control mice it can be concluded that SENP1<sup>ff</sup> CD19-Cre B cells are increasingly apoptotic and an increased proliferation rate is necessary to fill the empty Fol B cell niche. Transitional and MZ B cells show normal proliferation levels which goes in line with the insignificant decrease of total cell number. However, it can not be explained why after  $\alpha$ IL7R blocking all B cell subsets show an increased rate of apoptosis, whereas only Fol B cells show an increased proliferation rate.



To further investigate survival capacities of SENP1<sup>ff</sup> CD19-Cre B cells, isolated splenocytes were *in vitro* stimulated with LPS and IL4, a TLR4 antagonist and T<sub>H</sub>2 T cell derived cytokine, respectively. T and B cells were co-cultured in this system and it could be seen that T cells were proliferating normal, however that B cells from the SENP1<sup>ff</sup> CD19-Cre mice were decreasing in total cell number in the culture.

One explanation on the general reduction of B cells can be drawn from the work of Van Nguyen et al. (2012). They showed in a co-culture model of fetal liver hematopoietic stem cells (FL-HSCs) with OP9 cells a severe reduction of B and T cells (co-culture with OP9-DL cells) when SENP1 was knocked out. They further could show that this is caused by the lack of deSUMOylation of STAT5, which lead to an accumulation of SUMOylated STAT5 and disruption of subsequent IL7R signalling. This accumulation of SUMOylated STAT5 in the B cells of SENP1<sup>ff</sup> CD19-Cre mice still needs to be shown. Interestingly, they show the same effects for B and T cells, however we can only see a minor reduction of T cells in the SENP1<sup>ff</sup> and SENP1<sup>ff</sup> CD19-Cre mice. This may again strengthen the hypothesis that B cells are more sensitive to disruptions in the SUMOylation pathway than other cells.

Nonetheless, the question if B cells in culture failed to proliferate or if they underwent premature apoptosis needed to be answered. For this two experiments were performed. In the first experiment the different stages of cell cycle were analysed, one and two days after LPS and IL4 stimulation. It could be observed that SENP1<sup>ff</sup> CD19-Cre B cells responded quicker to stimulation on day one, which can be seen in an increase of cells in the S-phase, however, on day two more cells were dying than proliferating. These findings suggest that SENP1<sup>ff</sup> CD19-Cre B cells undergo activation induced cell death (AICD) upon stimulation. However, on day four of stimulation, all cells that survived the SENP1 KO and therefore AICD, proliferated normal. SENP1 KO survivors are not to be mistaken for CD19-Cre escapees. Knockout survivors have a SENP1 deficiency whereas in Cre escapees the Cre induced recombination and knockout of SENP1 did not occur and SENP1 is wildtype, however in this system hypomorphic. Further than that, a two fold increase of accumulating cells in the G<sub>2</sub>/M phase can be observed, which is linked by Di Virgilio et al. (2013) to the persistence of unrepaired DNA damage. An

additional link of SUMOylation and apoptosis is drawn by Jiang et al. (2012) who pointed out that SUMOylation represses the transcriptional activity of XBP1, which eventually leads to apoptosis. They further show that SENP1 deficiency can promote apoptosis through excessive XBP1 SUMOylation. This has to be further elucidated as XBP1 is major factor in PC development and may be one of the main factors for the observed apoptosis in SENP1<sup>ff</sup> CD19-Cre B cells.

After observing a strong apoptotic phenotype in the SENP1 KO B cells neither Bax, a pro-apoptotic transcription factor, or p53, whose upregulation is an indicator of apoptosis, were upregulated. Only the expression of Bcl2, an anti-apoptotic factor, was nearly two fold increased. It can be speculated that all cells that did not upregulate Bcl2 died as a result of the SENP1 KO, and that Bcl2 upregulation is essential for the survival of these SENP1 KO cells. However, to further strengthen this speculation more pro- and anti-apoptotic factors have to be analysed.

#### **4.2 SENP1 in CSR & PC development**

So far we have investigated the naive state of SENP1 KO or SENP1 hypomorph cells *in vivo* and their survival capacities after LPS and IL4 stimulation *in vitro*. But since it is known that the majority of transcription factors that are important for the maintenance of the germinal centre (GC) reaction or for induction of plasma cell (PC) development are SUMOylated the question arises how defective deSUMOylation will manifest itself in these B cell stages. Some of the known transcription factors which are SUMOylated or indirectly regulated by SUMO, and that are involved in the GC reaction and PC development are Bcl6 (Kuwata and Nakamura, 2008), Bach2 (Kono et al., 2008; Tashiro et al., 2004), Mitf1 (Murakami and Arnheiter, 2005), Xbp1 (Chen and Qi, 2010; Jiang et al., 2012) and BLIMP1 (Shimshon et al., 2011; Ying et al., 2012). These transcription factors can be divided in two groups. Bach2, Mitf1 Bcl6, and Pax5 (the latter two not being SUMOylated) regulate and promote the B cell stage in the GC reaction and are responsible for proliferation, CSR and affinity maturation (through SHM) (Shapiro-Shelef and Calame, 2005). Their counterparts are BLIMP1, Xbp1 and IRF4 (which is not SUMOylated), these factors promote and regulate the differentiation into PCs,

cessation of cell cycle and immunoglobulin secretion, changes in cell surface proteins and homing (Shapiro-Shelef and Calame, 2005).

However, also other factors that play a role in late B cell development are regulated by SUMOylation. DNA damage response, for example, which is highly important in class switch recombination (CSR) and somatic hypermutation (SHM), is regulated by SUMO. Another prominent SUMOylated regulatory mechanism is the cell cycle control. P53 (Muller et al., 2000; Rodriguez et al., 1999; Shen et al., 1996a), Rad52 (Altmannova et al., 2010), HDAC2 (Brandl et al., 2012), NEMO (Huang et al., 2003; Mabb et al., 2006; Wuerzberger-Davis et al., 2007) and I $\kappa$ B (Desterro et al., 1998; Wuerzberger-Davis et al., 2007) of the NF- $\kappa$ B pathway and MDM2 (Buschmann et al., 2000; Lee et al., 2006) are strongly modified by SUMO and therefore may alter B cell development and differentiation in response to antigen. Because of the vast range of SUMO targets and their various influences towards or against GC and PC development no expectations on a possible outcome of a SENP1 KO could be made.

Isolated splenic B cells were stimulated *in vitro* to undergo CSR and SHM and to further develop into PCs. The isolated SENP1 KO cells of the SENP1 CD19-Cre mice that survived initial AICD, did differentiate into PCs more than the control cells. The rate of IgG1 switched cells was less. This indicates a stronger selection or differentiation for PC, even though the immunoglobulin isotype switch is impaired.

These results stand in contrast to the expectations gained from publications by Shimshon et al. (2011) that in a system of impaired deSUMOylation of BLIMP1, PC development should be absent or decreased. Shimshon et al. (2011) observed proteasomal degradation of BLIMP1 after coexpression with a mutant inactive SENP1, therefore impaired deSUMOylation. Kallies et al. (2004) also showed *in vivo* that a BLIMP1 knockout can still induce the PC developmental program but renders no fully developed long-lived PCs. Ying et al. (2012), however, could not observe BLIMP1 degradation subsequent to defective deSUMOylation, and contrary to Shimshon et al. hypothesise that SUMOylation of BLIMP1 acts as an attenuator of repression, therefore a SENP1 KO should render a more potent

BLIMP1 activity and increased induction of PC development. This goes in line with the *in vitro* data of the SENP1<sup>ff</sup> CD19-Cre mice.

These *in vitro* results were backed up by *in vivo* experiments, where JHT/SENP1<sup>ff</sup> CD19-Cre BM chimeras were immunized with sheep red blood cells (SRBC) to induce a GC reaction with subsequent CSR and PC differentiation. These mice showed, just as naive mice, a strong reduction of the general splenic B cell population and a reduction of recirculated mature BM B cells. However, the reduction of the different B cell subpopulations in total cell number was not as strong as in naive mice. This varied between the separate experiments and can be accounted to an artefact of the generation of BM chimeras. The most important finding of this experiment, however, was the confirmation of the *in vitro* data. As seen in the *in vitro* stimulation also in the *in vivo* immunization, 14 days after SRBC injection, PC numbers were significantly increased in the JHT/SENP1<sup>ff</sup> CD19-Cre BM chimeras compared to controls. Also the number of GC B cells was increased, however the amount of unswitched IgM positive PCs was significantly higher and IgG1 switched B cells was lower, just as the secreted IgG1 in the sera of the mice.

These results lead to the conclusion that B cells that survive a SENP1 KO are more prone to undergo PC differentiation and that these PC either are not as capable of undergoing CSR or that these cells do switch to IgG1, however IgG1 positive cells are not surviving as good. One explanation for both scenarios could be the defective DNA damage response mechanisms during CSR.

The isotype of an antibody is determined by the constant region of the heavy chain ( $C_H$ ) and determines its molecular function. The switching of an isotype, or class, of an antibody is achieved through an intrachromosomal deletional recombination event of the heavy chain locus at switch regions 5' of every constant region (except  $C_{\delta}$ ). CSR and SHM are induced by activation-induced (cytidine) deaminase (AID) which induces single and subsequently double strand breaks (DSBs) at the switch regions. The loose DSBs are then rearranged and repaired through non-homologous end joining (NHEJ) by Ku70, Ku80, XRCC4 and ligase IV. All proteins except ligase IV are SUMOylated. Ku70 is not directly SUMOylated, but is stabilized indirectly through SUMO (Yurchenko et al., 2008). Ku80 is directly SUMOylated,

however impaired SUMOylation seems not to affect localisation on site of DNA DSBs (Koike and Koike, 2008) and SUMOylation of XRCC4 is so far only confirmed in humans, where SUMO modification regulates the localisation on and function of DNA DSB repair (Yurchenko et al., 2006).

Disruption of this highly complex switchboard of SUMOylation, only regarding DNA damage repair (DDR) in GC B cells in the SENP1<sup>ff</sup> CD19-Cre mice, affects molecular processes at many different levels, and its outcome cannot be predicted. Impairment through defective deSUMOylation may in the end either lead to a hyperactive repair system, where damage is repaired before isotype rearrangement or to a defective system where isotypes cannot be switched and therefore a functional BCR can not be expressed, which may lead to apoptosis. This has to be further analysed.

### **4.3 SENP2**

As SENP1 and SENP2 both deconjugate SUMO1 and are in many cases reported to be able to compensate for each other, it was decided to generate a SENP2 conditional KO mouse to investigate their different regulatory roles in SUMOylation. Furthermore to receive a global inability of deSUMOylation it is planned to cross the two strains together.

So far one batch of gene targeted stem cells has been generated and injected into blastocysts which were transplanted into surrogate mothers. Two female chimeric mice were born and subsequently bred with C57BL/6. However, non of the 57 littermates carried the SENP2 targeted allele. As was uncovered after blastocyste injection, the mouse embryonic stem cells used for the gene targeting were trisomic for chromosome 8, which may explain the failure of germline transmission of the targeted allele.

A second gene targeting in different embryonic stem cells was generated and cells are now ready for blastocyste injection.

## 5. Summary

SUMOylation is a highly dynamic and reversible posttranslational protein modification closely related to ubiquitination. SUMOylation regulates a vast array of different cellular functions, such as cell cycle, nuclear transport, DNA damage response, proliferation and transcriptional activation. Several groups have shown in *in vitro* studies how important SUMOylation is for early B cell development and survival as well as for later plasma cell differentiation. This thesis focuses on the deSUMOylation protease SENP1 and its *in vivo* effects on B cell development and differentiation. For this a conditional SENP1 knockout mouse model was crossed to the CD19-Cre mouse strain to generate a B cell specific SENP1 knockout mouse.

In our conditional SENP1<sup>ff</sup> CD19-Cre mouse model we observed normal numbers of all B cell subsets in the bone marrow. However in the spleen we observed an impairment of B cell survival, based on a 50% reduction of the follicular B cell compartment, whereas the marginal zone B cell compartment was unchanged. T cell numbers were comparable to control mice.

Further, impairments of B cell survival in SENP1<sup>ff</sup> CD19-Cre mice were analysed after *in vivo* blocking of IL7R signalling. The  $\alpha$ IL7R treatment in mature mice blocked new B cell formation in the bone marrow and increased apoptosis rates could be observed in splenic SENP1 KO B cells. Additionally, a higher turnover rate of B cells was measured by *in vivo* BrdU incorporation.

Since it is known that the majority of transcription factors that are important for the maintenance of the germinal centre reaction or for induction of plasma cell development are SUMOylated, the question arose, how defective deSUMOylation will manifest itself in these processes. The majority of *in vitro* cultured splenic B cells, stimulated to undergo class switch recombination and plasma cell differentiation underwent activation induced cell death. However, the surviving cells increasingly differentiated into IgM expressing plasma cells. Class switch recombination to IgG1 was reduced. These observations stood in line with observation made in *in vivo* sheep red blood cell immunization experiments, which showed increased amounts of germinal centres and germinal centre B cells, as well

as increased amounts of plasma cells differentiation in combination with decreased class switch to IgG1.

These results lead to the conclusion that SENP1 KO B cells increasingly undergo apoptosis, however, B cells that survive SENP1 deficiency are more prone to undergo plasma cell differentiation. Further, the precursors of these plasma cells either are not as capable of undergoing class switch recombination or they do switch to IgG1 and succumb to activation induced cell death. One possible explanation for both scenarios could be a defective DNA damage response mechanisms during class switch recombination, caused by impaired deSUMOylation.

## 6. Zusammenfassung

SUMOylierung ist eine dynamische und reversible posttranslationale Protein Modifizierung, ähnlich der Ubiquitinierung. SUMOylierung reguliert ein breites Spektrum an zellulären Prozessen, wie z. B. den Zellzyklus, nukleären Transport, DNA Reparatur Mechanismen, Proliferation und Transkription. Mehrere Publikationen zeigen *in vitro*, wie wichtig SUMOylierung für frühe B Zell Entwicklung und Überleben ist, sowie später zur Plasma Zell Differenzierung. Diese Dissertation ist fokussiert auf die deSUMOylierungs Protease SENP1 und ihre Auswirkungen auf B Zell Entwicklung und Differenzierung. Dazu wurden konditionelle SENP1 knockout Mäuse mit CD19-Cre Mäusen verkreuzt um einen B Zell spezifischen SENP1 knockout zu erhalten.

In diesem konditionellen SENP1<sup>ff</sup> CD19-Cre Mausmodell konnten im Knochenmark keine abnormalen B Zell Populationen festgestellt werden. In der Milz wurde jedoch eine 50%ige Einschränkung der Überlebenskapazität der B Zellen gemessen, die alleine auf das Follikuläre B Zell Kompartiment zurückzuführen ist. Marginal Zone B Zellen verhielten sich wildtypisch. Auch T Zell Populationen waren unverändert im Vergleich zu Kontrollgruppen.

Weitere Einschränkungen in der Überlebenskapazität von SENP1<sup>ff</sup> CD19-Cre B Zellen wurden untersucht durch *in vivo* IL7R Blockade mit  $\alpha$ IL7R Antikörpern. Dies führt zu einem Block in der frühen B Zell Entwicklung im Knochenmark, wobei eine Verminderung der verbleibenden reifen B Zellen in der Milz zu beobachten war, zurückzuführen auf eine erhöhte Apoptose Rate. Des Weiteren wurde ein erhöhter B Zell Umsatz in der Milz mithilfe von BrdU *in vivo* Inkorporation gemessen.

Es ist bekannt, dass eine Vielzahl der Transkriptionsfaktoren die die Germinal Center Reaction und die Induktion von Plasma Zell Produktion regulieren, SUMOyliert werden. Daher wurde untersucht, wie defektive deSUMOylierung diese Prozesse beeinträchtigt. Die Mehrzahl der aus der Milz gewonnenen, *in vitro* kultivierten B Zellen, die zur Class Switch Rekombination und Plasma Zell Differenzierung angeregt wurden, starben durch activation induced cell death



(AICD). Wobei die überlebenden B Zellen überwiegend zu IgM positiven Plasma Zellen differenzierten und class switch zu IgG1 reduziert war. Diese Beobachtung wurde bestätigt durch *in vivo* Immunisierung mit Schaf Erythrozyten (SRBC), die zu einer erhöhten Germinal Centre B Zell Bildung und Plasma Zell Differenzierung führte, aber auch einen verminderten class switch zu IgG1 zeigte.

Diese Ergebnisse lassen schlussfolgern, dass SENP1 knockout B Zellen eine erhöhte Apoptose Rate aufweisen, aber auch, dass B Zellen, die eine SENP1 Defizienz überleben vermehrt zu IgM positiven Plasma Zellen differenzieren. Des Weiteren wurde gezeigt, dass Plasma Zell Vorgänger Zellen entweder vermindert zu IgG1 switchen, oder nach einem erfolgreichen class switch zu IgG1 durch AICD sterben. Eine Erklärung für beide Szenarien könnte durch ein defektives DNA Reparatur System in SENP1 defizienten Zellen geliefert werden, welches essenziell ist für einen erfolgreichen Isotypen switch.

## 7. Reference List

- Allman, D., and Pillai, S. (2008). Peripheral B cell subsets. *Curr Opin Immunol* *20*, 149-157.
- Altmannova, V., Eckert-Boulet, N., Arneric, M., Kolesar, P., Chaloupkova, R., Damborsky, J., Sung, P., Zhao, X., Lisby, M., and Krejci, L. (2010). Rad52 SUMOylation affects the efficiency of the DNA repair. *Nucleic Acids Res* *38*, 4708-4721.
- Azuma, Y., Arnaoutov, A., and Dasso, M. (2003). SUMO-2/3 regulates topoisomerase II in mitosis. *J Cell Biol* *163*, 477-487.
- Bayer, P., Arndt, A., Metzger, S., Mahajan, R., Melchior, F., Jaenicke, R., and Becker, J. (1998). Structure determination of the small ubiquitin-related modifier SUMO-1. *J Mol Biol* *280*, 275-286.
- Bednarski, J.J., Nickless, A., Bhattacharya, D., Amin, R.H., Schlissel, M.S., and Sleckman, B.P. (2012). RAG-induced DNA double-strand breaks signal through Pim2 to promote pre-B cell survival and limit proliferation. *J Exp Med* *209*, 11-17.
- Bernardi, R., and Pandolfi, P.P. (2007). Structure, dynamics and functions of promyelocytic leukaemia nuclear bodies. *Nat Rev Mol Cell Biol* *8*, 1006-1016.
- Bertolotto, C., Lesueur, F., Giuliano, S., Strub, T., de Lichy, M., Bille, K., Dessen, P., d'Hayer, B., Mohamdi, H., Remenieras, A., *et al.* (2011). A SUMOylation-defective MITF germline mutation predisposes to melanoma and renal carcinoma. *Nature* *480*, 94-98.
- Bienko, M., Green, C.M., Crosetto, N., Rudolf, F., Zapart, G., Coull, B., Kannouche, P., Wider, G., Peter, M., Lehmann, A.R., *et al.* (2005). Ubiquitin-binding domains in Y-family polymerases regulate translesion synthesis. *Science* *310*, 1821-1824.
- Bischof, O., Kirsh, O., Pearson, M., Itahana, K., Pelicci, P.G., and Dejean, A. (2002). Deconstructing PML-induced premature senescence. *EMBO J* *21*, 3358-3369.
- Bischof, O., Nacerddine, K., and Dejean, A. (2005). Human papillomavirus oncoprotein E7 targets the promyelocytic leukemia protein and circumvents cellular senescence via the Rb and p53 tumor suppressor pathways. *Mol Cell Biol* *25*, 1013-1024.
- Bischof, O., Schwamborn, K., Martin, N., Werner, A., Sustmann, C., Grosschedl, R., and Dejean, A. (2006). The E3 SUMO ligase PIASy is a regulator of cellular senescence and apoptosis. *Mol Cell* *22*, 783-794.
- Bode, A.M., and Dong, Z. (2004). Post-translational modification of p53 in tumorigenesis. *Nat Rev Cancer* *4*, 793-805.
- Brandl, A., Wagner, T., Uhlig, K.M., Knauer, S.K., Stauber, R.H., Melchior, F., Schneider, G., Heinzl, T., and Kramer, O.H. (2012). Dynamically regulated

sumoylation of HDAC2 controls p53 deacetylation and restricts apoptosis following genotoxic stress. *J Mol Cell Biol* 4, 284-293.

Buschmann, T., Fuchs, S.Y., Lee, C.G., Pan, Z.Q., and Ronai, Z. (2000). SUMO-1 modification of Mdm2 prevents its self-ubiquitination and increases Mdm2 ability to ubiquitinate p53. *Cell* 101, 753-762.

Chen, H., and Qi, L. (2010). SUMO modification regulates the transcriptional activity of XBP1. *Biochem J* 429, 95-102.

Cheng, J., Kang, X., Zhang, S., and Yeh, E.T. (2007). SUMO-specific protease 1 is essential for stabilization of HIF1alpha during hypoxia. *Cell* 131, 584-595.

Chiles, T.C. (2004). Regulation and function of cyclin D2 in B lymphocyte subsets. *J Immunol* 173, 2901-2907.

Chomczynski, P., and Qasba, P.K. (1984). Alkaline transfer of DNA to plastic membrane. *Biochem Biophys Res Commun* 122, 340-344.

Cooper, A.B., Sawai, C.M., Sicinska, E., Powers, S.E., Sicinski, P., Clark, M.R., and Aifantis, I. (2006). A unique function for cyclin D3 in early B cell development. *Nat Immunol* 7, 489-497.

Critchlow, S.E., Bowater, R.P., and Jackson, S.P. (1997). Mammalian DNA double-strand break repair protein XRCC4 interacts with DNA ligase IV. *Curr Biol* 7, 588-598.

Cumano, A., and Rajewsky, K. (1986). Clonal recruitment and somatic mutation in the generation of immunological memory to the hapten NP. *EMBO J* 5, 2459-2468.

David, G., Neptune, M.A., and DePinho, R.A. (2002). SUMO-1 modification of histone deacetylase 1 (HDAC1) modulates its biological activities. *J Biol Chem* 277, 23658-23663.

de Stanchina, E., Querido, E., Narita, M., Davuluri, R.V., Pandolfi, P.P., Ferbeyre, G., and Lowe, S.W. (2004). PML is a direct p53 target that modulates p53 effector functions. *Mol Cell* 13, 523-535.

Delmer, A., Ajchenbaum-Cymbalista, F., Tang, R., Ramond, S., Faussat, A.M., Marie, J.P., and Zittoun, R. (1995). Overexpression of cyclin D2 in chronic B-cell malignancies. *Blood* 85, 2870-2876.

Desterro, J.M., Rodriguez, M.S., and Hay, R.T. (1998). SUMO-1 modification of I $\kappa$ B $\alpha$  inhibits NF- $\kappa$ B activation. *Mol Cell* 2, 233-239.

Di Virgilio, M., Callen, E., Yamane, A., Zhang, W., Jankovic, M., Gitlin, A.D., Feldhahn, N., Resch, W., Oliveira, T.Y., Chait, B.T., *et al.* (2013). Rif1 prevents resection of DNA breaks and promotes immunoglobulin class switching. *Science* 339, 711-715.

Dohmen, R.J. (2004). SUMO protein modification. *Biochim Biophys Acta* 1695, 113-131.

- Drag, M., and Salvesen, G.S. (2008). DeSUMOylating enzymes--SENPs. *IUBMB Life* *60*, 734-742.
- Eggan, K., Rode, A., Jentsch, I., Samuel, C., Hennek, T., Tintrup, H., Zevnik, B., Erwin, J., Loring, J., Jackson-Grusby, L., *et al.* (2002). Male and female mice derived from the same embryonic stem cell clone by tetraploid embryo complementation. *Nat Biotechnol* *20*, 455-459.
- Eladad, S., Ye, T.Z., Hu, P., Leversha, M., Beresten, S., Matunis, M.J., and Ellis, N.A. (2005). Intra-nuclear trafficking of the BLM helicase to DNA damage-induced foci is regulated by SUMO modification. *Hum Mol Genet* *14*, 1351-1365.
- Everett, R.D., Rechter, S., Papior, P., Tavalai, N., Stamminger, T., and Orr, A. (2006). PML contributes to a cellular mechanism of repression of herpes simplex virus type 1 infection that is inactivated by ICP0. *J Virol* *80*, 7995-8005.
- Flick, K., Ouni, I., Wohlschlegel, J.A., Capati, C., McDonald, W.H., Yates, J.R., and Kaiser, P. (2004). Proteolysis-independent regulation of the transcription factor Met4 by a single Lys 48-linked ubiquitin chain. *Nat Cell Biol* *6*, 634-641.
- Fox, C.J., Hammerman, P.S., Cinalli, R.M., Master, S.R., Chodosh, L.A., and Thompson, C.B. (2003). The serine/threonine kinase Pim-2 is a transcriptionally regulated apoptotic inhibitor. *Genes Dev* *17*, 1841-1854.
- Friedberg, E.C., Lehmann, A.R., and Fuchs, R.P. (2005). Trading places: how do DNA polymerases switch during translesion DNA synthesis? *Mol Cell* *18*, 499-505.
- Gao, C., Ho, C.C., Reineke, E., Lam, M., Cheng, X., Stanya, K.J., Liu, Y., Chakraborty, S., Shih, H.M., and Kao, H.Y. (2008). Histone deacetylase 7 promotes PML sumoylation and is essential for PML nuclear body formation. *Mol Cell Biol* *28*, 5658-5667.
- Geiss-Friedlander, R., and Melchior, F. (2007). Concepts in sumoylation: a decade on. *Nat Rev Mol Cell Biol* *8*, 947-956.
- Girdwood, D., Bumpass, D., Vaughan, O.A., Thain, A., Anderson, L.A., Snowden, A.W., Garcia-Wilson, E., Perkins, N.D., and Hay, R.T. (2003). P300 transcriptional repression is mediated by SUMO modification. *Mol Cell* *11*, 1043-1054.
- Gocke, C.B., Yu, H., and Kang, J. (2005). Systematic identification and analysis of mammalian small ubiquitin-like modifier substrates. *J Biol Chem* *280*, 5004-5012.
- Golebiowski, F., Matic, I., Tatham, M.H., Cole, C., Yin, Y., Nakamura, A., Cox, J., Barton, G.J., Mann, M., and Hay, R.T. (2009). System-wide changes to SUMO modifications in response to heat shock. *Sci Signal* *2*, ra24.
- Goodson, M.L., Hong, Y., Rogers, R., Matunis, M.J., Park-Sarge, O.K., and Sarge, K.D. (2001). Sumo-1 modification regulates the DNA binding activity of heat shock transcription factor 2, a promyelocytic leukemia nuclear body associated transcription factor. *J Biol Chem* *276*, 18513-18518.

- Gu, H., Zou, Y.R., and Rajewsky, K. (1993). Independent control of immunoglobulin switch recombination at individual switch regions evidenced through Cre-loxP-mediated gene targeting. *Cell* 73, 1155-1164.
- Guo, D., Li, M., Zhang, Y., Yang, P., Eckenrode, S., Hopkins, D., Zheng, W., Purohit, S., Podolsky, R.H., Muir, A., *et al.* (2004). A functional variant of SUMO4, a new I kappa B alpha modifier, is associated with type 1 diabetes. *Nat Genet* 36, 837-841.
- Gurrieri, C., Nafa, K., Merghoub, T., Bernardi, R., Capodieci, P., Biondi, A., Nimer, S., Douer, D., Cordon-Cardo, C., Gallagher, R., and Pandolfi, P.P. (2004). Mutations of the PML tumor suppressor gene in acute promyelocytic leukemia. *Blood* 103, 2358-2362.
- Gutierrez, G.J., and Ronai, Z. (2006). Ubiquitin and SUMO systems in the regulation of mitotic checkpoints. *Trends Biochem Sci* 31, 324-332.
- Haas, A.L., Ahrens, P., Bright, P.M., and Ankel, H. (1987). Interferon induces a 15-kilodalton protein exhibiting marked homology to ubiquitin. *J Biol Chem* 262, 11315-11323.
- Haglund, K., and Dikic, I. (2005). Ubiquitylation and cell signaling. *EMBO J* 24, 3353-3359.
- Hang, J., and Dasso, M. (2002). Association of the human SUMO-1 protease SENP2 with the nuclear pore. *J Biol Chem* 277, 19961-19966.
- Hardeland, U., Steinacher, R., Jiricny, J., and Schar, P. (2002). Modification of the human thymine-DNA glycosylase by ubiquitin-like proteins facilitates enzymatic turnover. *EMBO J* 21, 1456-1464.
- Hardy, R.R., and Hayakawa, K. (2001). B cell development pathways. *Annu Rev Immunol* 19, 595-621.
- Hay, R.T. (2007). SUMO-specific proteases: a twist in the tail. *Trends Cell Biol* 17, 370-376.
- Hershko, A., and Ciechanover, A. (1992). The ubiquitin system for protein degradation. *Annu Rev Biochem* 61, 761-807.
- Herzenberg, L.A., and Black, S.J. (1980). Regulatory circuits and antibody responses. *Eur J Immunol* 10, 1-11.
- Hochstrasser, M. (2001). SP-RING for SUMO: new functions bloom for a ubiquitin-like protein. *Cell* 107, 5-8.
- Hoegel, C., Pfander, B., Moldovan, G.L., Pyrowolakis, G., and Jentsch, S. (2002). RAD6-dependent DNA repair is linked to modification of PCNA by ubiquitin and SUMO. *Nature* 419, 135-141.
- Hoeller, D., Hecker, C.M., and Dikic, I. (2006). Ubiquitin and ubiquitin-like proteins in cancer pathogenesis. *Nat Rev Cancer* 6, 776-788.

- Hogan, M.E., Rooney, T.F., and Austin, R.H. (1987). Evidence for kinks in DNA folding in the nucleosome. *Nature* *328*, 554-557.
- Hong, Y., Rogers, R., Matunis, M.J., Mayhew, C.N., Goodson, M.L., Park-Sarge, O.K., and Sarge, K.D. (2001). Regulation of heat shock transcription factor 1 by stress-induced SUMO-1 modification. *J Biol Chem* *276*, 40263-40267.
- Howard, T.D., Akots, G., and Bowden, D.W. (1996). Physical and genetic mapping of the muscle phosphofructokinase gene (PFKM): reassignment to human chromosome 12q. *Genomics* *34*, 122-127.
- Huang, T.T., Wuerzberger-Davis, S.M., Wu, Z.H., and Miyamoto, S. (2003). Sequential modification of NEMO/IKKgamma by SUMO-1 and ubiquitin mediates NF-kappaB activation by genotoxic stress. *Cell* *115*, 565-576.
- Hurley, J.H., Lee, S., and Prag, G. (2006). Ubiquitin-binding domains. *Biochem J* *399*, 361-372.
- Igawa, T., Sato, Y., Takata, K., Fushimi, S., Tamura, M., Nakamura, N., Maeda, Y., Orita, Y., Tanimoto, M., and Yoshino, T. (2011). Cyclin D2 is overexpressed in proliferation centers of chronic lymphocytic leukemia/small lymphocytic lymphoma. *Cancer Sci* *102*, 2103-2107.
- Inoue, H., Nojima, H., and Okayama, H. (1990). High efficiency transformation of *Escherichia coli* with plasmids. *Gene* *96*, 23-28.
- Jackson, P.K. (2001). A new RING for SUMO: wrestling transcriptional responses into nuclear bodies with PIAS family E3 SUMO ligases. *Genes Dev* *15*, 3053-3058.
- Jacques, C., Baris, O., Prunier-Mirebeau, D., Savagner, F., Rodien, P., Rohmer, V., Franc, B., Guyetant, S., Malthiery, Y., and Reynier, P. (2005). Two-step differential expression analysis reveals a new set of genes involved in thyroid oncocytic tumors. *J Clin Endocrinol Metab* *90*, 2314-2320.
- Jacquiau, H.R., van Waardenburg, R.C., Reid, R.J., Woo, M.H., Guo, H., Johnson, E.S., and Bjornsti, M.A. (2005). Defects in SUMO (small ubiquitin-related modifier) conjugation and deconjugation alter cell sensitivity to DNA topoisomerase I-induced DNA damage. *J Biol Chem* *280*, 23566-23575.
- Jeggo, P.A., and Lobrich, M. (2007). DNA double-strand breaks: their cellular and clinical impact? *Oncogene* *26*, 7717-7719.
- Jentsch, S., and Pyrowolakis, G. (2000). Ubiquitin and its kin: how close are the family ties? *Trends Cell Biol* *10*, 335-342.
- Jiang, Z., Fan, Q., Zhang, Z., Zou, Y., Cai, R., Wang, Q., Zuo, Y., and Cheng, J. (2012). SENP1 deficiency promotes ER stress-induced apoptosis by increasing XBP1 SUMOylation. *Cell Cycle* *11*, 1118-1122.

- Jin, C., Shiyanova, T., Shen, Z., and Liao, X. (2001). Heteronuclear nuclear magnetic resonance assignments, structure and dynamics of SUMO-1, a human ubiquitin-like protein. *Int J Biol Macromol* *28*, 227-234.
- Johnson, E.S. (2004). Protein modification by SUMO. *Annu Rev Biochem* *73*, 355-382.
- Johnson, E.S., and Blobel, G. (1999). Cell cycle-regulated attachment of the ubiquitin-related protein SUMO to the yeast septins. *J Cell Biol* *147*, 981-994.
- Johnson, K., Shapiro-Shelef, M., Tunyaplin, C., and Calame, K. (2005). Regulatory events in early and late B-cell differentiation. *Mol Immunol* *42*, 749-761.
- Kagey, M.H., Melhuish, T.A., and Wotton, D. (2003). The polycomb protein Pc2 is a SUMO E3. *Cell* *113*, 127-137.
- Kallies, A., Hasbold, J., Tarlinton, D.M., Dietrich, W., Corcoran, L.M., Hodgkin, P.D., and Nutt, S.L. (2004). Plasma cell ontogeny defined by quantitative changes in blimp-1 expression. *J Exp Med* *200*, 967-977.
- Kamitani, T., Kito, K., Nguyen, H.P., and Yeh, E.T. (1997). Characterization of NEDD8, a developmentally down-regulated ubiquitin-like protein. *J Biol Chem* *272*, 28557-28562.
- Kannouche, P.L., Wing, J., and Lehmann, A.R. (2004). Interaction of human DNA polymerase eta with monoubiquitinated PCNA: a possible mechanism for the polymerase switch in response to DNA damage. *Mol Cell* *14*, 491-500.
- Kim, J.H., and Baek, S.H. (2009). Emerging roles of desumoylating enzymes. *Biochim Biophys Acta* *1792*, 155-162.
- Kim, K.I., Baek, S.H., and Chung, C.H. (2002). Versatile protein tag, SUMO: its enzymology and biological function. *J Cell Physiol* *191*, 257-268.
- Kirsh, O., Seeler, J.S., Pichler, A., Gast, A., Muller, S., Miska, E., Mathieu, M., Harel-Bellan, A., Kouzarides, T., Melchior, F., and Dejean, A. (2002). The SUMO E3 ligase RanBP2 promotes modification of the HDAC4 deacetylase. *EMBO J* *21*, 2682-2691.
- Koike, M., and Koike, A. (2008). Accumulation of Ku80 proteins at DNA double-strand breaks in living cells. *Exp Cell Res* *314*, 1061-1070.
- Koken, M.H., Linares-Cruz, G., Quignon, F., Viron, A., Chelbi-Alix, M.K., Sobczak-Thepot, J., Juhlin, L., Degos, L., Calvo, F., and de The, H. (1995). The PML growth-suppressor has an altered expression in human oncogenesis. *Oncogene* *10*, 1315-1324.
- Kono, K., Harano, Y., Hoshino, H., Kobayashi, M., Bazett-Jones, D.P., Muto, A., Igarashi, K., and Tashiro, S. (2008). The mobility of Bach2 nuclear foci is regulated by SUMO-1 modification. *Exp Cell Res* *314*, 903-913.

- Kuhn, R., and Schwenk, F. (1997). Advances in gene targeting methods. *Curr Opin Immunol* 9, 183-188.
- Kurahashi, S., Hayakawa, F., Miyata, Y., Yasuda, T., Minami, Y., Tsuzuki, S., Abe, A., and Naoe, T. (2011). PAX5-PML acts as a dual dominant-negative form of both PAX5 and PML. *Oncogene* 30, 1822-1830.
- Kuwata, T., and Nakamura, T. (2008). BCL11A is a SUMOylated protein and recruits SUMO-conjugation enzymes in its nuclear body. *Genes Cells* 13, 931-940.
- Lam, E.W., Glassford, J., Banerji, L., Thomas, N.S., Sicinski, P., and Klaus, G.G. (2000). Cyclin D3 compensates for loss of cyclin D2 in mouse B-lymphocytes activated via the antigen receptor and CD40. *J Biol Chem* 275, 3479-3484.
- Lee, J., Lee, Y., Lee, M.J., Park, E., Kang, S.H., Chung, C.H., Lee, K.H., and Kim, K. (2008). Dual modification of BMAL1 by SUMO2/3 and ubiquitin promotes circadian activation of the CLOCK/BMAL1 complex. *Mol Cell Biol* 28, 6056-6065.
- Lee, M.H., Lee, S.W., Lee, E.J., Choi, S.J., Chung, S.S., Lee, J.I., Cho, J.M., Seol, J.H., Baek, S.H., Kim, K.I., *et al.* (2006). SUMO-specific protease SUSP4 positively regulates p53 by promoting Mdm2 self-ubiquitination. *Nat Cell Biol* 8, 1424-1431.
- Lee, M.H., Mabb, A.M., Gill, G.B., Yeh, E.T., and Miyamoto, S. (2011). NF-kappaB induction of the SUMO protease SENP2: A negative feedback loop to attenuate cell survival response to genotoxic stress. *Mol Cell* 43, 180-191.
- Li, S.J., and Hochstrasser, M. (1999). A new protease required for cell-cycle progression in yeast. *Nature* 398, 246-251.
- Li, S.J., and Hochstrasser, M. (2000). The yeast ULP2 (SMT4) gene encodes a novel protease specific for the ubiquitin-like Smt3 protein. *Mol Cell Biol* 20, 2367-2377.
- Li, T., Santockyte, R., Shen, R.F., Tekle, E., Wang, G., Yang, D.C., and Chock, P.B. (2006). Expression of SUMO-2/3 induced senescence through p53- and pRB-mediated pathways. *J Biol Chem* 281, 36221-36227.
- Lieber, M.R., Ma, Y., Pannicke, U., and Schwarz, K. (2004). The mechanism of vertebrate nonhomologous DNA end joining and its role in V(D)J recombination. *DNA Repair (Amst)* 3, 817-826.
- Lin, X., Liang, M., Liang, Y.Y., Brunnicardi, F.C., and Feng, X.H. (2003). SUMO-1/Ubc9 promotes nuclear accumulation and metabolic stability of tumor suppressor Smad4. *J Biol Chem* 278, 31043-31048.
- Liu, Y.C., Pan, J., Zhang, C., Fan, W., Collinge, M., Bender, J.R., and Weissman, S.M. (1999). A MHC-encoded ubiquitin-like protein (FAT10) binds noncovalently to the spindle assembly checkpoint protein MAD2. *Proc Natl Acad Sci U S A* 96, 4313-4318.
- Loeb, K.R., and Haas, A.L. (1992). The interferon-inducible 15-kDa ubiquitin homolog conjugates to intracellular proteins. *J Biol Chem* 267, 7806-7813.



- Lorick, K.L., Jensen, J.P., Fang, S., Ong, A.M., Hatakeyama, S., and Weissman, A.M. (1999). RING fingers mediate ubiquitin-conjugating enzyme (E2)-dependent ubiquitination. *Proc Natl Acad Sci U S A* *96*, 11364-11369.
- Lyons, A.B., and Parish, C.R. (1994). Determination of lymphocyte division by flow cytometry. *J Immunol Methods* *171*, 131-137.
- Mabb, A.M., Wuerzberger-Davis, S.M., and Miyamoto, S. (2006). PIASy mediates NEMO sumoylation and NF-kappaB activation in response to genotoxic stress. *Nat Cell Biol* *8*, 986-993.
- Mallette, F.A., Goumard, S., Gaumont-Leclerc, M.F., Moiseeva, O., and Ferbeyre, G. (2004). Human fibroblasts require the Rb family of tumor suppressors, but not p53, for PML-induced senescence. *Oncogene* *23*, 91-99.
- Mataraza, J.M., Tumang, J.R., Gumina, M.R., Gurdak, S.M., Rothstein, T.L., and Chiles, T.C. (2006). Disruption of cyclin D3 blocks proliferation of normal B-1a cells, but loss of cyclin D3 is compensated by cyclin D2 in cyclin D3-deficient mice. *J Immunol* *177*, 787-795.
- Matic, I., van Hagen, M., Schimmel, J., Macek, B., Ogg, S.C., Tatham, M.H., Hay, R.T., Lamond, A.I., Mann, M., and Vertegaal, A.C. (2008). In vivo identification of human small ubiquitin-like modifier polymerization sites by high accuracy mass spectrometry and an in vitro to in vivo strategy. *Mol Cell Proteomics* *7*, 132-144.
- Melchior, F. (2000). SUMO--nonclassical ubiquitin. *Annu Rev Cell Dev Biol* *16*, 591-626.
- Meluh, P.B., and Koshland, D. (1995). Evidence that the MIF2 gene of *Saccharomyces cerevisiae* encodes a centromere protein with homology to the mammalian centromere protein CENP-C. *Mol Biol Cell* *6*, 793-807.
- Mendoza, H.M., Shen, L.N., Botting, C., Lewis, A., Chen, J., Ink, B., and Hay, R.T. (2003). NEDP1, a highly conserved cysteine protease that deNEDDylates Cullins. *J Biol Chem* *278*, 25637-25643.
- Miller, A.J., Levy, C., Davis, I.J., Razin, E., and Fisher, D.E. (2005). Sumoylation of MITF and its related family members TFE3 and TFEB. *J Biol Chem* *280*, 146-155.
- Miltenyi, S., Muller, W., Weichel, W., and Radbruch, A. (1990). High gradient magnetic cell separation with MACS. *Cytometry* *11*, 231-238.
- Minty, A., Dumont, X., Kaghad, M., and Caput, D. (2000). Covalent modification of p73alpha by SUMO-1. Two-hybrid screening with p73 identifies novel SUMO-1-interacting proteins and a SUMO-1 interaction motif. *J Biol Chem* *275*, 36316-36323.
- Modesti, M., Junop, M.S., Ghirlando, R., van de Rakt, M., Gellert, M., Yang, W., and Kanaar, R. (2003). Tetramerization and DNA ligase IV interaction of the DNA double-strand break repair protein XRCC4 are mutually exclusive. *J Mol Biol* *334*, 215-228.

- Mohamedali, A., Soeiro, I., Lea, N.C., Glassford, J., Banerji, L., Mufti, G.J., Lam, E.W., and Thomas, N.S. (2003). Cyclin D2 controls B cell progenitor numbers. *J Leukoc Biol* 74, 1139-1143.
- Moldovan, G.L., Pfander, B., and Jentsch, S. (2006). PCNA controls establishment of sister chromatid cohesion during S phase. *Mol Cell* 23, 723-732.
- Moldovan, G.L., Pfander, B., and Jentsch, S. (2007). PCNA, the maestro of the replication fork. *Cell* 129, 665-679.
- Morris, J.R., Pangon, L., Boutell, C., Katagiri, T., Keep, N.H., and Solomon, E. (2006). Genetic analysis of BRCA1 ubiquitin ligase activity and its relationship to breast cancer susceptibility. *Hum Mol Genet* 15, 599-606.
- Mukhopadhyay, D., and Dasso, M. (2007). Modification in reverse: the SUMO proteases. *Trends Biochem Sci* 32, 286-295.
- Muller, S., Berger, M., Lehembre, F., Seeler, J.S., Haupt, Y., and Dejean, A. (2000). c-Jun and p53 activity is modulated by SUMO-1 modification. *J Biol Chem* 275, 13321-13329.
- Muller, S., Hoege, C., Pyrowolakis, G., and Jentsch, S. (2001). SUMO, ubiquitin's mysterious cousin. *Nat Rev Mol Cell Biol* 2, 202-210.
- Mullis, K.B., and Faloona, F.A. (1987). Specific synthesis of DNA in vitro via a polymerase-catalyzed chain reaction. *Methods Enzymol* 155, 335-350.
- Murakami, H., and Arnheiter, H. (2005). Sumoylation modulates transcriptional activity of MITF in a promoter-specific manner. *Pigment Cell Res* 18, 265-277.
- Nacerddine, K., Lehembre, F., Bhaumik, M., Artus, J., Cohen-Tannoudji, M., Babinet, C., Pandolfi, P.P., and Dejean, A. (2005). The SUMO pathway is essential for nuclear integrity and chromosome segregation in mice. *Dev Cell* 9, 769-779.
- Nutt, S.L., Taubenheim, N., Hasbold, J., Corcoran, L.M., and Hodgkin, P.D. (2011). The genetic network controlling plasma cell differentiation. *Semin Immunol* 23, 341-349.
- Owerbach, D., McKay, E.M., Yeh, E.T., Gabbay, K.H., and Bohren, K.M. (2005). A proline-90 residue unique to SUMO-4 prevents maturation and sumoylation. *Biochem Biophys Res Commun* 337, 517-520.
- Papouli, E., Chen, S., Davies, A.A., Huttner, D., Krejci, L., Sung, P., and Ulrich, H.D. (2005). Crosstalk between SUMO and ubiquitin on PCNA is mediated by recruitment of the helicase Srs2p. *Mol Cell* 19, 123-133.
- Park, M.A., Seok, Y.J., Jeong, G., and Lee, J.S. (2008). SUMO1 negatively regulates BRCA1-mediated transcription, via modulation of promoter occupancy. *Nucleic Acids Res* 36, 263-283.

- Peled, J.U., Yu, J.J., Venkatesh, J., Bi, E., Ding, B.B., Krupski-Downs, M., Shaknovich, R., Sicinski, P., Diamond, B., Scharff, M.D., and Ye, B.H. (2010). Requirement for cyclin D3 in germinal center formation and function. *Cell Res* 20, 631-646.
- Petrie, K., Guidez, F., Howell, L., Healy, L., Waxman, S., Greaves, M., and Zelent, A. (2003). The histone deacetylase 9 gene encodes multiple protein isoforms. *J Biol Chem* 278, 16059-16072.
- Pettitt, S.J., Liang, Q., Rairdan, X.Y., Moran, J.L., Prosser, H.M., Beier, D.R., Lloyd, K.C., Bradley, A., and Skarnes, W.C. (2009). Agouti C57BL/6N embryonic stem cells for mouse genetic resources. *Nat Methods* 6, 493-495.
- Pfander, B., Moldovan, G.L., Sacher, M., Hoege, C., and Jentsch, S. (2005). SUMO-modified PCNA recruits Srs2 to prevent recombination during S phase. *Nature* 436, 428-433.
- Pham, C.T., MacIvor, D.M., Hug, B.A., Heusel, J.W., and Ley, T.J. (1996). Long-range disruption of gene expression by a selectable marker cassette. *Proc Natl Acad Sci U S A* 93, 13090-13095.
- Pichler, A., Gast, A., Seeler, J.S., Dejean, A., and Melchior, F. (2002). The nucleoporin RanBP2 has SUMO1 E3 ligase activity. *Cell* 108, 109-120.
- Pichler, A., Knipscheer, P., Oberhofer, E., van Dijk, W.J., Korner, R., Olsen, J.V., Jentsch, S., Melchior, F., and Sixma, T.K. (2005). SUMO modification of the ubiquitin-conjugating enzyme E2-25K. *Nat Struct Mol Biol* 12, 264-269.
- Rickert, R.C., Roes, J., and Rajewsky, K. (1997). B lymphocyte-specific, Cre-mediated mutagenesis in mice. *Nucleic Acids Res* 25, 1317-1318.
- Rodriguez, M.S., Dargemont, C., and Hay, R.T. (2001). SUMO-1 conjugation in vivo requires both a consensus modification motif and nuclear targeting. *J Biol Chem* 276, 12654-12659.
- Rodriguez, M.S., Desterro, J.M., Lain, S., Midgley, C.A., Lane, D.P., and Hay, R.T. (1999). SUMO-1 modification activates the transcriptional response of p53. *EMBO J* 18, 6455-6461.
- Rooney, S., Chaudhuri, J., and Alt, F.W. (2004). The role of the non-homologous end-joining pathway in lymphocyte development. *Immunol Rev* 200, 115-131.
- Ross, S., Best, J.L., Zon, L.I., and Gill, G. (2002). SUMO-1 modification represses Sp3 transcriptional activation and modulates its subnuclear localization. *Mol Cell* 10, 831-842.
- Sacher, M., Pfander, B., Hoege, C., and Jentsch, S. (2006). Control of Rad52 recombination activity by double-strand break-induced SUMO modification. *Nat Cell Biol* 8, 1284-1290.

- Saiki, R.K., Gelfand, D.H., Stoffel, S., Scharf, S.J., Higuchi, R., Horn, G.T., Mullis, K.B., and Erlich, H.A. (1988). Primer-directed enzymatic amplification of DNA with a thermostable DNA polymerase. *Science* 239, 487-491.
- Saitoh, H., Sparrow, D.B., Shiomi, T., Pu, R.T., Nishimoto, T., Mohun, T.J., and Dasso, M. (1998). Ubc9p and the conjugation of SUMO-1 to RanGAP1 and RanBP2. *Curr Biol* 8, 121-124.
- Sambrook, J., and Gething, M.J. (1989). Protein structure. Chaperones, paperones. *Nature* 342, 224-225.
- Seeler, J.S., and Dejean, A. (1999). The PML nuclear bodies: actors or extras? *Curr Opin Genet Dev* 9, 362-367.
- Seeler, J.S., and Dejean, A. (2003). Nuclear and unclear functions of SUMO. *Nat Rev Mol Cell Biol* 4, 690-699.
- Seufert, W., Futcher, B., and Jentsch, S. (1995). Role of a ubiquitin-conjugating enzyme in degradation of S- and M-phase cyclins. *Nature* 373, 78-81.
- Shapiro-Shelef, M., and Calame, K. (2005). Regulation of plasma-cell development. *Nat Rev Immunol* 5, 230-242.
- Shen, Z., Pardington-Purtymun, P.E., Comeaux, J.C., Moyzis, R.K., and Chen, D.J. (1996a). Associations of UBE2I with RAD52, UBL1, p53, and RAD51 proteins in a yeast two-hybrid system. *Genomics* 37, 183-186.
- Shen, Z., Pardington-Purtymun, P.E., Comeaux, J.C., Moyzis, R.K., and Chen, D.J. (1996b). UBL1, a human ubiquitin-like protein associating with human RAD51/RAD52 proteins. *Genomics* 36, 271-279.
- Sheng, W., and Liao, X. (2002). Solution structure of a yeast ubiquitin-like protein Smt3: the role of structurally less defined sequences in protein-protein recognitions. *Protein Sci* 11, 1482-1491.
- Shimshon, L., Michaeli, A., Hadar, R., Nutt, S.L., David, Y., Navon, A., Waisman, A., and Tirosh, B. (2011). SUMOylation of Blimp-1 promotes its proteasomal degradation. *FEBS Lett* 585, 2405-2409.
- Stavnezer, J., Guikema, J.E., and Schrader, C.E. (2008). Mechanism and regulation of class switch recombination. *Annu Rev Immunol* 26, 261-292.
- Steinacher, R., and Schar, P. (2005). Functionality of human thymine DNA glycosylase requires SUMO-regulated changes in protein conformation. *Curr Biol* 15, 616-623.
- Stuurman, N., Meijne, A.M., van der Pol, A.J., de Jong, L., van Driel, R., and van Renswoude, J. (1990). The nuclear matrix from cells of different origin. Evidence for a common set of matrix proteins. *J Biol Chem* 265, 5460-5465.

- Tashiro, S., Muto, A., Tanimoto, K., Tsuchiya, H., Suzuki, H., Hoshino, H., Yoshida, M., Walter, J., and Igarashi, K. (2004). Repression of PML nuclear body-associated transcription by oxidative stress-activated Bach2. *Mol Cell Biol* 24, 3473-3484.
- Tatham, M.H., Jaffray, E., Vaughan, O.A., Desterro, J.M., Botting, C.H., Naismith, J.H., and Hay, R.T. (2001). Polymeric chains of SUMO-2 and SUMO-3 are conjugated to protein substrates by SAE1/SAE2 and Ubc9. *J Biol Chem* 276, 35368-35374.
- Terris, B., Baldin, V., Dubois, S., Degott, C., Flejou, J.F., Henin, D., and Dejean, A. (1995). PML nuclear bodies are general targets for inflammation and cell proliferation. *Cancer Res* 55, 1590-1597.
- Ulrich, H.D. (2009). Regulating post-translational modifications of the eukaryotic replication clamp PCNA. *DNA Repair (Amst)* 8, 461-469.
- Ulrich, H.D., Vogel, S., and Davies, A.A. (2005). SUMO keeps a check on recombination during DNA replication. *Cell Cycle* 4, 1699-1702.
- Ungureanu, D., Vanhatupa, S., Kotaja, N., Yang, J., Aittomaki, S., Janne, O.A., Palvimo, J.J., and Silvennoinen, O. (2003). PIAS proteins promote SUMO-1 conjugation to STAT1. *Blood* 102, 3311-3313.
- Van Nguyen, T., Angkasekwinai, P., Dou, H., Lin, F.M., Lu, L.S., Cheng, J., Chin, Y.E., Dong, C., and Yeh, E.T. (2012). SUMO-specific protease 1 is critical for early lymphoid development through regulation of STAT5 activation. *Mol Cell* 45, 210-221.
- Vigasova, D., Sarangi, P., Kolesar, P., Vlasakova, D., Slezakova, Z., Altmannova, V., Nikulenkov, F., Anrather, D., Gith, R., Zhao, X., *et al.* (2013). Lif1 SUMOylation and its role in non-homologous end-joining. *Nucleic Acids Res* 41, 5341-5353.
- Villagra, N.T., Navascues, J., Casafont, I., Val-Bernal, J.F., Lafarga, M., and Berciano, M.T. (2006). The PML-nuclear inclusion of human supraoptic neurons: a new compartment with SUMO-1- and ubiquitin-proteasome-associated domains. *Neurobiol Dis* 21, 181-193.
- Wan, J., Subramonian, D., and Zhang, X.D. (2012). SUMOylation in control of accurate chromosome segregation during mitosis. *Curr Protein Pept Sci* 13, 467-481.
- Wu, K., Yamoah, K., Dolios, G., Gan-Erdene, T., Tan, P., Chen, A., Lee, C.G., Wei, N., Wilkinson, K.D., Wang, R., and Pan, Z.Q. (2003). DEN1 is a dual function protease capable of processing the C terminus of Nedd8 and deconjugating hyper-neddylated CUL1. *J Biol Chem* 278, 28882-28891.
- Wuerzberger-Davis, S.M., Nakamura, Y., Seufzer, B.J., and Miyamoto, S. (2007). NF-kappaB activation by combinations of NEMO SUMOylation and ATM activation stresses in the absence of DNA damage. *Oncogene* 26, 641-651.
- The GeneCards Human Gene Database - Asb8, (March 18, 2013), Retrieved October 14, 2013, from <http://www.genecards.org/cgi-bin/carddisp.pl?gene=ASB8>

The GeneCards Human Gene Database - COL2A1, (March 18, 2013), Retrieved October 14, 2013, from <http://www.genecards.org/cgi-bin/carddisp.pl?gene=COL2A1>

The GeneCards Human Gene Database - TMEM106C, (March 18, 2013), Retrieved October 14, 2013, from <http://www.genecards.org/cgi-bin/carddisp.pl?gene=TMEM106C>

Xu, Z., and Au, S.W. (2005). Mapping residues of SUMO precursors essential in differential maturation by SUMO-specific protease, SENP1. *Biochem J* 386, 325-330.

Yamaguchi, T., Sharma, P., Athanasiou, M., Kumar, A., Yamada, S., and Kuehn, M.R. (2005). Mutation of SENP1/SuPr-2 reveals an essential role for desumoylation in mouse development. *Mol Cell Biol* 25, 5171-5182.

Yang, S.H., Jaffray, E., Hay, R.T., and Sharrocks, A.D. (2003). Dynamic interplay of the SUMO and ERK pathways in regulating Elk-1 transcriptional activity. *Mol Cell* 12, 63-74.

Yang, S.H., and Sharrocks, A.D. (2013). Ubc9 acetylation: a new route for achieving specificity in substrate SUMOylation. *EMBO J* 32, 773-774.

Yang, Y., Tse, A.K., Li, P., Ma, Q., Xiang, S., Nicosia, S.V., Seto, E., Zhang, X., and Bai, W. (2011). Inhibition of androgen receptor activity by histone deacetylase 4 through receptor SUMOylation. *Oncogene* 30, 2207-2218.

Yeh, E.T., Gong, L., and Kamitani, T. (2000). Ubiquitin-like proteins: new wines in new bottles. *Gene* 248, 1-14.

Ying, H.Y., Su, S.T., Hsu, P.H., Chang, C.C., Lin, I.Y., Tseng, Y.H., Tsai, M.D., Shih, H.M., and Lin, K.I. (2012). SUMOylation of Blimp-1 is critical for plasma cell differentiation. *EMBO Rep* 13, 631-637.

Yu, L., Ji, W., Zhang, H., Renda, M.J., He, Y., Lin, S., Cheng, E.C., Chen, H., Krause, D.S., and Min, W. (2010). SENP1-mediated GATA1 deSUMOylation is critical for definitive erythropoiesis. *J Exp Med* 207, 1183-1195.

Yurchenko, V., Xue, Z., Gama, V., Matsuyama, S., and Sadofsky, M.J. (2008). Ku70 is stabilized by increased cellular SUMO. *Biochem Biophys Res Commun* 366, 263-268.

Yurchenko, V., Xue, Z., and Sadofsky, M.J. (2006). SUMO modification of human XRCC4 regulates its localization and function in DNA double-strand break repair. *Mol Cell Biol* 26, 1786-1794.

Zhang, F.P., Mikkonen, L., Toppari, J., Palvimo, J.J., Thesleff, I., and Janne, O.A. (2008). Sumo-1 function is dispensable in normal mouse development. *Mol Cell Biol* 28, 5381-5390.

Zhao, J. (2007). Sumoylation regulates diverse biological processes. *Cell Mol Life Sci* 64, 3017-3033.

Zhong, S., Hu, P., Ye, T.Z., Stan, R., Ellis, N.A., and Pandolfi, P.P. (1999). A role for PML and the nuclear body in genomic stability. *Oncogene* 18, 7941-7947.

Zhong, S., Muller, S., Ronchetti, S., Freemont, P.S., Dejean, A., and Pandolfi, P.P. (2000). Role of SUMO-1-modified PML in nuclear body formation. *Blood* 95, 2748-2752.

Zhou, C., Yang, Y., and Jong, A.Y. (1990). Mini-prep in ten minutes. *Biotechniques* 8, 172-173.

## **8. Acknowledgements**



## 9. Versicherung

Ich versichere, dass ich die von mir vorgelegte Dissertation selbständig angefertigt, die benutzten Quellen und Hilfsmittel vollständig angegeben und die Stellen der Arbeit - einschließlich Tabellen, Karten und Abbildungen -, die anderen Werken im Wortlaut oder dem Sinn nach entnommen sind, in jedem Einzelfall als Entlehnung kenntlich gemacht habe; dass diese Dissertation noch keiner anderen Fakultät oder Universität zur Prüfung vorgelegen hat; dass sie noch nicht veröffentlicht worden ist sowie, dass ich eine solche Veröffentlichung vor Abschluss des Promotionsverfahrens nicht vornehmen werde. Die Bestimmungen dieser Promotionsordnung sind mir bekannt. Die von mir vorgelegte Dissertation ist von Prof. Dr. Ari Waisman betreut worden.

Mainz, 29. November 2013



Christian Reichhold

## **10. Lebenslauf**

## **11. Publikationen**